

379  
N818  
NOV 10 1975

KINETICS AND MECHANISM OF SUBSTITUTION REACTIONS  
OF TUNGSTEN CARBONYL COMPLEXES CONTAINING  
BIDENTATE SULFUR LIGANDS

DISSERTATION

Presented to the Graduate Council of the  
North Texas State University in Partial  
Fulfillment of the Requirements

For the Degree of

DOCTOR OF PHILOSOPHY

By

Linda D. Schultz, B.A., M.S.

Denton, Texas

December, 1975

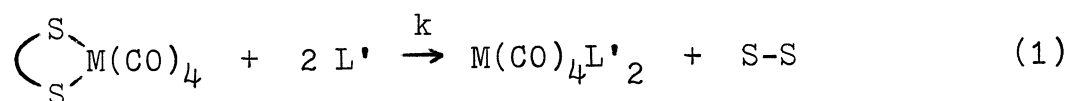
© Copyright by

Linda D. Schultz

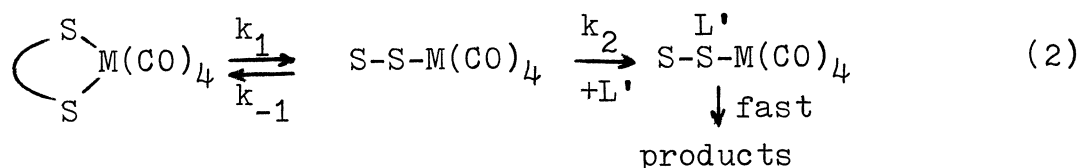
1975

Schultz, Linda D., Kinetics and Mechanism of Substitution Reactions of Tungsten Carbonyl Complexes Containing Bidentate Sulfur Ligands. Doctor of Philosophy (Chemistry), December, 1975, 98 pp., 9 tables, 35 illustrations, bibliography, 65 titles.

Previous investigations of the kinetics and mechanism of the substitution reaction of bidentate substituted transition metal carbonyl complexes with Lewis bases (L') to yield the cis disubstituted bidentate substitution product (1), where M = Cr, Mo, or W and S-S = DTO (2,2,7,7-tetramethyl-3,6-dithiaoctane) or DTN (2,2,8,8-tetramethyl-3,7-dithianonane) have suggested that this reaction proceeds



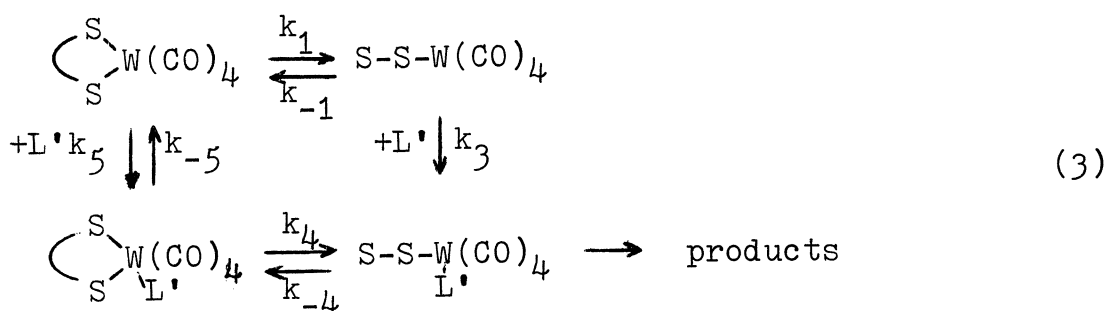
via a mechanism (2) involving initial reversible dissociation of one end of the bidentate sulfur ligand followed by rapid attack of L' on the resulting five-coordinate intermediate.



However, in the case of bidentate = DTN,  $k_1$  was found to exhibit dependence upon the identity of L', an observation inconsistent with this mechanism. Therefore, it was considered necessary to investigate these systems in much greater detail.

Kinetic studies were made of the substitution reactions of  $(\text{DTO})\text{W}(\text{CO})_4$  and  $(\text{DTN})\text{W}(\text{CO})_4$  with a series of phosphorus ligands including trimethyl, triethyl, triisopropyl, triphenyl, and constrained phosphite and tri-n-butylphosphine and triphenylphosphine in xylene at various temperatures.

The kinetic data were found to be consistent with three discrete pathways, which may be encompassed in reaction scheme (3).



The pathway followed for each system studied was found to be dependent upon the identity of the substrate and the steric and electronic properties of  $\text{L}'$ . Path A, governed by  $k_1, k_{-1}, k_2, k_3$ , was followed by the systems  $(\text{DTO})\text{W}(\text{CO})_4$  with trimethyl, triethyl, triisopropyl, triphenyl, and constrained phosphite and triphenylphosphine and  $(\text{DTN})\text{W}(\text{CO})_4$  with triisopropyl, triphenyl, and constrained phosphite and triphenylphosphine. Path B, governed by  $k_1, k_{-1}, k_2, k_3, k_{-4}, k_{-5}$ , was followed by the systems  $(\text{DTN})\text{W}(\text{CO})_4$  with trimethyl and triethyl phosphite. Path C, governed by  $k_1, k_{-1}, k_2, k_3, k_4, k_5$ , was followed by the reactions of both  $(\text{DTO})\text{W}(\text{CO})_4$  and  $(\text{DTN})\text{W}(\text{CO})_4$  with tri-n-butylphosphine.

The intermediate species  $(DTN)W(CO)_4P(OCH_2)_3CCH_3$ , with the DTN moiety bonded to the metal atom through only one sulfur donor atom, whose presence was predicted by this mechanism, was detected during the course of the substitution reaction between  $(DTN)W(CO)_4$  and the constrained phosphite. This compound was isolated and characterized.

Activation parameters were calculated for the reactions of  $(DTO)W(CO)_4$  and  $(DTN)W(CO)_4$  with triisopropyl phosphite and tri-n-butylphosphine. On the basis of these activation parameters, the ground state energy for the DTO complex is calculated to be about 5.6 kcal/mole lower than that of the DTN complex. The entropies of activation indicate  $k_1$  and  $k_5$  to be  $I_d$  and  $I_a$  processes respectively.



## PREFACE

The author wishes to express her gratitude to Mr. Jim Henderson for checking the purity of liquid phosphorus ligands by GLC. I wish also to thank Mr. Ahmad Moradi and Mr. Jerry Pardue for assistance and advice in the laboratory.

Financial support of this work by the Robert A. Welch Foundation and the North Texas State University Faculty Research Fund is gratefully acknowledged.

TABLE OF CONTENTS

	Page
LIST OF TABLES . . . . .	iv
LIST OF ILLUSTRATIONS . . . . .	v
Chapter	
I. INTRODUCTION . . . . .	1
History and General Properties	
Bonding	
Reactions	
The Problem	
II. EXPERIMENTAL . . . . .	25
Preparation and Purification of Materials	
Determination of Rates	
III. RESULTS . . . . .	43
(DTO)W(CO) <sub>4</sub>	
(DTN)W(CO) <sub>4</sub>	
IV. DISCUSSION . . . . .	74
Path A	
Path B	
Path C	
V. CONCLUSIONS . . . . .	91
BIBLIOGRAPHY . . . . .	95

## LIST OF TABLES

Table	Page
I. Rates of Reaction of $(\text{DTO})\text{W}(\text{CO})_4$ with Phosphorus Ligands in Xylene . . . . .	45
II. Rate Constants for Reaction of $(\text{DTO})\text{W}(\text{CO})_4$ with Phosphorus Ligands in Xylene . . . . .	51
III. Activation Parameters for Reaction of $(\text{DTO})\text{W}(\text{CO})_4$ with Triisopropyl Phosphite in Xylene . . . . .	54
IV. Second Order Rate Constants for Reaction of $(\text{DTO})\text{W}(\text{CO})_4$ with Tri- <u>n</u> -butylphosphine in Xylene . . . . .	58
V. Rates of Reaction of $(\text{DTN})\text{W}(\text{CO})_4$ with Phosphorus Ligands in Xylene . . . . .	59
VI. Rate Constants for Reaction of $(\text{DTN})\text{W}(\text{CO})_4$ with Phosphorus Ligands in Xylene . . . . .	65
VII. Activation Parameters for Reaction of $(\text{DTN})\text{W}(\text{CO})_4$ with Triisopropyl Phosphite in Xylene . . . . .	69
VIII. Second Order Rate Constants for Reaction of $(\text{DTN})\text{W}(\text{CO})_4$ with Tri- <u>n</u> -butylphosphine in Xylene . . . . .	73
IX. Cone Angles of Phosphorus Ligands . . . . .	84



## LIST OF ILLUSTRATIONS

Figure	Page
1. Valence Bond Representation of Transition Metal-Carbon Monoxide Bond . . . . .	5
2. Detailed Valence Bond Representation of Transition Metal-Carbon Monoxide Bond . . .	5
3. Molecular Orbital Representation of Carbon Monoxide-Transition Metal Bond . . . . .	6
4. Synergic Bonding . . . . .	7
5. Fenske "Direct Donation" Effect. . . . .	9
6. Substitution Reaction Mechanism Involving Rate Determining Dissociation of Carbon Monoxide	11
7. Substitution Reaction Mechanism Involving Rate Determining Attack of L' at Metal Atom. . .	13
8. Substitution Reaction Mechanism Involving Rate Determining Attack of L' at Carbonyl Carbon	14
9. Mechanism I. . . . .	20
10. Mechanism II . . . . .	21
11. Substrate-Ligand Interaction . . . . .	24
12. Gas Chromatogram of Purified Triisopropyl Phosphite . . . . .	27
13. Mass Spectrum of Purified Triisopropyl Phosphite . . . . .	28
14. Reaction Flask Used for Kinetic Studies. . . . .	37

LIST OF ILLUSTRATIONS Continued

Figure	Page
15. Visible Spectra of $(DTN)W(CO)_4$ and $(DTN)W(CO)_4P(OCH_2)_3CCH_3$ . . . . .	40
16. Plot of Time vs. Absorbance for Reaction of $(DTN)W(CO)_4$ with $P(OCH_2)_3CCH_3$ at $66.5^\circ C$ Monitored at Two Different Wavelengths. . . . .	41
17. Plot of $k_{obs}$ vs. $[L']$ for Reaction of Various Phosphorus Ligands with $(DTO)W(CO)_4$ in Xylene at $99.9^\circ C$ . . . . .	49
18. Plot of $1/k_{obs}$ vs. $1/[L']$ for Reaction of $(DTO)W(CO)_4$ with Various Phosphorus Ligands in Xylene at $99.9^\circ C$ . . . . .	50
19. Plot of $k_{obs}$ vs. $[L']$ for Reaction of Triisopropyl Phosphite with $(DTO)W(CO)_4$ at Different Temperatures. . . . .	52
20. Plot of $1/k_{obs}$ vs. $1/[L']$ for Reaction of Triisopropyl Phosphite with $(DTO)W(CO)_4$ at Different Temperatures . . . . .	53
21. Eyring Plot of Rate Constants of Reaction of $(DTO)W(CO)_4$ with Triisopropyl Phosphite in Xylene at Different Temperatures . . . . .	55
22. Plot of $k_{obs}$ vs. $[L']$ for Reactions of Tri-n-butylphosphine with $(DTO)W(CO)_4$ at Different Temperatures. . . . .	56
23. Plot of $1/k_{obs}$ vs. $1/[L']$ for Reaction of $(DTO)W(CO)_4$ with Tri-n-butylphosphine at Various Temperatures. . . . .	57

LIST OF ILLUSTRATIONS Continued

Figure	Page
24. Plot of $k_{\text{obs}}$ vs. $[L']$ for Reactions of Various Phosphorus Ligands with $(\text{DTN})\text{W}(\text{CO})_4$ in Xylene at $66.5^\circ \text{C}$ . . . . .	63
25. Plot of $1/k_{\text{obs}}$ vs. $1/[L']$ for Reaction of $(\text{DTN})\text{W}(\text{CO})_4$ with Various Phosphorus Ligands in Xylene at $66.5^\circ \text{C}$ . . . . .	64
26. Plot of $k_{\text{obs}}$ vs. $[L']$ for Reaction of Triisopropyl Phosphite with $(\text{DTN})\text{W}(\text{CO})_4$ at Different Temperatures. . . . .	67
27. Plot of $1/k_{\text{obs}}$ vs. $1/[L']$ for Reaction of Triisopropyl Phosphite with $(\text{DTN})\text{W}(\text{CO})_4$ at Different Temperatures . . . . .	68
28. Eyring Plot of Rate Constants of Reaction of $(\text{DTN})\text{W}(\text{CO})_4$ with Triisopropyl Phosphite in Xylene at Different Temperatures . . . . .	70
29. Plot of $k_{\text{obs}}$ vs. $[L']$ for Reaction of Tri-n-butylphosphine with $(\text{DTN})\text{W}(\text{CO})_4$ at Different Temperatures. . . . .	71
30. Plot of $1/k_{\text{obs}}$ vs. $1/[L']$ for Reaction of Tri-n-butylphosphine with $(\text{DTN})\text{W}(\text{CO})_4$ at Different Temperatures in Xylene. . . . .	72
31. Potential Energy Diagram for Reaction of (bidentate) $\text{W}(\text{CO})_4$ with Triisopropyl Phosphite in Xylene . . . . .	79
32. Carbonyl Stretching Spectra in Chloroform of Products and Substrate for $(\text{DTN})\text{W}(\text{CO})_4 + \text{P}(\text{OCH}_2)_3\text{CCH}_3$ . . . . .	82

LIST OF ILLUSTRATIONS Continued

Figure	Page
33. Substitution Reaction Mechanism Involving Chelate Ring Reclosure with Expulsion of L' . . . . .	85
34. Substitution Reaction Mechanism Involving reversible Dissociation and Direct Attack of L'. . . . .	89
35. Substitution Reaction Mechanism Scheme for Reaction of Tundsten Carbonyl Complexes Containing Bidentate Sulfur Ligands with Monodentate Phosphorus Ligands. . . . .	92

## CHAPTER I

### INTRODUCTION

#### History and General Properties

The chemistry of transition metal carbonyl complexes and their derivatives has proven to be a fruitful field of study for inorganic chemists. This investigation began in 1890 with the synthesis of tetracarbonylnickel(0) by Mond, Langer, and Quinke<sup>1</sup>. One year later, in 1891, the discovery of iron pentacarbonyl was announced by Berthelot<sup>2</sup>. Further research by Hieber and coworkers<sup>3</sup> in Germany during the 1920's and 1930's initiated an extensive study of these interesting compounds and their properties by a veritable host of chemists. An insight into the beginnings of transition metal carbonyl chemistry may be gained from a series of review articles by Trout<sup>4-7</sup>. A measure of the current development of this field may be gained from the fact that metal carbonyl complexes of some type have now been reported for all of the transition metals<sup>8</sup> and many and diverse derivatives of these complexes have been synthesized<sup>9</sup>. A large number of excellent review articles now exist on different aspects of these compounds. These review articles will not be listed here, but will be cited when appropriate.

Transition metal carbonyl complexes consist of a metal

atom in a low negative, zero, or low positive oxidation state bonded to carbon monoxide (a neutral molecule). This may be contrasted with the "classical complexes" in which the metal atom has a well defined oxidation number and the ligands have a discrete electron population<sup>8</sup>. The structures of these compounds encompass a wide variety of stereochemistries<sup>10</sup> and some structures have yet to be completely solved. These complexes may be mononuclear or polynuclear (have one or more central metal atoms), and the carbonyl groups may be either terminal (bonded to only one metal atom) or bridging (bonded to more than one metal atom). In some compounds, such as  $\text{Fe}_3(\text{CO})_{12}$ , both types of carbonyl groups are present. This discussion, however, will be limited to mononuclear carbonyls, of octahedral geometry, containing only terminal carbonyl groups.

Although both the carbon and oxygen atoms of carbon monoxide have a lone pair of electrons available for coordination, the oxygen atom is the more electronegative, and thus the lone pair on the carbon is more readily available for bond formation. Indeed, in most cases examined, bonding in transition metal carbonyl complexes has been shown to occur through the carbon atom.

With few exceptions, transition metal carbonyl complexes obey Sidgwick's rule, i.e. the metal attains the electronic configuration of the next rare gas. An interesting discus-

sion of the theoretical basis of this rule, also known as the "eighteen-electron rule" or the "effective atomic number" (EAN) rule, has been given by Mitchell and Parish<sup>11</sup>. This rule is essentially an extension of the Lewis octet rule, and its primary importance is its use as a tool in predicting the coordination number of transition metal carbonyl complexes, since few other classes of compounds obey it with high frequency<sup>12</sup>.

A number of other unusual and useful properties of the transition metal carbonyl complexes have made them the object of extensive research. Most of these compounds are diamagnetic, electrically neutral, and moderately inert<sup>8</sup>. Some metal carbonyl complexes are volatile, and most are hydrophobic and soluble in organic solvents. A large number and variety of derivatives may be prepared by simple thermal or photochemical processes. Many of the parent compounds and their derivatives have differing colors, and all have characteristic infrared spectra in the carbonyl stretching region, 2200 to 1700  $\text{cm}^{-1}$ . This region of the spectrum is free from interference from other vibrational modes of the molecule, with the exception of the M-H stretch, and from observation of the number of bands and their positions and intensities it is possible to predict the molecular symmetry of the compound under investigation<sup>13,14</sup>. Indeed, the presence of these interesting properties has made transition metal carbonyl complexes excellent models with which to study

many inorganic reactions.

The very formation of transition metal carbonyl species is initially startling when it is considered that the transition metals have high heats of atomization and carbon monoxide is a generally inert molecule. Furthermore, the electron donating ability of carbon monoxide is negligible<sup>8</sup>. In addition, the low oxidation state of the central metal atom should yield a prohibitively high formal charge on the metal. The stability and ease of formation of these compounds, which might seem anomalous in view of the preceding, may be explained by a consideration of the bonding between the transition metal and carbon monoxide.

#### Bonding

Pauling suggested that complexes should be most stable when the electronegativity of the ligand was such that the metal atom achieved an essentially neutral charge. This rule of thumb is known as the "electroneutrality principle". Since the metal is bonded to an element of relatively low electronegativity in the case of transition metal carbonyl complexes, Pauling suggested that a possible mechanism for delocalizing the electron density on the transition metal atom would be "back bonding", or partial double bond resonance, which would stabilize the system by shifting the electron density from the electropositive metal atom to the more electronegative oxygen atom, as shown in Figure 1.



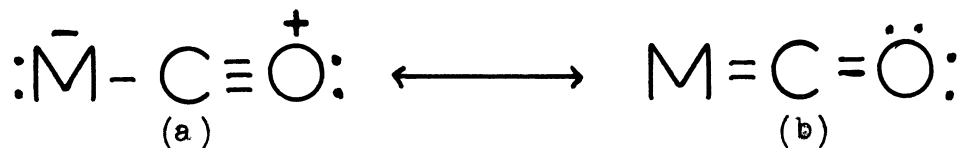


Fig. 1--Valence bond representation of transition metal-carbon monoxide bond.

The contribution of canonical form (b) to the structure makes this increased stability possible. A closer examination of this process indicates that this delocalization of charge must occur by overlap of a p orbital of the carbon with a d or d-hybrid orbital of the proper symmetry on the metal atom<sup>12</sup> as illustrated in Figure 2. This arrangement makes the carbon p orbital unavailable for a pi bond to the oxygen.

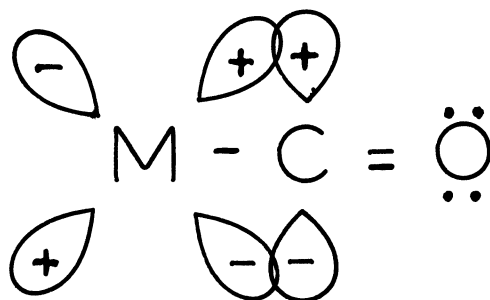


Fig. 2--Detailed valence bond representation of the transition metal-carbon monoxide bond.

The molecular orbital (MO) theoretical approach to this system is more detailed and probably more accurate<sup>8</sup>, as illustrated in Figure 3. There first occurs a dative overlap of the filled carbon sp-hybrid orbital with the empty d-hybrid orbital on the metal to form a sigma bond (Fig. 3a).

Secondly, there is a dative overlap of a filled d-pi or hybrid d-pi metal orbital of proper symmetry with a vacant pi antibonding orbital of carbon monoxide (Fig. 3b).

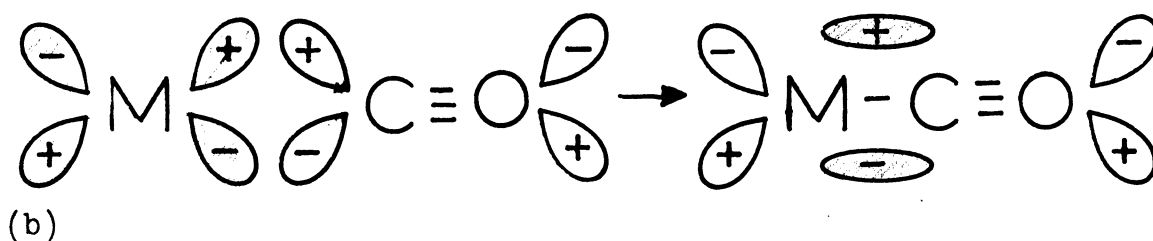
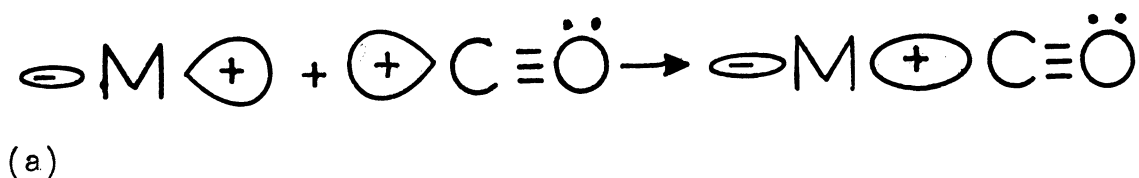
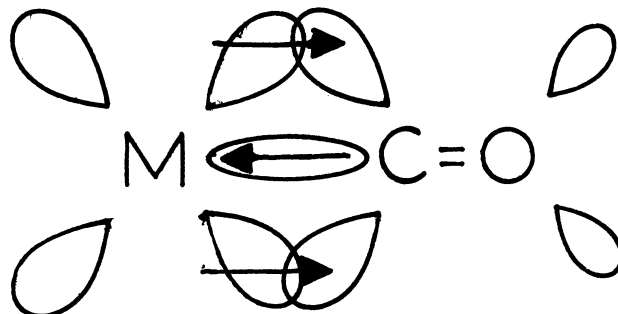


Fig. 3--Molecular orbital representation of carbon monoxide-transition metal bond.

The simultaneous existence of the two types of bonding in this system, sigma and pi, leads to reinforcement of the carbon monoxide-metal bond since as the carbon donates electron density to the metal via the sigma bond it attains a more positive charge which induces an increase in "back bonding" involving the pi bond. This "back bonding" makes the carbon monoxide as a whole negative and increases its basicity, leading to enhancement of sigma donation. This mechanism of mutual reinforcement is known as "synergic bonding" and is illustrated in Figure 4.

pi donating from M  
 decreased negative charge on M



sigma donation from CO  
 increased positive charge on C

Fig. 4--Synergic bonding

The main sources of information about the multiple nature of transition metal-carbon monoxide bonds are bond lengths and vibrational spectra. The information on bond lengths which has been examined supports the present theory of bonding quite well<sup>8</sup>. The carbonyl stretching spectra, as previously mentioned, are easily accessible for study. Analyses of these spectra have been greatly facilitated by the development of the Cotton-Kraihanzel energy factored force field<sup>15,16</sup>. This approach attempts to simplify the interpretation of spectra through calculation of carbonyl stretching force constants, which are a more utilitarian index of the bonding properties of the complexes than are the frequencies themselves. Studies of the variation of

these force constants with the degree of substitution and nature of substituents in substitution products of transition metal carbonyl complexes have been made with hundreds of compounds<sup>17</sup>, and they have proved to be a major tool in the study of bonding in metal carbonyls.

However, a measure of disagreement exists as to the actual mechanism of these bonding interactions. Cotton and coworkers<sup>15,18-20</sup> developed a theory attributing all changes in carbonyl force constants to variation in the pi bonding abilities among the differing ligands and the resultant changes in the occupancy of the pi antibonding orbitals of the carbonyl groups. Angelici<sup>21,22</sup> attributed these trends in stretching frequencies and the attendant force constants to sigma bonding effects only, although this conclusion is now questioned<sup>23</sup>. The recent theoretical work of Fenske and coworkers<sup>24,25</sup> strongly indicates that the predominant effects on frequencies and force constants within a series of compounds are a result of the occupancy of the pi antibonding orbitals, and the sigma bonding properties of the substituent have only a minimal effect.

A third operational mechanism which has been proposed is the Fenske "direct donation" effect<sup>24,25</sup>. This mechanism involves a through space interaction between the  $p_z$  orbital of the substituent and the pi antibonding orbitals of the appropriate symmetry on the equatorial carbonyl groups as illustrated in Figure 5.

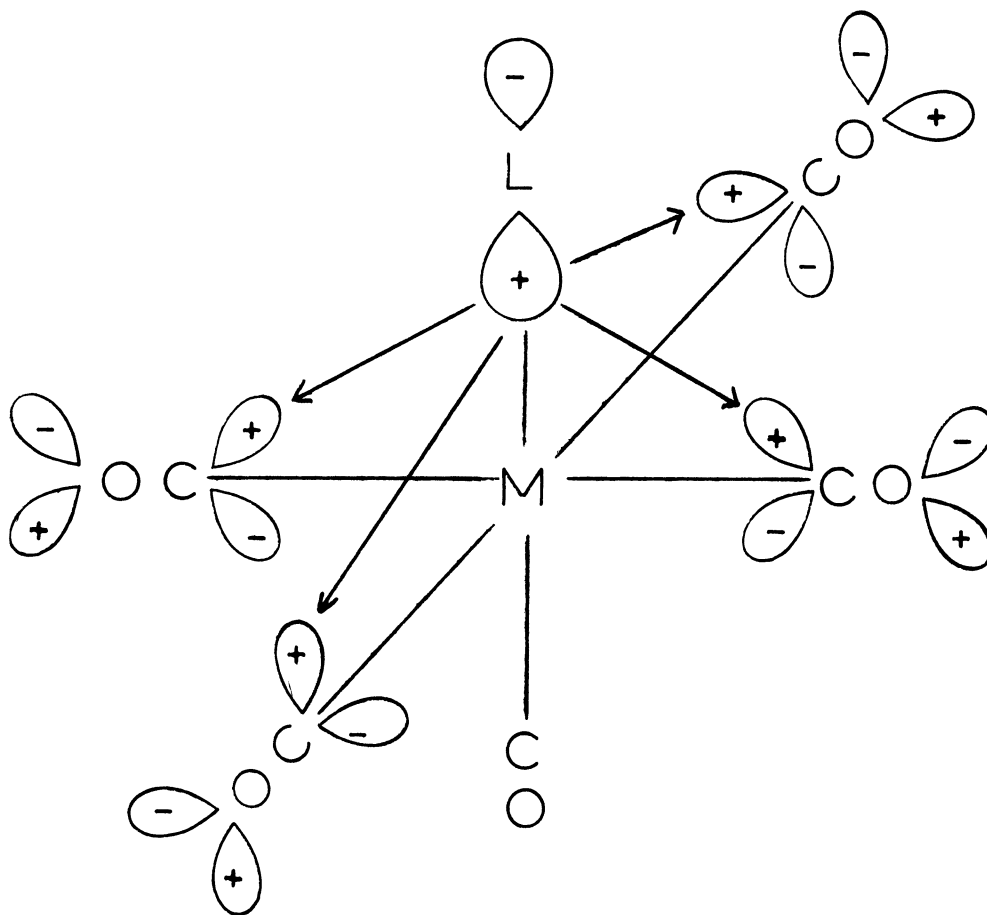


Fig. 5--Fenske "direct donation" effect

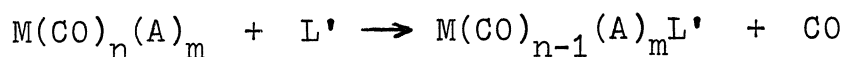
MacDiarmid and coworkers<sup>26</sup> have independently derived a similar theory. The "direct donation" effect has also received support from the work of Keeling, Kettle, and Paul<sup>27</sup> and Dobson<sup>28,29</sup>.

These interacting factors complicate the interpretation of bonding in transition metal carbonyl complexes based solely on observation of the carbonyl stretching spectrum and add validity to the view of Basolo and Pearson<sup>30</sup> that

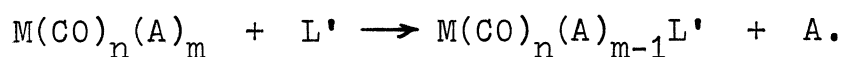
the prediction of metal-carbon bond strengths based solely on carbonyl stretching frequencies and the resultant force constants is a questionable procedure. Therefore, in recent years the focus of the study of bonding in transition metal carbonyl complexes has shifted from spectrochemical methods to kinetic studies of the reactions of these compounds.

### Reactions

Although transition metal carbonyl complexes undergo a plethora of chemical reactions, the most important single class of reactions must be considered to be substitution reactions in which either the carbonyl moiety or a substituent is replaced by a Lewis base ( $L'$ ):



or



The rate laws for these reactions are primarily of three basic types. The first type of behavior observed involves a first order reaction independent of the concentration of the ligand. The rate law for this reaction is expressed by

$$-d[\text{Substrate}]/dt = k_1[\text{Substrate}].$$

A common example of this type of rate behavior, and one which has been well documented<sup>31</sup>, is a mechanism involving

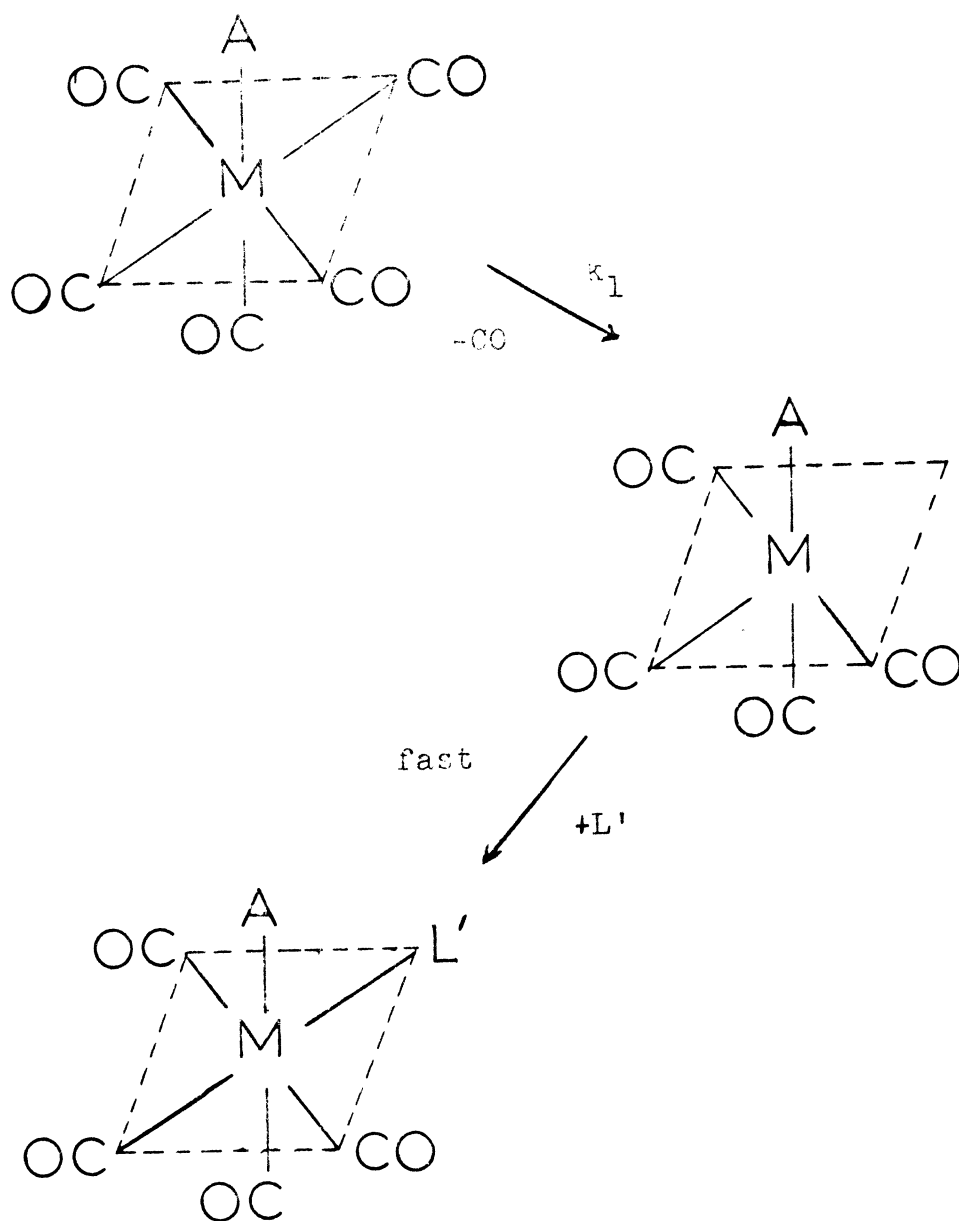


Fig. 6--Substitution reaction mechanism involving rate determining dissociation of carbon monoxide.

unimolecular rate determining dissociation of a carbonyl group, as shown in Figure 6.

The second mode of rate behavior observed for substitution reactions of transition metal carbonyl complexes yields a second order rate law dependent upon the concentrations of both complex and ligand,

$$-d[\text{Substrate}]/dt = k_2[\text{Substrate}][\text{L}'].$$

For reactions involving exclusively carbonyl replacement, the ligand dependency has been attributed to either formation of a seven-coordinate intermediate arising from nucleophilic attack at the metal atom, as illustrated in Figure 7, or attack by the ligand at the carbonyl carbon, as shown in Figure 8. It is difficult to differentiate between these two processes, since the rate laws and products are identical. It has been shown theoretically<sup>32</sup> that the carbonyl carbon is a favored site of nucleophilic attack in the hexacarbonyls of vanadium, chromium, and manganese. In the case of reactions of  $\text{M}(\text{CO})_6$ , where  $\text{M} = \text{Cr}, \text{Mo}, \text{or } \text{W}$ , with tetra-(n-butyl)ammonium halides, the small chromium species undergoes attack at the carbonyl carbon, while the larger metal atoms react via a seven-coordinate intermediate<sup>33</sup>.

The third class of reactions involves a mixed order rate law and may be considered as a combination of the previous two types. The rate law has the form



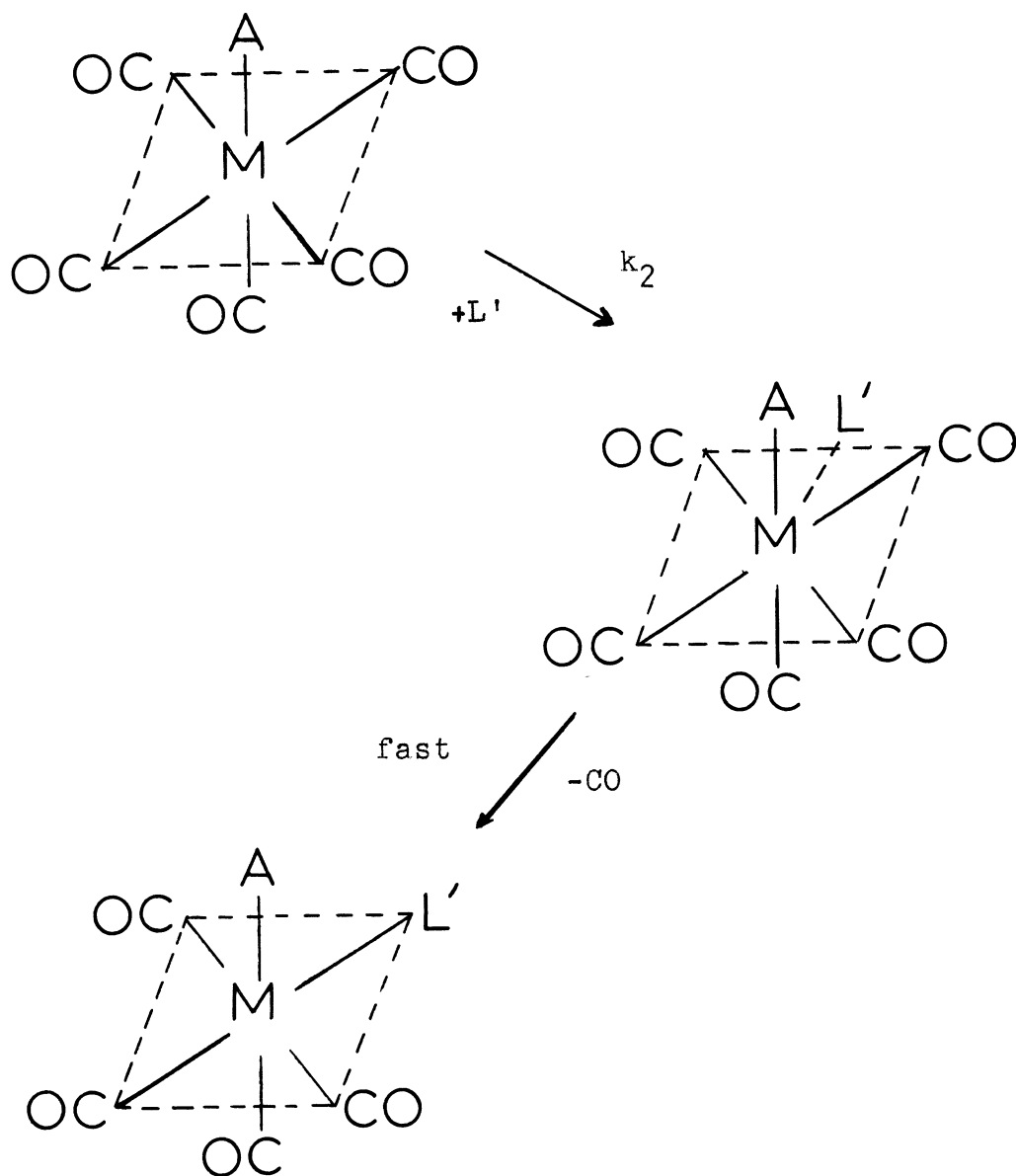


Fig. 7--Substitution reaction mechanism involving rate determining attack of  $L'$  at metal atom.

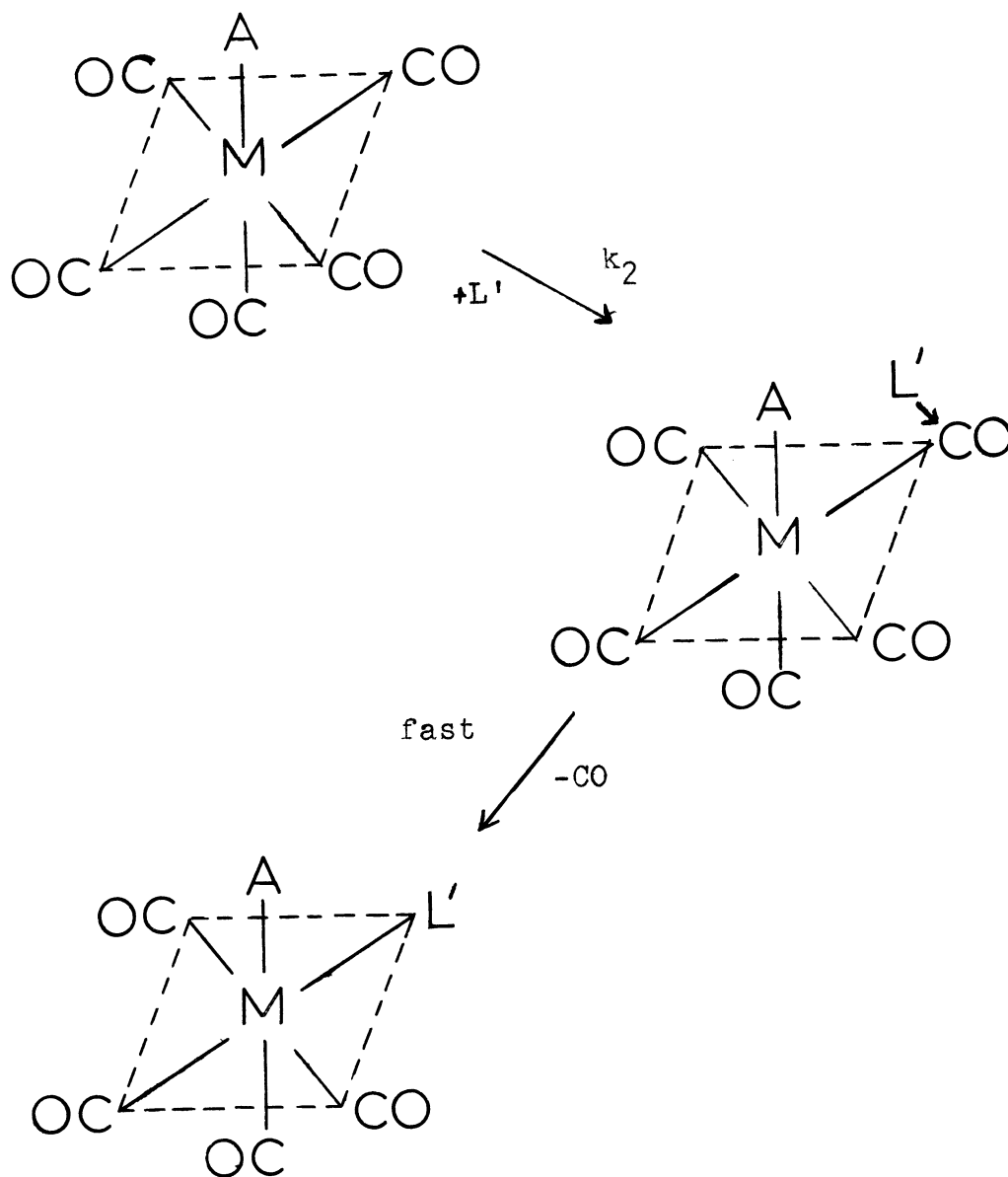


Fig. 8--Substitution reaction mechanism involving rate determining attack of  $L'$  at carbonyl carbon.

$$-d[\text{Substrate}]/dt = k_1[\text{Substrate}] + k_2[\text{L}'][\text{Substrate}]$$

and is indicative of competing first and second order reactions. Covey and Brown<sup>34</sup> have studied a system of this type involving substitution reactions of  $\text{Mo}(\text{CO})_5(\text{amine})$  complexes. In actuality, this third type of mechanism is the general case and the other examples may be considered as limiting behavior.

These three behavioral types may be distinguished by studying the reaction rates under pseudo first order conditions employing a large (twenty-fold or greater) excess of ligand. In this situation, the ligand concentration remains essentially constant during the course of the reaction and may be incorporated into an observed rate constant  $k_{\text{obs}}$ , with  $k_{\text{obs}} = k_{\text{true}}[\text{L}']$ . When the reaction rates are measured at a number of differing concentrations of  $\text{L}'$ , all of suitable excess, the true reaction type and rate constants can be deduced from a plot of  $k_{\text{obs}}$  versus  $[\text{L}']$ .

For the first reaction type discussed, the rate law was

$$-d[\text{Substrate}]/dt = k_1[\text{Substrate}].$$

Under pseudo first order conditions, this will become

$$-d[\text{Substrate}]/dt = k_{\text{obs}}[\text{Substrate}],$$

where  $k_{\text{obs}} = k_1$ .

A plot of  $k_{\text{obs}}$  versus ligand concentration for this system

would be linear with zero slope and an intercept of  $k_1$ .

The second reaction type was characterized by the rate law

$$-d[\text{Substrate}] / dt = k_2[L'][\text{Substrate}].$$

This expression, under pseudo first order conditions, will reduce to

$$-d[\text{Substrate}] / dt = k_{\text{obs}}[\text{Substrate}],$$

with  $k_{\text{obs}} = k_2[L']$ .

A plot of  $k_{\text{obs}}$  versus ligand concentration for this system would be linear, with a zero intercept and a slope of  $k_2$ .

The general, non-limiting reaction type was characterized by the rate law

$$-d[\text{Substrate}] / dt = k_1[\text{Substrate}] + k_2[\text{Substrate}][L'] .$$

Under pseudo first order reaction conditions, this expression would also reduce to

$$-d[\text{Substrate}] / dt = k_{\text{obs}}[\text{Substrate}] ,$$

where  $k_{\text{obs}} = k_1 + k_2[L']$ .

A plot of  $k_{\text{obs}}$  versus ligand concentration for this system would be linear with a slope of  $k_2$  and an intercept of  $k_1$ . Non-linear behavior of a plot of  $k_{\text{obs}}$  versus  $[L']$  is indicative of a more complex mechanism than those discussed above.

## The Problem

As the study of bonding in octahedral metal carbonyl complexes shifted from almost exclusive consideration of infrared spectral data to kinetic and mechanistic investigations, one topic of interest became the substitution reactions of (bidentate) $M(CO)_4$  complexes with Lewis bases. These reactions had the option of proceeding via replacement of the bidentate ligand to yield cis or trans  $M(CO)_4L'_2$  compounds or by substitution of a carbonyl group to form cis or trans (bidentate) $M(CO)_3L'$  complexes. In the majority of cases, the mode of reaction has been found to depend primarily upon the steric and electronic nature of the bidentate ligand and to be essentially independent of the identity of  $L'$ ,<sup>35,36</sup>.

Angelici and Graham<sup>37-40</sup> investigated the kinetics of the reactions of 2,2'-dipyridyl (dipy), o-phenanthroline (phen), various substituted phenanthrolines, and 1,2-diamino-2-methylpropane (dmp) complexes of Cr, Mo, and W with various phosphites to yield the carbonyl dissociation products. The chromium derivatives reacted according to a first order rate law involving rate determining loss of a carbonyl,

$$\text{rate} = k[(\text{bidentate})\text{Cr}(\text{CO})_4],$$

while the molybdenum and tungsten complexes were found to obey a mixed order rate law,

$$\text{rate} = k_1 [(\text{bidentate})\text{M}(\text{CO})_4] + k_2 [(\text{bidentate})\text{M}(\text{CO})_4] [\text{L}']$$

indicative of a combination of mechanisms of the types illustrated in Figures 6 and 7. The lack of a second order term in the case of the chromium complexes was attributed to steric factors which would prevent the formation of a seven-coordinate intermediate. However, the labilization of carbon monoxide observed in these systems, as indicated by the first order term, was inexplicable in terms of the then accepted pi bonding arguments. Accordingly, it was deemed necessary to investigate similar reactions in complexes coordinating through a different donor atom, since dipy, phen, and dmp all coordinate through nitrogen.

Therefore, Faber and Dobson<sup>41</sup> investigated the kinetics of the phosphorus bidentate systems  $(\text{diphos})\text{Cr}(\text{CO})_4$  and  $(\text{diphos})\text{Mo}(\text{CO})_4$  ( $\text{diphos} = (\text{C}_6\text{H}_5)_2\text{PCH}_2\text{CH}_2\text{P}(\text{C}_6\text{H}_5)_2$ ) with Lewis bases to yield the carbonyl substitution products and the reaction of  $(\text{dpae})\text{Cr}(\text{CO})_4$  ( $\text{dpae} = 1,2\text{-bis-diphenylarsenoethane}$ ), which coordinates through arsenic, with triethyl phosphite to yield the bidentate substitution product<sup>42</sup>. An investigation of the substitution reactions of the sulfur bidentate compounds  $(\text{DTH})\text{Cr}(\text{CO})_4$  and  $(\text{DTH})\text{Mo}(\text{CO})_4$  ( $\text{DTH} = 2,5\text{-dithiahexane}$ ) with phosphites<sup>43</sup> showed the reaction products to be solely cis and trans  $\text{M}(\text{CO})_4(\text{phosphite})_2$  and the rate law to be

$$\text{rate} = k[(\text{DTH})\text{M}(\text{CO})_4][\text{phosphite}].$$

This rate law could be explained by either of the two mechanisms shown in Figures 9 and 10.

In the case of mechanism I, a simple direct attack of L' at the metal atom to yield a seven-coordinate activated complex or intermediate, the rate law is a simple second order expression,

$$\text{rate} = k[(\text{bidentate})\text{M}(\text{CO})_4][\text{L}'].$$

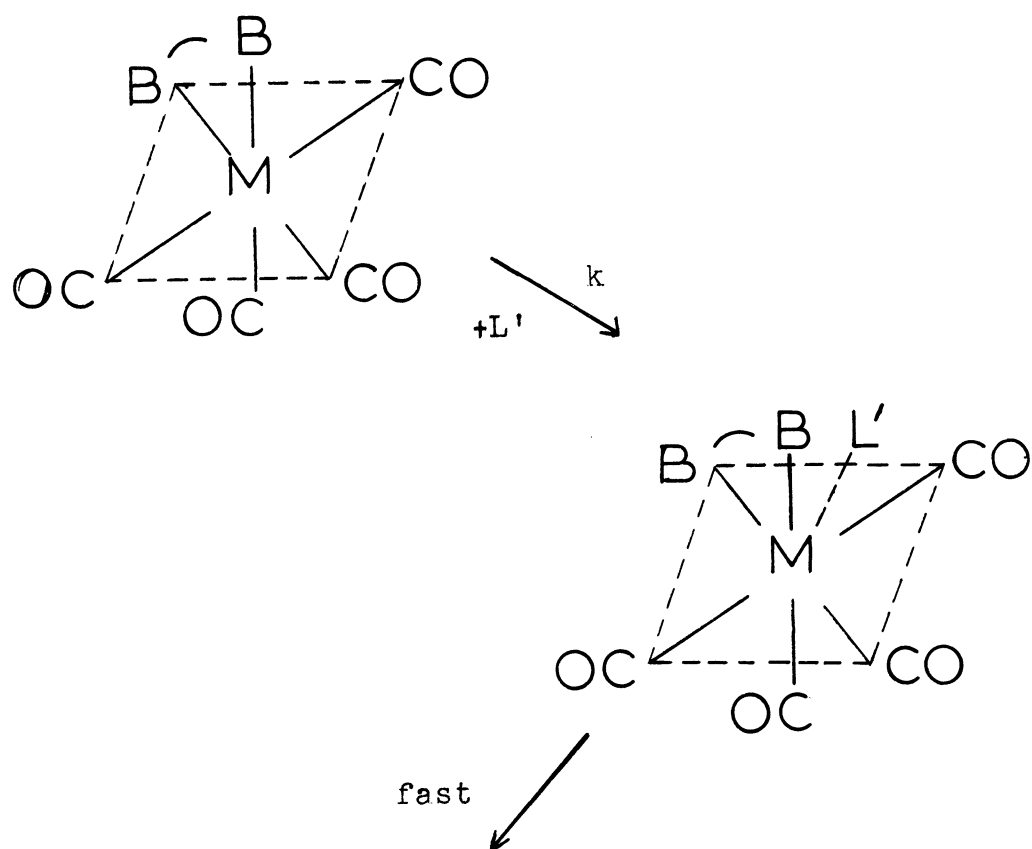
Mechanism II, a reversible dissociation of one end of the bidentate ligand followed by attack of L' upon the resulting five-coordinate intermediate, will yield the following rate law (steady state approximation)<sup>44</sup>:

$$\text{rate} = \frac{k_1 k_2 [(\text{bidentate})\text{M}(\text{CO})_4][\text{L}']}{(k_{-1} + k_2[\text{L}'])}.$$

If  $k_{-1} \gg k_2[\text{L}']$ , this expression will reduce to

$$\text{rate} = \left( \frac{k_1 k_2}{k_{-1}} \right) [(\text{bidentate})\text{M}(\text{CO})_4][\text{L}'],$$

an expression which is indistinguishable from that for the simple direct attack mechanism above. But, these two paths may be separated on the basis of activation parameters, since the direct attack mechanism should exhibit a markedly unfavorable entropy of activation due to the change in coordination number, while the entropy of activation for the



## PRODUCTS

Fig. 9--Mechanism I: Direct attack by  $L'$  on metal



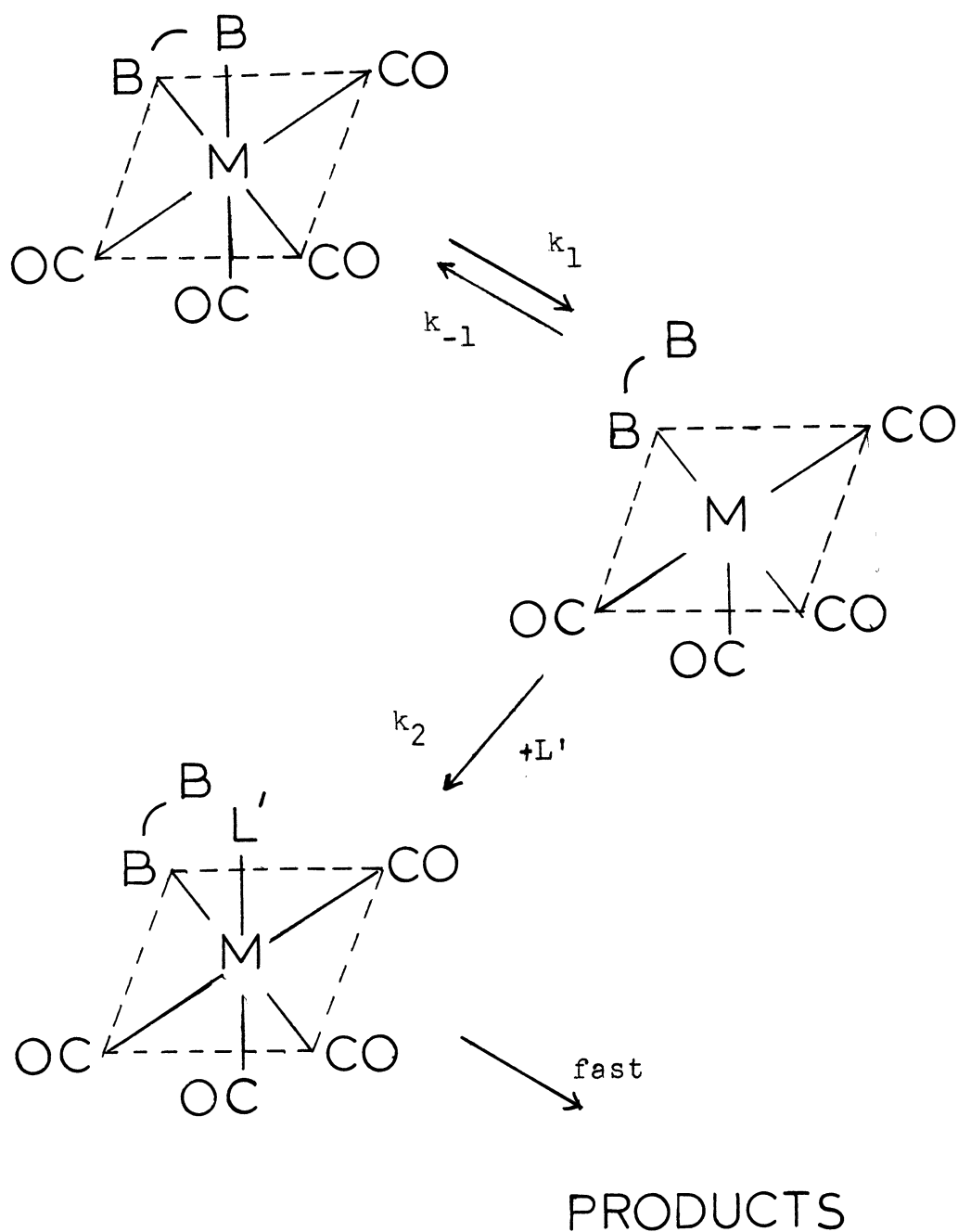


Fig. 10--Mechanism II: Reversible dissociation of one end of bidentate ligand followed by attack of  $L'$ .

reversible dissociation mechanism should be small. On this basis, it was postulated that the Cr complex reacted via mechanism II and the Mo complex reacted by mechanism I.

A search was undertaken for a system in which differentiation of mechanisms I and II would be simpler and more pronounced, i.e. a system in which  $k_{-1}$  would not be much greater in magnitude than  $k_2[L']$ . Such a system was found in the reaction of  $(tmen)Cr(CO)_4$  ( $tmen = N,N,N',N'$ -tetramethylethylenediamine) with phosphites<sup>45</sup>. For this reaction, the term  $k_2[L']$  is not negligible compared to  $k_{-1}$  and a mixed order reaction is observed, i.e. a plot of  $k_{obs}$  versus  $[L']$  is non-linear. This is to be expected since, under pseudo first order conditions, for mechanism II the  $k_{obs}$  term may be expressed by

$$k_{obs} = (k_1 k_2 L') / (k_{-1} + k_2[L']).$$

Therefore, a plot of  $k_{obs}$  vs.  $[L']$  for a reaction following this pathway should exhibit second order behavior at low concentrations of  $L'$  and first order behavior at higher  $L'$  concentrations. However, this expression for  $k_{obs}$  may be rearranged to yield

$$1 / k_{obs} = 1 / k_1 + k_{-1} / (k_1 k_2 [L']).$$

This expression will yield a linear plot of  $1/k_{obs}$  versus  $1/[L']$  with an intercept of  $1/k_1$  and a slope of  $k_{-1}/k_1 k_2$ .

Such a plot was indeed obtained for the substitution reactions of  $(tmen)Cr(CO)_4$ , indicating mechanism II to be the preferred pathway for this complex.

Dobson<sup>46</sup> further investigated reactions of this type by studying the reactions of  $(DTO)M(CO)_4$  (DTO = 2,2,7,7-tetramethyl-3,6-dithiaoctane and M = Cr, Mo, and W) with phosphites. These compounds are analogous to the DTH systems with the exception of bulky t-butyl groups on the sulfur donor atoms replacing the methyl groups of DTH. It was hoped that these steric effects would inhibit  $k_{-1}$  and allow a choice between mechanisms I and II. This hypothesis proved correct and curving plots of  $k_{obs}$  versus  $[L']$  and linear plots of  $1/k_{obs}$  versus  $1/[L']$  were noted. Therefore, mechanism II was proposed as the operational mechanism in this system also.

This line of investigation was extended by Faber and Dobson<sup>47</sup> to include the 6-membered chelate ring system  $(DTN)M(CO)_4$  (DTN = 2,2,8,8-tetramethyl-3,7-dithianonane), which differs from the DTO system by the inclusion of an additional  $CH_2$  in the chelate backbone. Once again, rate behavior indicative of mechanism II was observed. However, when this reaction was run with different phosphites, the values of  $k_1$  obtained from the intercepts of the  $1/k_{obs}$  vs.  $1/[L']$  plots differed. Since mechanism II requires the reversible dissociation of one end of the bidentate ligand, governed by  $k_1$ , to be independent of  $L'$ , no change

in the value of  $k_1$  should be observed with the variation of phosphites. To explain this inconsistency, a ligand-substrate interaction of the type illustrated in Figure 11, which would aid in the dissociation of one end of the bidentate ligand, was postulated<sup>47</sup>.

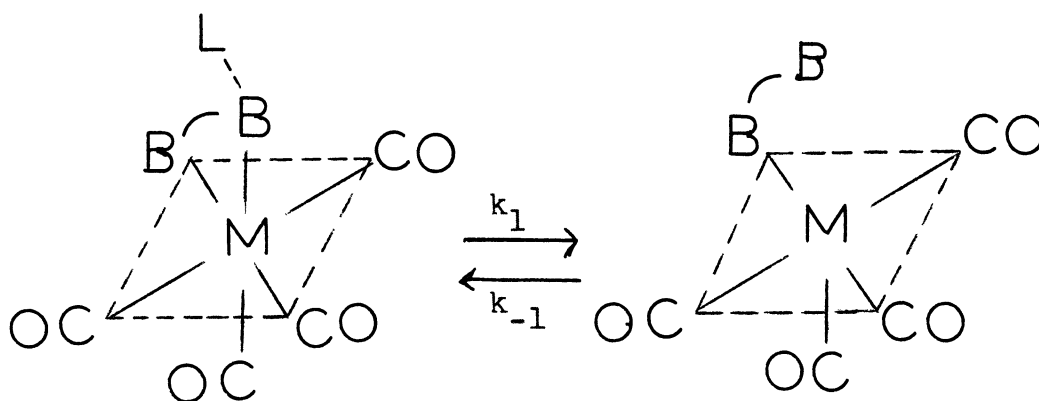


Fig. 11--Substrate-ligand interaction

However, efforts to obtain supportive evidence for such an interaction were unsuccessful. Therefore, it was deemed desirable to reinvestigate these systems in much greater detail to obtain a better understanding of these mechanisms.

## CHAPTER II

### EXPERIMENTAL

#### Preparation and Purification of Materials

##### General

Infrared spectra for identification purposes were run on a Perkin-Elmer 621 grating spectrophotometer calibrated against a band of water vapor at  $1869.4 \text{ cm}^{-1}$ <sup>48</sup>. Ultra-violet and visible spectra were obtained on a Cary 14 recording spectrophotometer. Proton NMR spectra were obtained on a JEOL JNM-PS-100 High Resolution NMR spectrophotometer. Chemical analyses were obtained from Galbraith Laboratories, Inc., Knoxville, Tenn. All samples for kinetic experiments were weighed on a Mettler balance, type H16, to 0.0001 g. Kinetic runs in the visible region were monitored on a Beckman model DU-2 direct reading spectrophotometer. Kinetic data were analyzed by a least squares treatment on an IBM 360, model 50 computer at the NTSU Computing Center. Limits of error are given in parenthesis and are one standard deviation.

The purity of all metal complexes was ascertained by examination of the infrared spectra, since the carbonyl stretching spectrum in the region  $1700\text{-}2200 \text{ cm}^{-1}$  may be used to detect the presence of other complexes of differing

degrees of substitution and because these complexes decompose upon heating and do not give sharp melting points. DTO and DTN ligands were checked for purity by examination of their NMR spectra<sup>46,47</sup>. Liquid phosphorus ligands were checked for purity by GLC on a Finnigan Corporation model 3200 gas chromatograph / mass spectrometer with a model 6000 data system utilizing a Zeta Research, Inc. model 130 Zeta plotter, series 100, and a Texas Instruments, Inc. Silent 700 electronic terminal for data output. The column used was a 5 ft x 2 mm id. glass U column with Silicone OV-1 packing on Chromosorb W-HP, 80-100 mesh. A sample chromatogram and peak analysis are shown in Figures 12 and 13 for purified triisopropyl phosphite.

#### Sulfur Ligands

DTO.--DTO was obtained from Phillips Petroleum Co., Special Products Division, Bartlesville, Okla., and was found to be suitable for use without further purification.

DTN.--DTN was prepared by the method of Fedorov and Savel'eva<sup>49</sup>. One mole of sodium (23 g) was allowed to react with 500 ml of absolute ethanol in a one liter 3-necked round-bottomed flask fitted with a reflux condenser, nitrogen inlet, and magnetic stirrer. After the sodium had completely reacted, one mole (90 g) of t-butyl mercaptan was added dropwise to the solution. After the reaction had

TRIIISOPROPYL PHOSPHITE

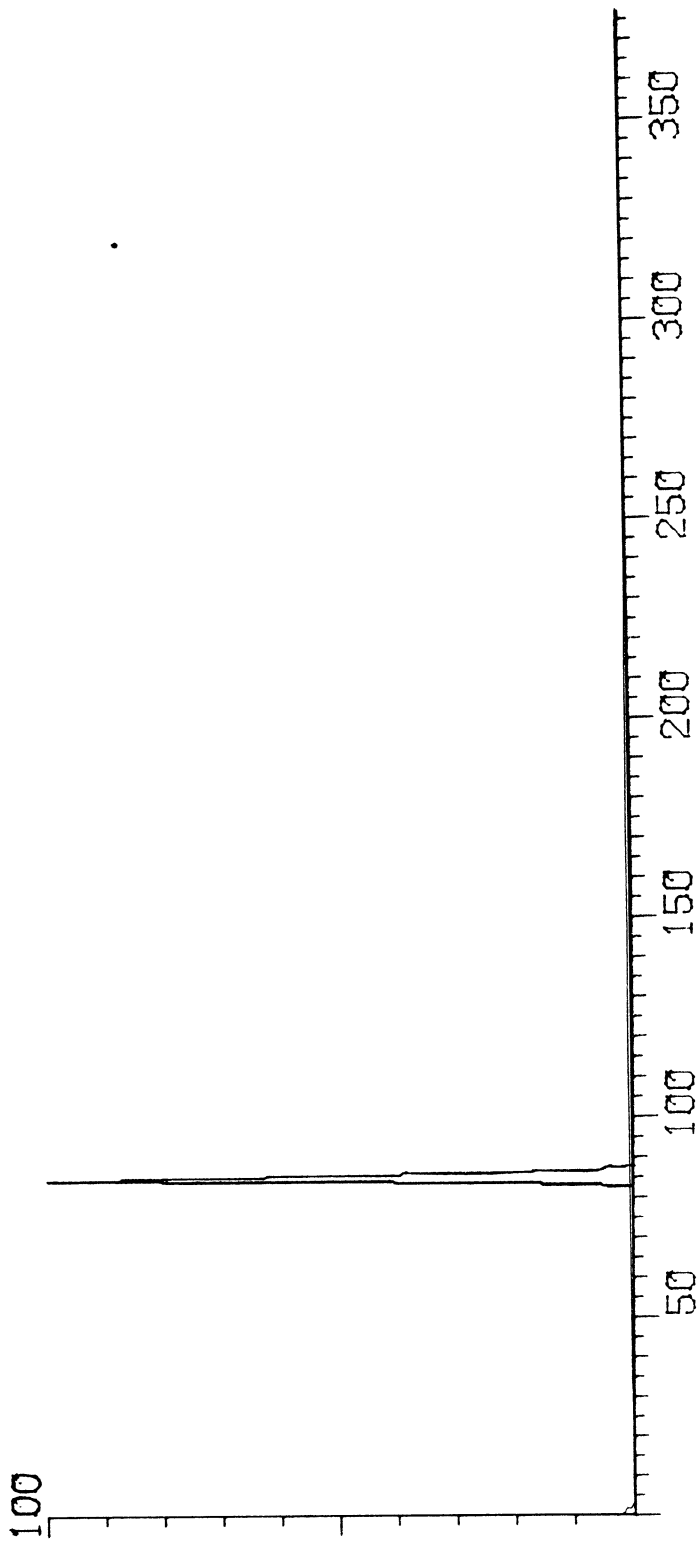


Fig. 12--Gas chromatogram of purified triisopropyl phosphite.

TRIIISOPROPYL PHOSPHITE

# 85

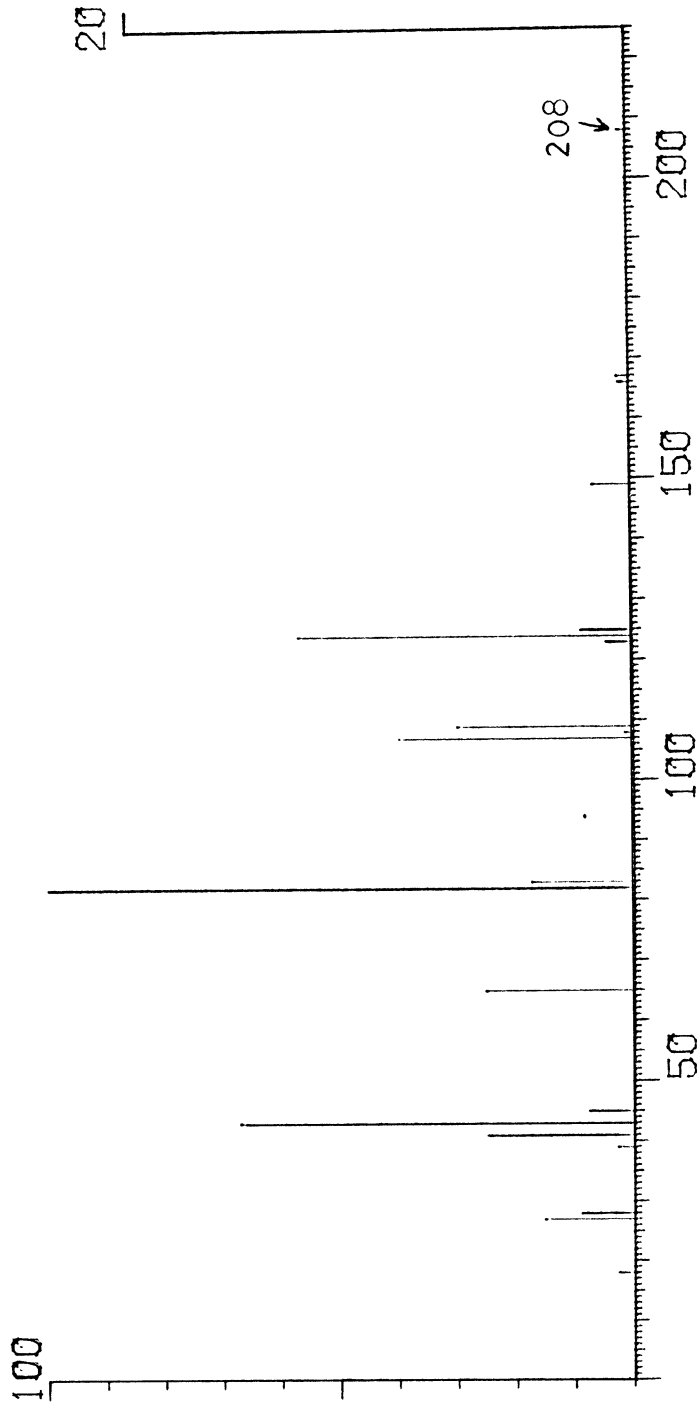


Fig. 13--Mass spectrum of purified triisopropyl phosphite.



stirred for two hours, 0.5 mole (101 g) of 1,3-dibromopropane was added dropwise, with ice cooling, and the mixture was stirred an additional hour at room temperature. The precipitated NaBr was then removed by filtration and the solvent was removed under vacuum. The DTN was then isolated by distillation under nitrogen at reduced pressure.

### Phosphorus Ligands

Trialkyl phosphites are generally considered to be very stable compounds and are frequently used "as obtained" or with minimal precautions as to purity for kinetic investigations. However, unless severe measures to ensure purity were observed, kinetic data for the systems studied in this investigation were not reproducible.

Pidcock et al.<sup>50</sup> have reported catalysis of substitution reactions resulting from contamination of trimethyl phosphite by phosphate. However, phosphates have boiling points markedly greater than those of the corresponding phosphites, and the impurities detected in this study were low-boiling species. These impurities possibly corresponded to adsorbed water and/or hydrolysis products, although they were not definitely identified. The effect of these impurities on reaction rates was inhibition. These contaminants seemed to be relatively inert, and the observed inhibition could be due to incorrect ligand concentrations resulting from inclusion of weight of impurities in the

sample weights used for calculation of ligand concentrations. The observed rate law would not be altered, but plots of  $k_{\text{obs}}$  versus ligand concentration would be affected, since the ligand concentrations reported would not be accurate.

All kinetic data reported in this investigation were obtained using phosphorus ligands which had been rigorously purified, using an appropriate method, and shown to be pure by GLC analysis. All liquid phosphorus ligands were stored under nitrogen in foil-wrapped flasks at atmospheric pressure, with the exception of tri-n-butylphosphine, which was kept under vacuum, and all kinetic runs involving these ligands were completed within one week of distillation, with the exception of tri-n-butylphosphine, which was only used within 48 hours of distillation. Results reported were shown to be reproducible with different batches of ligand.

Trimethyl phosphite.-- $\text{P}(\text{OCH}_3)_3$  was purchased from Aldrich Chemical Co., Milwaukee, Wis. Some older samples were shown by GLC to be only about 60 per cent pure. Trimethyl phosphite was purified by fractional distillation at 111-112 degrees C at atmospheric pressure over sodium and under nitrogen and shown to be pure by GLC prior to use.

Triethyl phosphite.-- $\text{P}(\text{OC}_2\text{H}_5)_3$  was purchased from Aldrich Chemical Co. and purified by fractional distillation

at 155-166 degrees C over sodium and under nitrogen at atmospheric pressure. The compound was then shown to be pure by GLC.

Triisopropyl phosphite.-- $\text{P}(\text{OCH}(\text{CH}_3)_2)_3$  was purchased from Aldrich Chemical Co. and purified by fractional distillation at 60-62 degrees C and 10 torr pressure over sodium. The ligand was then checked for purity by GLC.

Triphenyl phosphite.-- $\text{P}(\text{OC}_6\text{H}_5)_3$  was purchased from both Aldrich and Eastman Organic Chemical Co.'s and no significant difference in quality was noted. The ligand, as obtained, had a very noticeable odor of phenol, and this impurity was identified by GLC. The ligand was first distilled over a small amount of sodium at about 0.1 torr and 160 degrees C to remove as much phenol as possible. (Excess sodium appeared to result in decomposition of triphenyl phosphite under these conditions). The distillate was then redistilled without sodium at this temperature and pressure until no phenol was observed crystallized in the condenser and no odor of phenol could be detected. The ligand was then shown to be pure by GLC.

Tri-n-Butylphosphine.--  $\text{P}(\text{CH}_2\text{CH}_2\text{CH}_2\text{CH}_3)_3$  was purchased from Aldrich Chemical Co. and purified by distillation at 150 degrees C and 50 torr pressure over sodium. Although the ligand was then shown to be pure by GLC analysis, kinetic

results were not reproducible after about two days. Therefore, this ligand was stored under high vacuum and used only immediately after purification. Care was taken to reproduce results with different batches of ligand.

Triphenylphosphine.-- $P(C_6H_5)_3$  was purchased from Cincinnati Milacron, Reading, Ohio, and was recrystallized from absolute ethanol four times and dried under high vacuum. To obtain reproducible kinetic data, it was necessary to redry the ligand immediately prior to use.

"Constrained" phosphite.--4-methyl-2,6,7-trioxa-1-phosphabicyclo[2.2.2]octane,  $P(OCH_2)_3CCH_3$ , was prepared by the method of Verkade<sup>51</sup>. One mole of 1,1,1-tris(hydroxymethyl)ethane (120 g) and one mole of trimethyl phosphite (124 g) were combined and heated at reflux for 30 minutes. Methanol was then removed by distillation at atmospheric pressure. Unreacted trimethyl phosphite was removed by distillation under nitrogen at reduced pressure. The product was then purified by vacuum sublimation at 50 deg. C and 0.2 torr pressure. This sublimation was repeated four times before the compound was considered suitable for use. No problems in reproducibility of data were encountered with this ligand.

#### Complexes

(DTO)W(CO)<sub>4</sub>.--(DTO)W(CO)<sub>4</sub> was prepared by the method of

Dobson<sup>46</sup>. Tungsten hexacarbonyl (7.25 g) and 30 ml of DTO were heated at reflux in xylene for four hours under nitrogen. This solution was then cooled and filtered and the volume reduced to approximately one-fourth under reduced pressure. An excess of petroleum ether was then added to the solution, which was then placed in a freezer for 24 hours. The yellow crystals which precipitated from the solution were collected by suction filtration and recrystallized from toluene-hexane. Carbonyl stretching spectrum ( $\text{CHCl}_3$ ): 2019 (m), 1906 (vs), 1889 (vs), 1868 (s)  $\text{cm}^{-1}$ . (vs = very strong, s = strong, m = medium, w = weak, sh = shoulder)

$(\text{DTN})\text{W}(\text{CO})_4$ .--- $(\text{DTN})\text{W}(\text{CO})_4$  was prepared by the method of Dobson and Faber<sup>47</sup>. Tungsten hexacarbonyl (3 g) and DTN (2 g) were dissolved in 350 ml of hexane and irradiated with a Hanovia 450-W medium pressure UV lamp in an immersion reactor for one hour under nitrogen. The reaction solution was then cooled and filtered and placed in a freezer for 24 hours. The yellow product which precipitated from the solution was collected by suction filtration and recrystallized from toluene-hexane. Carbonyl stretching spectrum ( $\text{CHCl}_3$ ): 2019 (w), 1902 (vs), 1883 (s), 1848 (s)  $\text{cm}^{-1}$ .

$(\text{DTN})\text{W}(\text{CO})_4\text{P}(\text{OCH}_2)_3\text{CCH}_3$ .--- $(\text{DTN})\text{W}(\text{CO})_4\text{P}(\text{OCH}_2)_3\text{CCH}_3$  was detected as an intermediate in the reaction of  $(\text{DTN})\text{W}(\text{CO})_4$  with the constrained phosphite and was isolated by the following procedure: 0.5 g ( $1 \times 10^{-3}$  mole) of  $(\text{DTN})\text{W}(\text{CO})_4$

and 3 g ( $2 \times 10^{-2}$  mole) of  $\text{P}(\text{OCH}_2)_3\text{CCH}_3$  were dissolved in 150 ml of xylene in a 250 ml round-bottomed flask fitted with a stopcock and a rubber septum of the type used in kinetic flasks. The solution was kept under nitrogen and the flask was placed in a constant temperature bath at 66.5 degrees C. Samples were withdrawn periodically and monitored on the IR spectrophotometer. When the concentration of intermediate had reached a maximum (about 1500 seconds), the reaction was quenched by removing the flask from the bath and placing it in a freezer. After 24 hours, the solution was filtered and the solvent was almost totally removed under vacuum and approximately 50 ml of hexane was added to the flask, which was replaced in the freezer for an additional three hours. The solution was then filtered under nitrogen to remove precipitated  $\text{W}(\text{CO})_4(\text{P}(\text{OCH}_2)_3\text{CCH}_3)_2$  and unreacted starting materials. This filtrate was then taken to dryness under a stream of nitrogen to yield a pale yellow residue, consisting of  $(\text{DTN})\text{W}(\text{CO})_4\text{P}(\text{OCH}_2)_3\text{CCH}_3$  and unreacted  $\text{P}(\text{OCH}_2)_3\text{CCH}_3$ . This powder was then recrystallized from hexane three times to remove excess phosphite. The final yield of pure material was 8 mg. Carbonyl stretching spectrum ( $\text{CHCl}_3$ ): 2032 (w), 1921 (vs), 1905 (vs), 1882 (s)  $\text{cm}^{-1}$ . Anal. Calcd. for  $\text{C}_{20}\text{H}_{33}\text{O}_7\text{PS}_2\text{W}$ : C, 36.15; H, 5.01. Found: C, 35.81; H, 5.11.

The spectrum of  $(\text{DTN})\text{W}(\text{CO})_4\text{P}(\text{OCH}_2)_3\text{CCH}_3$  is intermediate to that of the starting material and final product:

(DTN)W(CO)<sub>4</sub> in CHCl<sub>3</sub><sup>47</sup>,

2019 (w), 1902 (vs), 1883 (s), 1848 (s) cm<sup>-1</sup>;

(DTN)W(CO)<sub>4</sub>P(OCH<sub>2</sub>)<sub>3</sub>CCH<sub>3</sub> in CHCl<sub>3</sub>,

2032 (w), 1921 (vs), 1905 (vs), 1882 (s) cm<sup>-1</sup>;

cis-W(CO)<sub>4</sub>(P(OCH<sub>2</sub>)<sub>3</sub>CCH<sub>3</sub>)<sub>2</sub> in CH<sub>2</sub>Cl<sub>2</sub><sup>52</sup>,

2045, (m), 1950 (vs), 1924 (sh) cm<sup>-1</sup>.

The spectrum may also be compared with that of (SPE)W(CO)<sub>4</sub> in CHCl<sub>3</sub><sup>53</sup> (SPE = 1-diphenylphosphino-2-(methylthio)ethane):

2023 (m), 1914 (s), 1897 (s), 1871 (ms) cm<sup>-1</sup>.

The similarities among these spectra indicate that the species isolated in this investigation is cis-(DTN)W(CO)<sub>4</sub>-P(OCH<sub>2</sub>)<sub>3</sub>CCH<sub>3</sub>, with the DTN ligand attached to the metal through only one sulfur donor atom.

### Solvents

Technical grade xylene was obtained from Scientific Products, Inc. and purified by fractional distillation over sodium (138-140 degrees C). The solvent was stored in an amber bottle under nitrogen prior to use.

### Determination of Rates

#### General

Reaction rates were determined by monitoring the decay of substrate absorption bands in the visible or infrared region of the spectrum, a procedure to which substituted metal carbonyl complexes are exceptionally well suited<sup>54</sup>.

All bands monitored for kinetic purposes were found to obey Beer's Law over the concentration range used. This was done by preparing a series of dilutions of the complex in the solvent used for kinetic studies, over an absorbance range of about 1.0 to 0.05 absorbance units, and observing a linear plot of absorbance versus dilution.

Kinetic studies were carried out in 100 ml volumetric flasks fitted with a stopcock and rubber septum, as shown in Figure 14, which permitted sampling without contamination of the reaction solution by air. All reactions were studied under an atmosphere of nitrogen by purging the flask with nitrogen prior to the run and adding reactants to the flask under a stream of nitrogen. The substrate was placed in the flask and a 50 ml solution of temperature equilibrated solvent-ligand solution of known concentration was added. Each ligand solution was individually prepared by weighing a separate sample of purified ligand, and these solutions were used immediately upon equilibration to the proper temperature (usually a maximum of fifteen minutes). After thorough shaking to ensure complete dissolution of the substrate, the reaction solution was placed in a constant temperature bath and allowed to reach thermal equilibrium (about five minutes). Reactions requiring temperatures higher than 80 degrees C were carried out in an oil bath; lower temperatures were achieved with a water bath. The Haake model R21 constant temperature circulators used maintained reaction



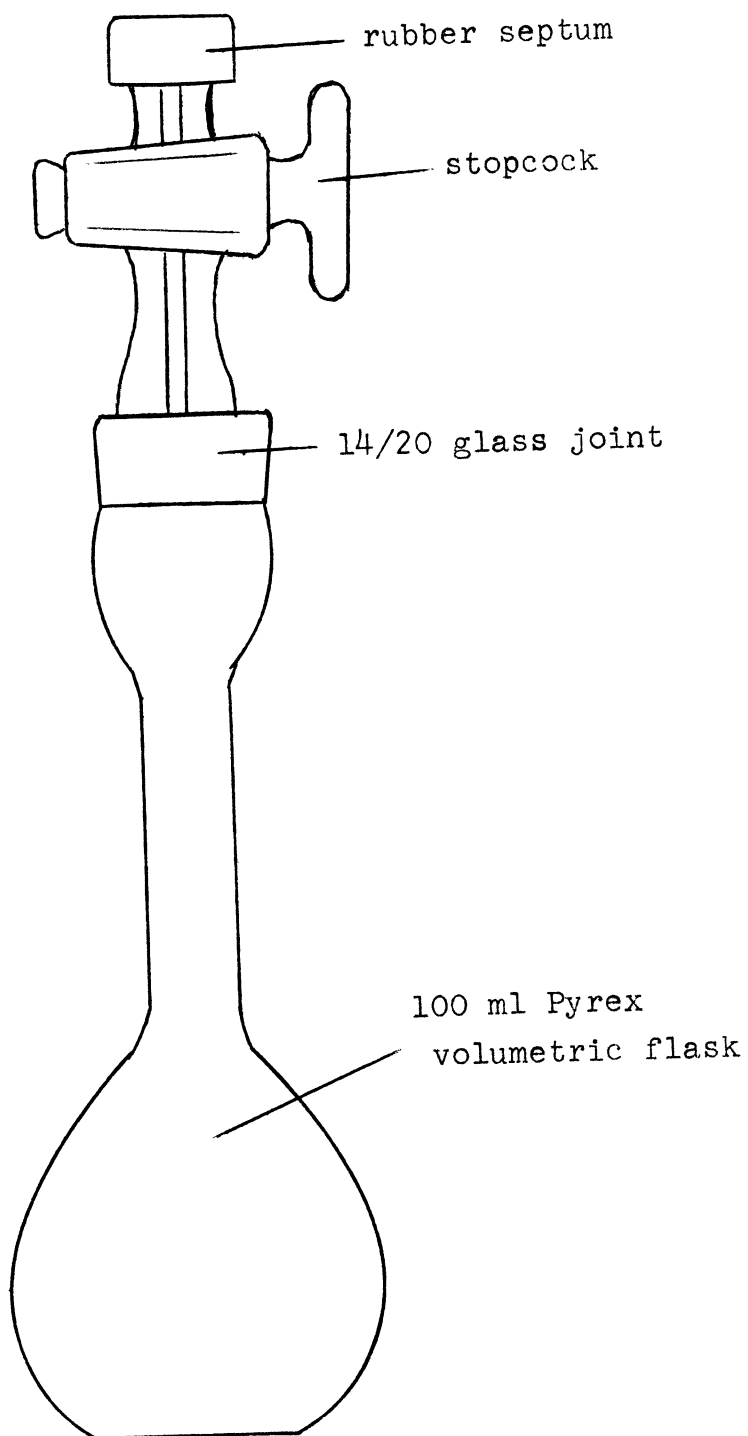


Fig. 14--Reaction flask used for kinetic studies.

temperatures to within 0.05 degree C. Small volumes of nitrogen were injected into the reaction vessel before samples were withdrawn using a glass syringe and a ten inch needle. Samples were withdrawn at timed intervals and immediately analyzed on the appropriate spectrophotometer.

Pseudo first order reaction conditions were obtained through use of ligand concentrations in 20-fold or greater excess of substrate concentrations. Substrate concentrations in the range of  $10^{-4}$  molar were used, since this concentration range gave an initial absorbance reading of approximately 1.0 at the wavelengths monitored in the visible region. Reactions were followed to at least two half lives (75 per cent completion). Products were identified by examination of the carbonyl stretching spectrum of the completed reaction solution.

#### Specific Conditions for Kinetic Reactions

Reactions of  $(\text{DTO})\text{W}(\text{CO})_4$  and  $(\text{DTN})\text{W}(\text{CO})_4$  with phosphites and phosphines were monitored on a Beckman DU-2 spectrophotometer in a 1 cm pyrex cell at 430 and 425 nm respectively. In the case of the reaction of  $(\text{DTN})\text{W}(\text{CO})_4$  with constrained phosphite, complex consecutive reactions were observed corresponding to the reaction of  $(\text{DTN})\text{W}(\text{CO})_4$  and the simultaneous decomposition of  $(\text{DTN})\text{W}(\text{CO})_4\text{P}(\text{OCH}_2)_3\text{CCH}_3$ . This complex behavior was caused by the presence of the two yellow species, both absorbing significantly at 425 nm, as

can be seen from the visible spectra in Figure 15.

In the case of reactions of  $(\text{DTO})\text{W}(\text{CO})_4$  and  $(\text{DTN})\text{W}(\text{CO})_4$  with trimethyl, triethyl, triisopropyl, and triphenyl phosphite, and for the reaction of  $(\text{DTO})\text{W}(\text{CO})_4$  with the constrained phosphite, a solvent-ligand blank differing from  $A_\infty$  by less than 0.01 absorbance units was employed and plots of  $\ln(A_t - A_{bl})$  versus time were linear to two or more half lives.

In the case of the reactions of both substrates with tri-n-butylphosphine and triphenylphosphine, a colored product was formed and plots of  $\ln(A_t - A_{bl})$  versus time were nonlinear. These reactions were monitored until a constant  $A_\infty$  was observed (six or more half lives); plots of  $\ln(A_t - A_\infty)$  vs. time were linear to at least 75 per cent completion.

The reaction of  $(\text{DTN})\text{W}(\text{CO})_4$  with the constrained phosphite was a complex consecutive reaction consisting of rapid initial formation of a colored intermediate, which slowly reacted to form colorless products. Plots of  $\ln(A_t - A_{bl})$  vs. time monitored at 425 nm were nonlinear during the course of the fast reaction, but became linear during the slow reaction, allowing calculation of the slower rate. The rapid reaction was monitored at 445 nm and linear plots of  $\ln(A_t - A_{bl})$  vs. time were obtained to over one half life before nonlinear behavior was observed, as shown in Figure 16. The rate of the fast reaction was calculated

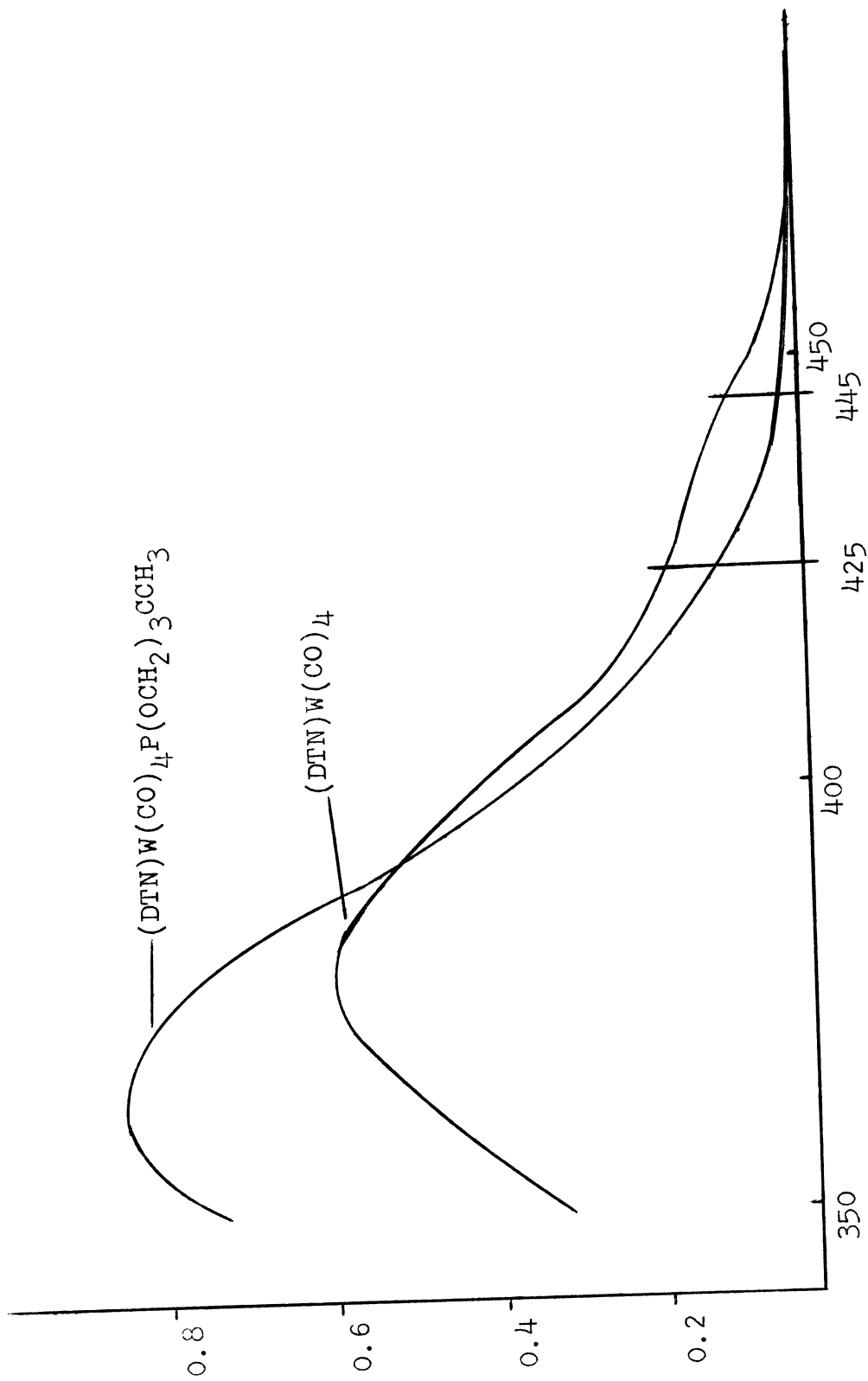


Fig. 15--Visible spectra of  $(\text{DTN})\text{W}(\text{CO})_4$  and  $(\text{DTN})\text{W}(\text{CO})_4\text{P}(\text{OCH}_2)_3\text{CCH}_3$   
 (Ordinate = absorbance, Abscissa = wavelength in nm)

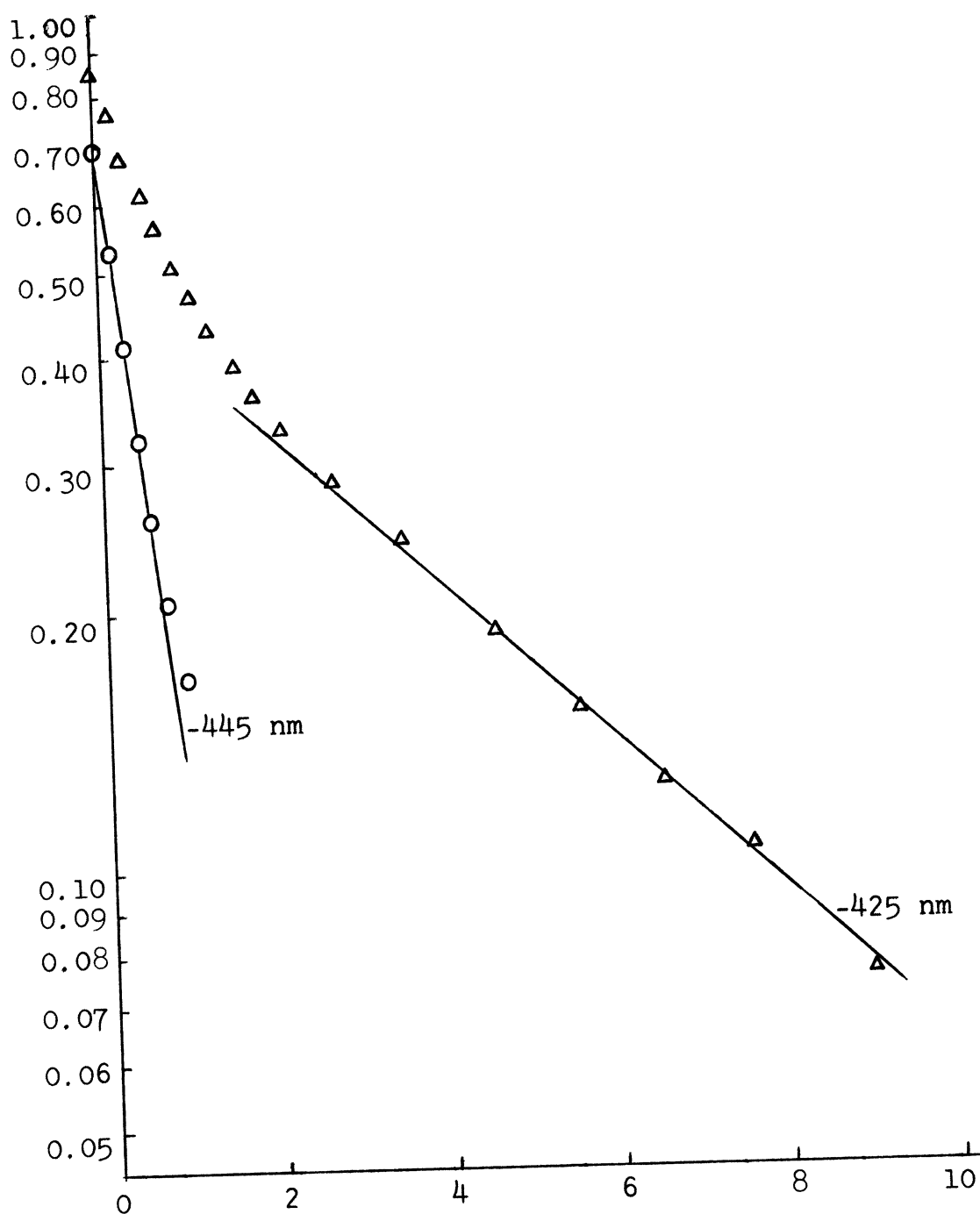


Fig. 16--Plot of time vs. absorbance for reaction of  $(DTN)W(CO)_4$  with  $P(OCH_2)_3CCH_3$  in xylene at  $66.5^\circ C$  monitored at two different wavelengths. (Ordinate = absorbance, Abscissa = time in sec x  $10^{-3}$ ).

from the initial linear portion of the plot.

The final products of all kinetic reactions studied were the cis and some trans disubstituted products, as determined from the infrared spectra of the carbonyl stretching region of the reaction solution after the reaction was complete. No evidence of carbonyl substitution products was observed in any of these systems.

## CHAPTER III

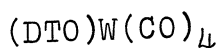
### RESULTS

The rates of all reactions studied were found to be dependent upon both the concentrations of substrate and substituting ligand. The substrate dependence was factored out through the use of pseudo first order reaction conditions as described in Chapter I:

$$\begin{aligned}\text{rate} &= k_{\text{true}}[\text{L}'][\text{Substrate}] \\ &= k_{\text{obs}}[\text{Substrate}]\end{aligned}$$

$$k_{\text{obs}} = k_{\text{true}}[\text{L}'],$$

and the rate laws were deduced from the behavior of the plots of  $k_{\text{obs}}$  vs. ligand concentration and  $1/k_{\text{obs}}$  versus  $1/[\text{L}']$ . Studies of the temperature dependence of reaction rates of  $(\text{DTO})\text{W}(\text{CO})_4$  and  $(\text{DTN})\text{W}(\text{CO})_4$  were made at three different temperatures with triisopropyl phosphite as a representative ligand and activation parameters were calculated. Similar studies of temperature dependence of reaction rates of both substrates were made using tri-n-butylphosphine as a nontypical ligand and activation parameters were calculated for these systems also.



Results of the kinetic studies of the substitution reactions of  $(\text{DTO})\text{W}(\text{CO})_4$  with a series of phosphites and phosphines in xylene at various temperatures are summarized in Table I.

Kinetic studies of the reaction of  $(\text{DTO})\text{W}(\text{CO})_4$  with "typical" ligands trimethyl, triisopropyl, triphenyl, and constrained phosphite and triphenylphosphine at 99.9 degrees C are summarized graphically in Figures 17 and 18 in the form of plots of  $k_{\text{obs}}$  versus ligand concentration and  $1/k_{\text{obs}}$  versus  $1/[\text{L}']$  respectively. From the non-linear behavior of the  $k_{\text{obs}}$  vs. ligand concentration plot and the linear nature of the reciprocal plot, it may be inferred that the active mechanism in these reactions is mechanism II, as illustrated in Figure 10, involving reversible dissociation of one end of the bidentate ligand followed by attack of  $\text{L}'$  upon the five-coordinate intermediate. Values of  $k_1$  and  $k_2/k_{-1}$  were calculated from the intercept and slope of the reciprocal plots as described in Chapter I. These values are summarized in Table II. The  $k_1$  values of these substitution reactions at 99.9°, within one standard deviation, do not differ and may be averaged to give a value of  $23.2 (9) \times 10^{-4} \text{ sec}^{-1}$ . This  $k_1$  value varies by 18.5 per cent and 13.4 per cent respectively from the  $k_1$  values of  $27.5 \times 10^{-4} \text{ sec}^{-1}$  for triethyl phosphite and  $26.3$



TABLE I  
 RATES OF REACTION OF  $(\text{DTO})\text{W}(\text{CO})_4$  WITH  
 PHOSPHORUS LIGANDS IN XYLENE

Ligand	Ligand Conc. moles/liter	Temperature degrees C	$k_{\text{obs}}$ $\times 10^4 \text{ sec.}^{-1}$	
$\text{P}(\text{OCH}_3)_3$	0.155	99.9	3.42 (1)	
	0.183		3.62 (1)	
	0.208		4.25 (1)	
	0.270		5.20 (1)	
	0.347		6.49 (5)	
	0.541		8.67 (4)	
	1.041		13.28 (4)	
$\text{P}(\text{OCH}(\text{CH}_3)_2)_3$	0.491	89.9	1.65 (1)	
	0.566		1.87 (1)	
	0.663		2.10 (1)	
	0.729		2.22 (1)	
	0.849		2.51 (1)	
	1.199		3.35 (2)	
	1.296		3.48 (2)	
	1.472		3.61 (2)	
	0.173		99.9	2.04 (1)
	0.266			2.97 (1)
0.340	3.70 (2)			
0.428	4.39 (2)			

I Continued

	0.512		5.20 (1)
	0.590		5.60 (2)
	0.823		7.31 (3)
	1.215		9.7 (1)
	0.179	109.9	6.06 (4)
	0.197		6.71 (3)
	0.246		7.84 (7)
	0.269		8.40 (1)
	0.312		9.74 (2)
	0.386		11.1 (1)
	0.468		13.09 (6)
	0.590		16.55 (8)
	0.808		19.0 (1)
	1.280		24.7 (1)
	1.702		30.3 (2)
P(OC <sub>6</sub> H <sub>5</sub> ) <sub>3</sub>	0.125	99.9	1.15 (2)
	0.167		1.54 (1)
	0.245		2.21 (2)
	0.303		2.61 (1)
	0.383		3.40 (6)
	0.399		3.53 (2)
	0.432		3.56 (6)
	0.752		6.1 (1)
	1.100		6.8 (2)
	1.798		8.5 (2)

I Continued

$P(C_6H_5)_3$	0.182	99.9	2.75 (5)
	0.243		3.32 (4)
	0.278		4.09 (2)
	0.326		4.33 (4)
	0.392		5.16 (9)
	0.967		9.25 (8)
	$P(OCH_2)_3CCH_3$	0.138	99.9
0.190			6.07 (7)
0.227			6.91 (4)
0.323			8.43 (8)
0.406			9.86 (7)
0.527			12.7 (2)
0.710			12.97 (5)
$P((CH_2)_3CH_3)_3$	0.172	89.9	1.71 (2)
	0.323		2.72 (3)
	0.440		3.31 (1)
	0.729		4.39 (4)
	0.962		5.37 (8)
	1.156		6.25 (4)
	1.394		7.26 (8)
	0.059	99.9	2.88 (2)
	0.085		4.41 (4)
	0.094		4.4 (1)
0.120		4.42 (6)	
0.160		5.1 (1)	

I Continued

0.239		5.26 (9)
0.240		5.6 (1)
0.285		6.2 (1)
0.389		6.61 (5)
0.519		8.45 (6)
0.702		10.0 (1)
0.772		11.7 (2)
1.028		13.7 (3)
1.419		17.4 (3)
2.063		22.7 (4)
0.093	109.9	8.54 (6)
0.129		9.1 (2)
0.184		10.59 (7)
0.250		11.7 (1)
0.335		12.7 (2)
0.501		17.8 (3)
0.903		26.6 (6)

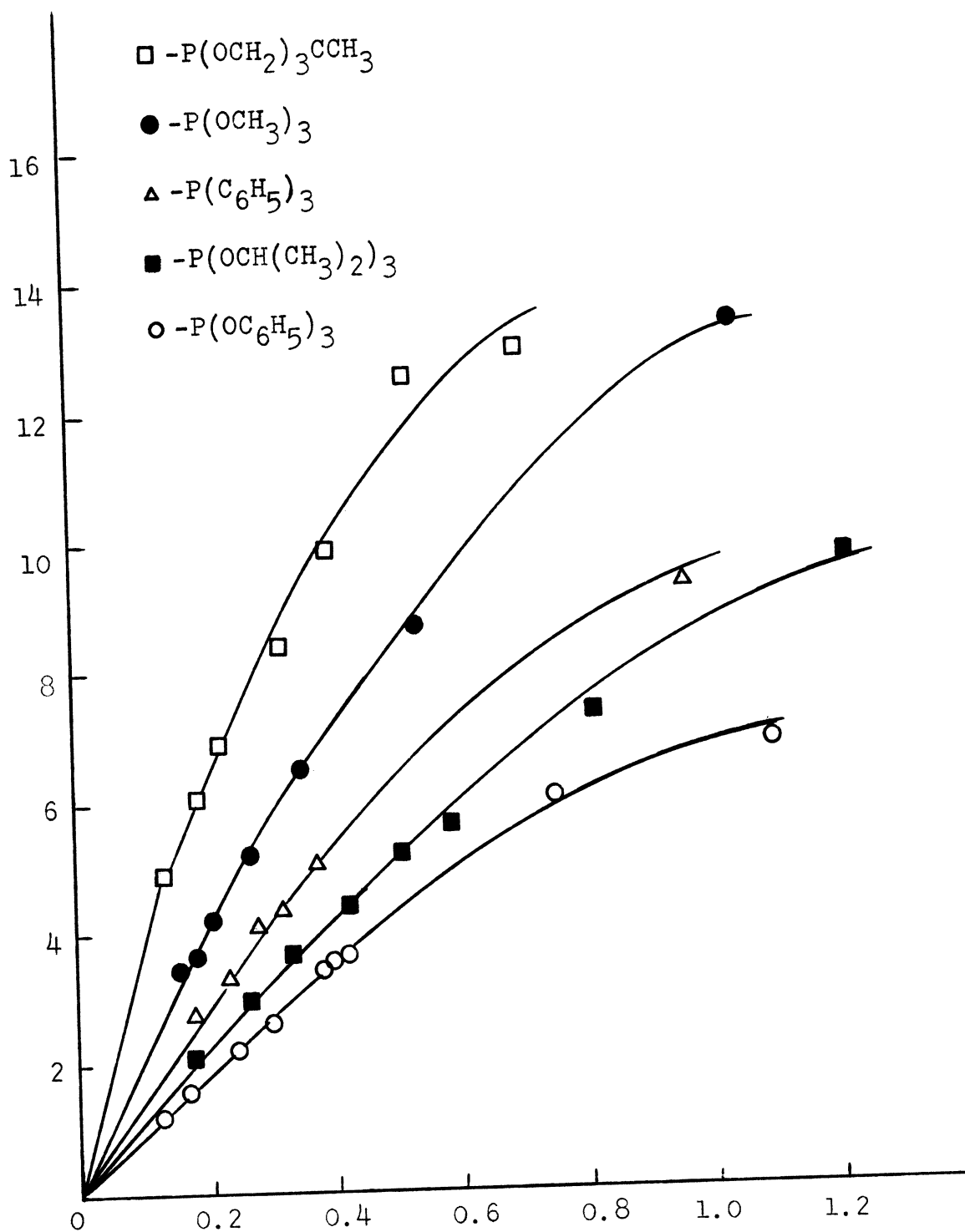


Fig. 17--Plot of  $k_{\text{obs}}$  vs.  $[\text{L}']$  for reaction of various phosphorus ligands with  $(\text{DTOW})(\text{CO})_4$  in xylene at  $99.9^\circ\text{C}$ . (Ordinate =  $k \times 10^4 \text{ sec}^{-1}$ , Abscissa =  $[\text{L}']$  in moles/l).

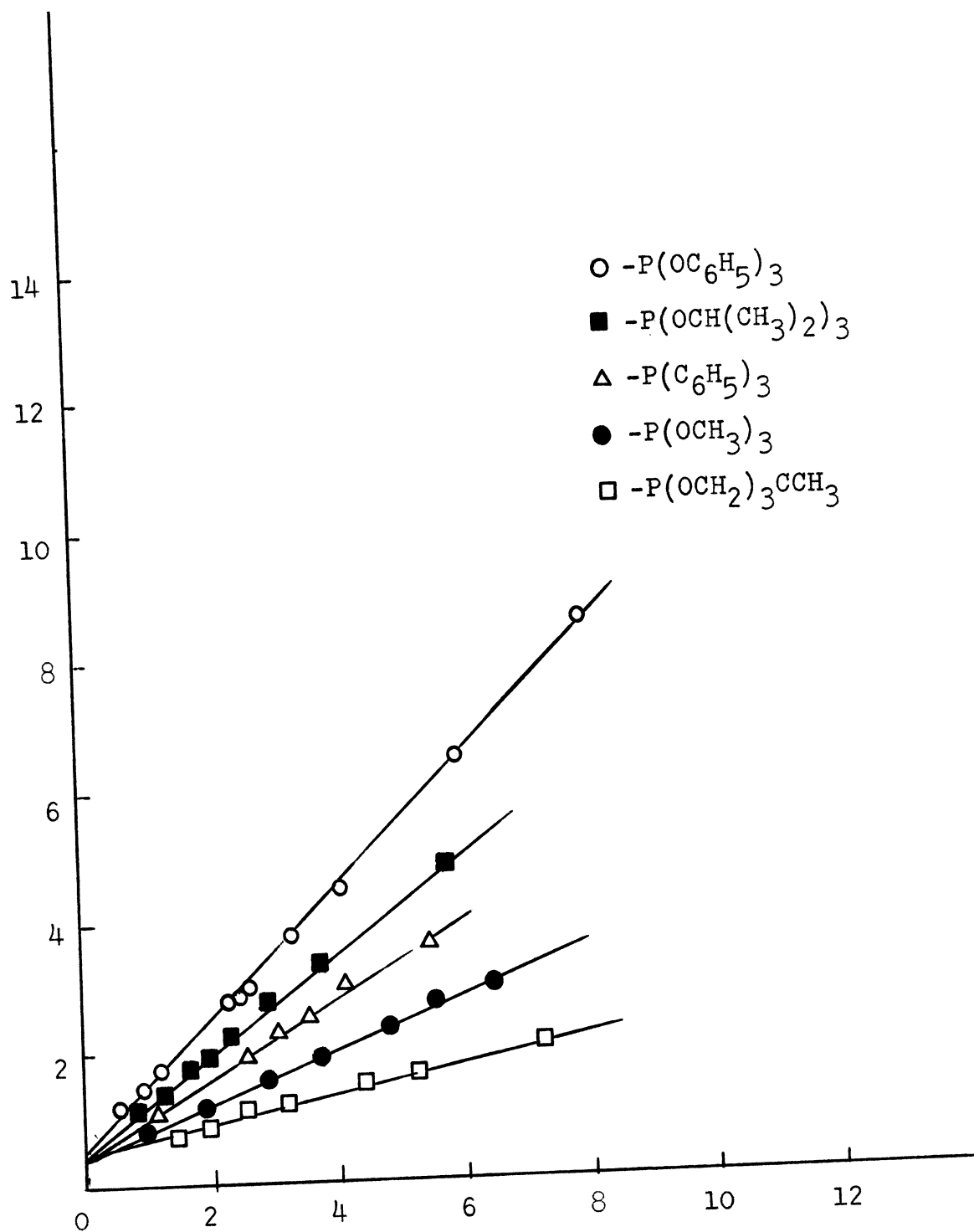


Fig. 18--Plot of  $1/k_{\text{obs}}$  vs.  $1/[\text{L}']$  for reaction of  $(\text{DTO})\text{W}(\text{CO})_4$  with various phosphorus ligands in xylene at  $99.9^\circ\text{C}$ . (Ordinate =  $1/k \times 10^{-3}$  sec, Abscissa =  $1/[\text{L}']$  1/mole).

$\times 10^{-4} \text{ sec}^{-1}$  for triisopropyl phosphite reported by Dobson<sup>46</sup> under identical experimental conditions. This is consistent with mechanism II, which predicts  $k_1$  to be independent of the identity of L'.

TABLE II  
RATE CONSTANTS FOR REACTION OF  $(\text{DTO})\text{W}(\text{CO})_4$   
WITH PHOSPHORUS LIGANDS IN XYLENE

Ligand	Temperature degrees C	$k_1$ $\times 10^4 \text{ sec}^{-1}$	$k_2/k_{-1}$ liter/mole
$\text{P}(\text{OCH}_3)_3$	99.9	26. (5)	0.93 (4)
$\text{P}(\text{OCH}(\text{CH}_3)_2)_3$	89.9	9.9 (7)	0.409 (9)
	99.9	23. (1)	0.557 (5)
	109.9	51. (4)	0.75 (1)
$\text{P}(\text{OC}_6\text{H}_5)_3$	99.9	24. (4)	0.413 (7)
$\text{P}(\text{OCH}_2)_3\text{CCH}_3$	99.9	23. (2)	1.96 (8)
$\text{P}(\text{C}_6\text{H}_5)_3$	99.9	20. (4)	0.85 (4)

Results of kinetic studies of the substitution reaction of  $(\text{DTO})\text{W}(\text{CO})_4$  with triisopropyl phosphite at three different temperatures are summarized graphically in Figures 19 and 20. The linearity of the reciprocal plots and curving nature of the  $k_{\text{obs}}$  vs. ligand concentration plots is consistent with mechanism II at all three temperatures investigated. The calculated values of  $k_1$  and  $k_{-1}/k_2$  gave linear

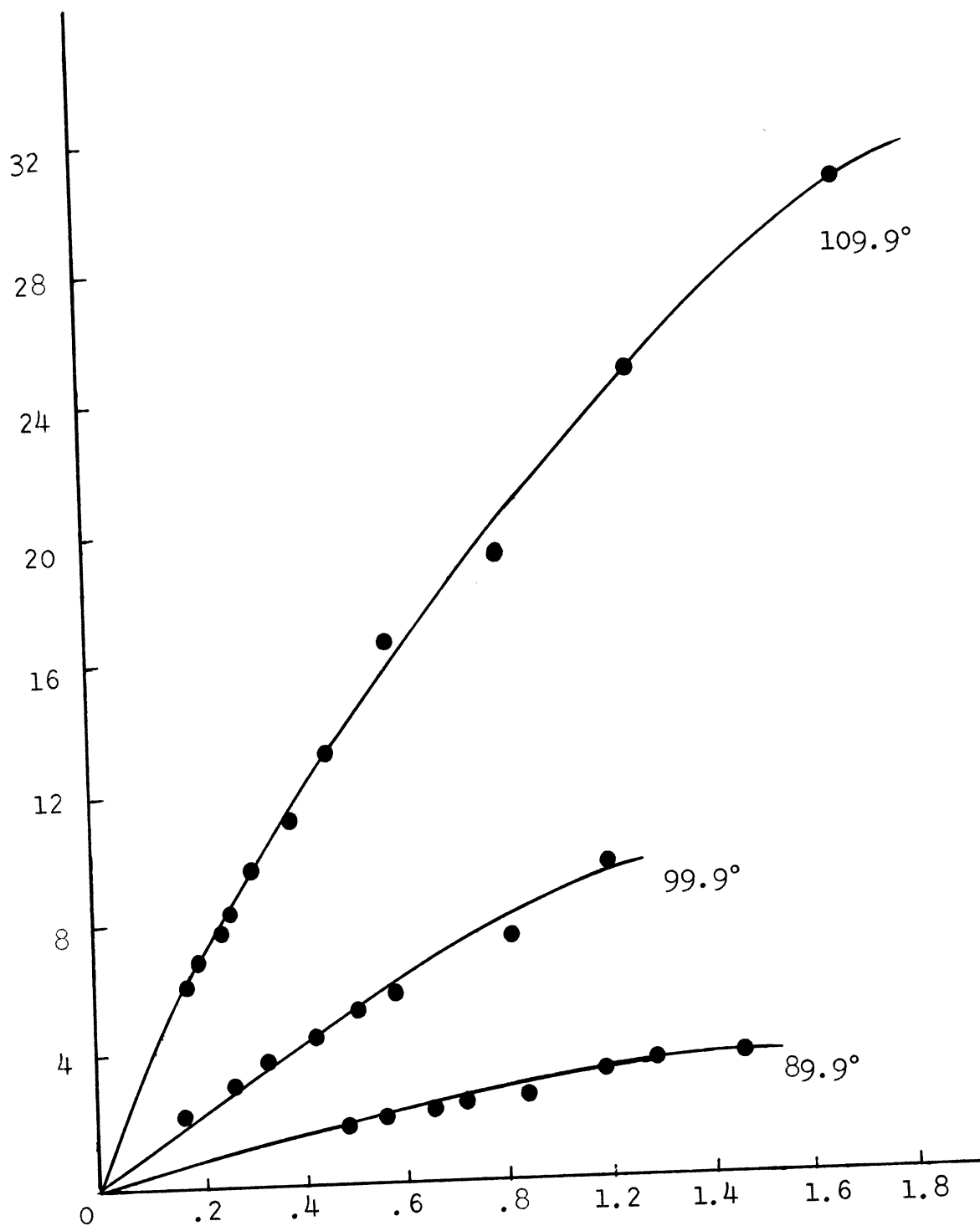


Fig. 19--Plot of  $k_{obs}$  vs.  $[L']$  for reaction of triisopropyl phosphite with  $(\text{DTO})\text{W}(\text{CO})_4$  at different temperatures. (Ordinate =  $k \times 10^4 \text{ sec}^{-1}$ , Abscissa =  $[L'] \times \text{moles/l}$ ).



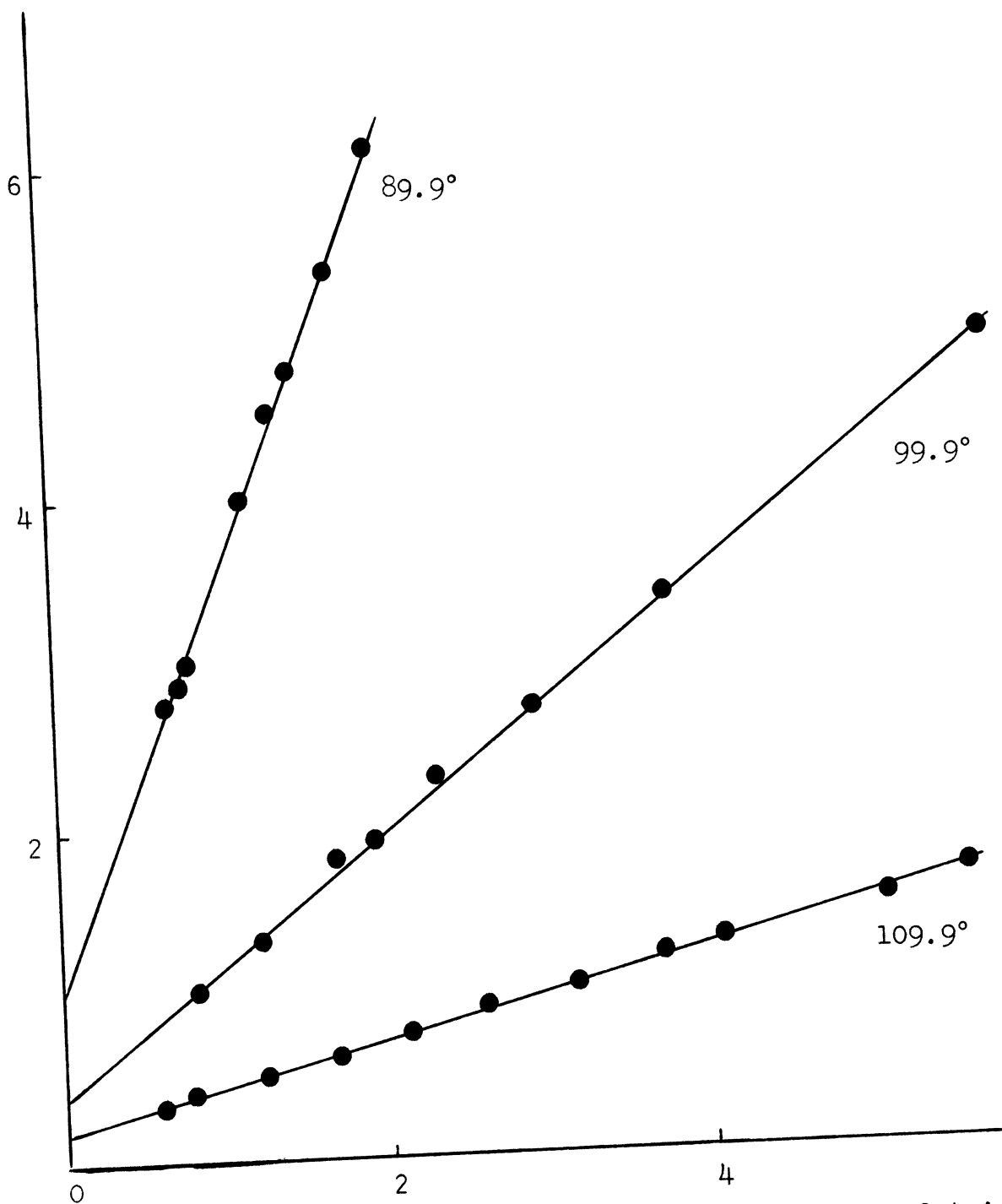


Fig. 20--Plot of  $1/k_{\text{obs}}$  vs.  $1/[L']$  for reaction of triisopropyl phosphite with  $(\text{DTO})\text{W}(\text{CO})_4$  at different temperatures. (Ordinate =  $1/k \times 10^3 \text{ sec}$ , Abscissa =  $1/[L'] \text{ 1/mole}$ ).

Eyring plots, as shown in Figure 21. Activation parameters were calculated from these rate constants and are presented in Table III.

TABLE III  
ACTIVATION PARAMETERS FOR REACTION OF  $(\text{DTO})\text{W}(\text{CO})_4$   
WITH TRIISOPROPYL PHOSPHITE IN XYLENE

Activation Parameter	Value
$\Delta H_1^*$	22.0 (3) kcal/mole
$\Delta S_1^*$	-12.1 (7) e.u.
$\Delta H_{-1}^* - \Delta H_2^*$	-9.12 (7) kcal/mole
$\Delta S_{-1}^* - \Delta S_2^*$	-23.3 (2) e.u.

Results of the kinetic studies of the reaction of  $(\text{DTO})\text{W}(\text{CO})_4$  with tri-n-butylphosphine at three different temperatures are summarized in the form of plots of  $k_{\text{obs}}$  vs. ligand concentration and  $1/k_{\text{obs}}$  versus  $1/[\text{L}']$  in Figures 22 and 23 respectively. Linear behavior of the  $k_{\text{obs}}$  versus ligand concentration plot and non-linear behavior of the reciprocal plot indicate the predominant mechanism in this system to be a direct attack mechanism, such as mechanism I in Figure 9. The non-zero intercept of this  $k_{\text{obs}}$  vs.  $[\text{L}']$  plot, however, indicates that competition from another mechanism must also be present in the system. Rate constants for this reaction were obtained from the slope of

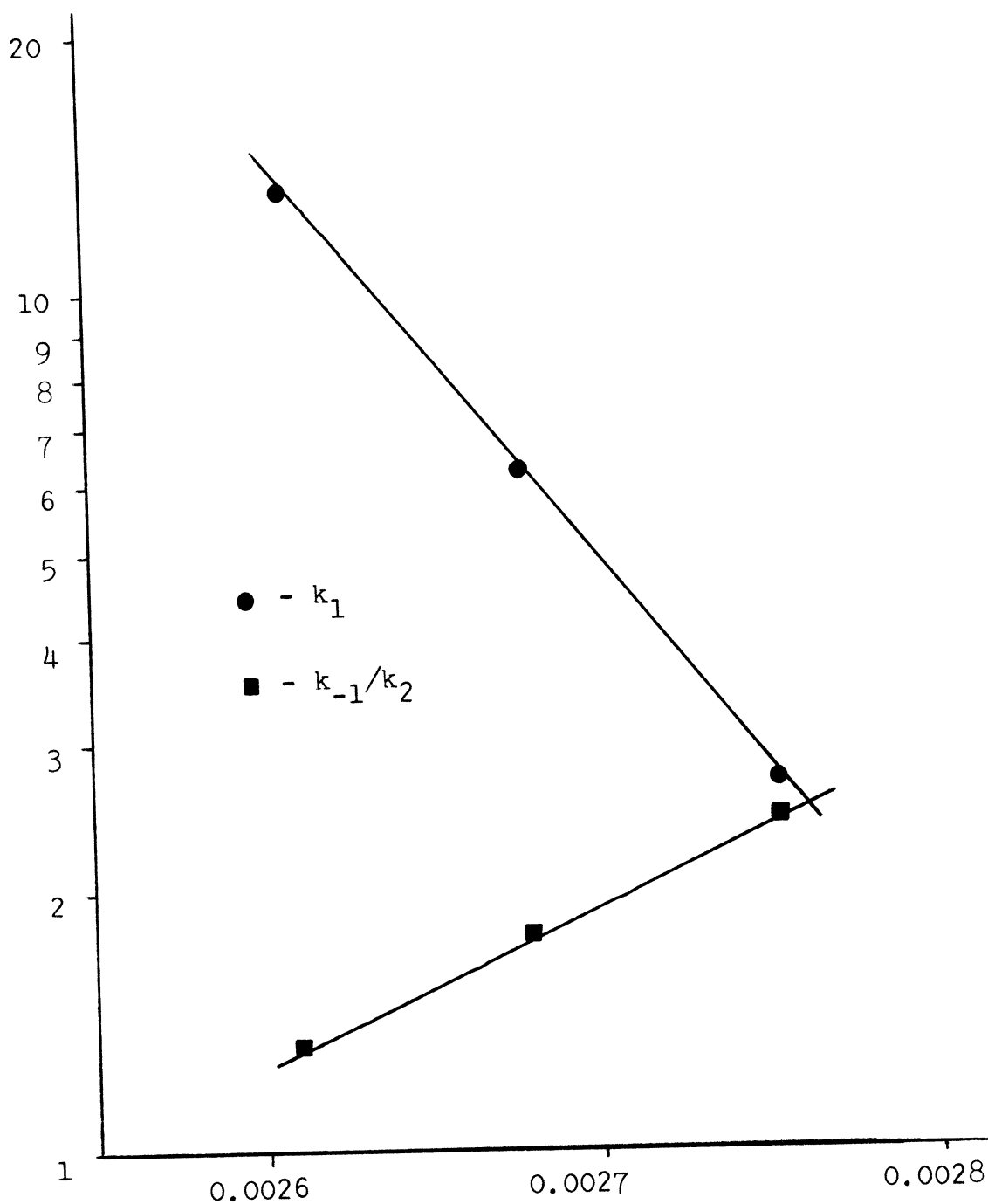


Fig. 21--Eyring plot of rate constants of reaction of  $(\text{DTO})\text{W}(\text{CO})_4$  with triisopropyl phosphite in xylene at different temperatures. (Ordinate =  $k_1/T \times 10^6 \text{ sec}^{-1} \text{ deg}^{-1}$  or  $k_{-1}/k_2$ , Abscissa =  $1/T \text{ degree}^{-1}$ ).

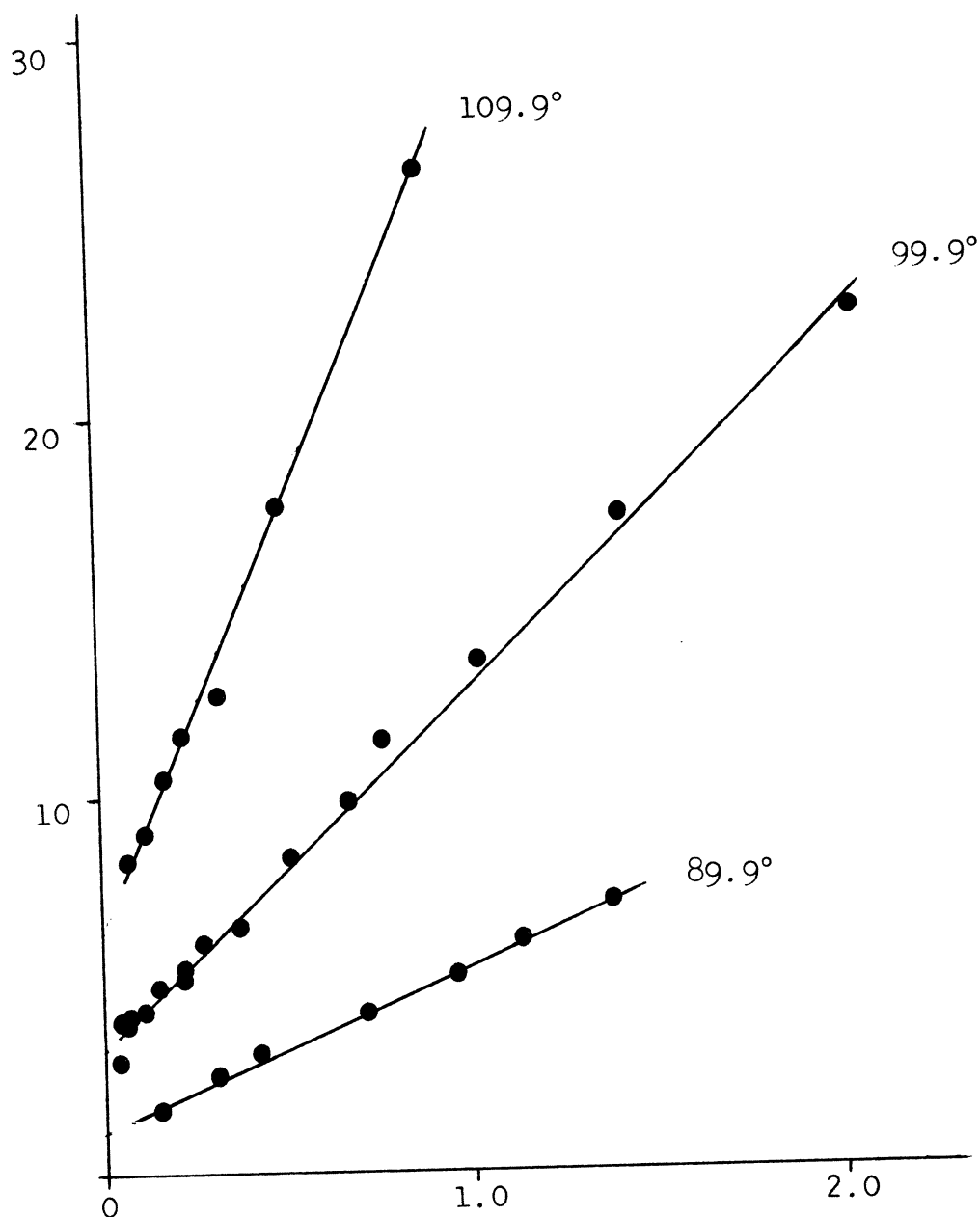


Fig. 22--Plot of  $k_{\text{obs}}$  vs.  $[L']$  for reactions of tri-n-butylphosphine with  $(\text{DTO})\text{W}(\text{CO})_4$  at different temperatures. (Ordinate =  $k \times 10^4 \text{ sec}^{-1}$ , Abscissa =  $[L']$  in moles/liter).

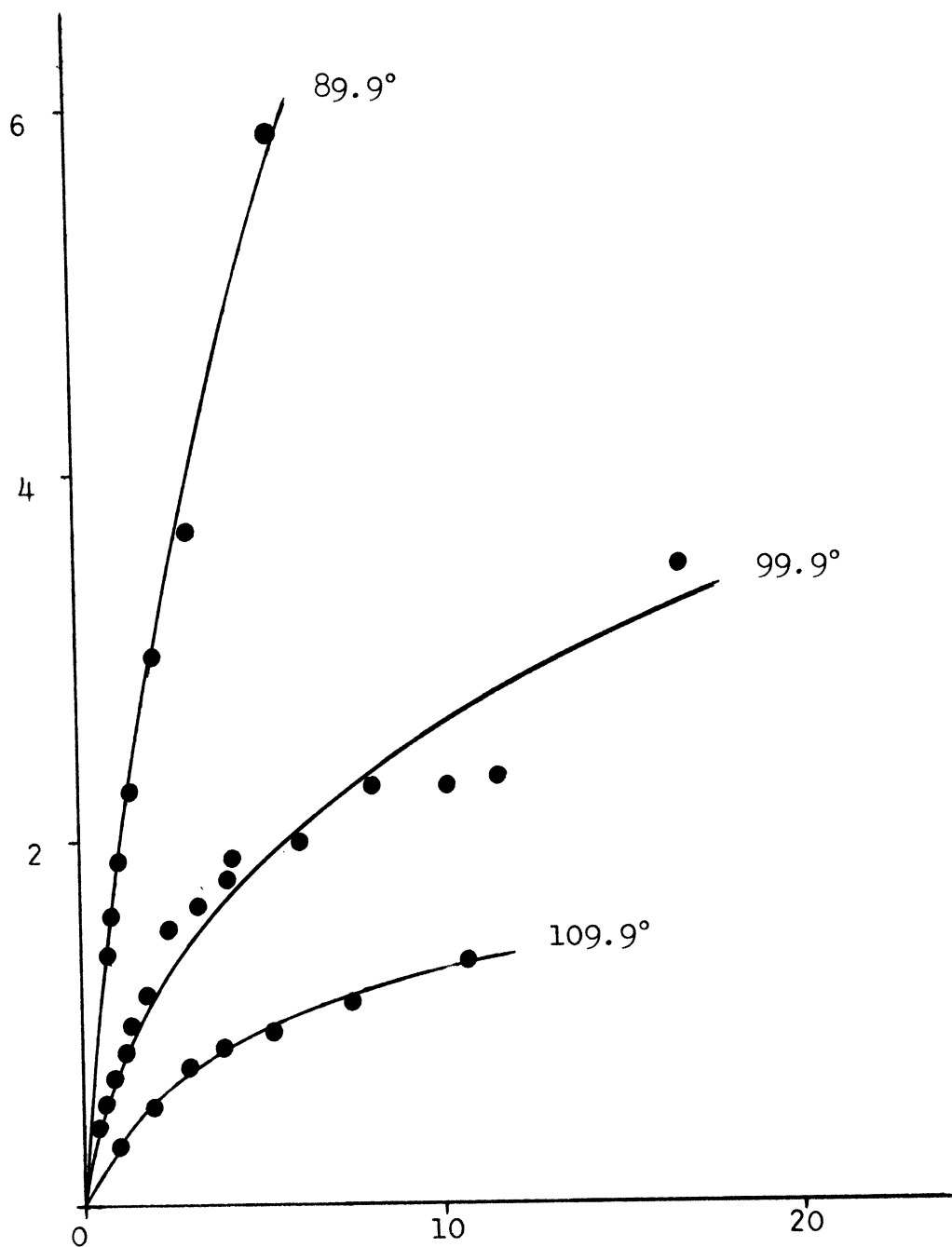


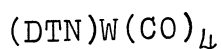
Fig. 23--Plot of  $1/k_{\text{obs}}$  vs.  $1/[L']$  for reaction of  $(\text{DTO})\text{W}(\text{CO})_4$  with tri-*n*-butylphosphine at various temperatures. (Ordinate =  $1/k \times 10^{-3}$  sec, Abscissa =  $1/[L']$  1/mole)

the  $k_{\text{obs}}$  vs. ligand concentration plots at each temperature and are summarized in Table IV.

TABLE IV  
SECOND ORDER RATE CONSTANTS FOR REACTION OF  $(\text{DTO})\text{W}(\text{CO})_4$   
WITH TRI-n-BUTYLPHOSPHINE IN XYLENE

Temperature degrees C	Rate Constant $\times 10^4$ liter / mole sec
89.9	4.4 (1)
99.9	9.6 (2)
109.9	22.5 (7)

From these rate constants, activation parameters for this system were calculated to be  $\Delta H^* = 22. (1)$  kcal/mole and  $\Delta S^* = -14. (3)$  e.u.



Results of the kinetic studies of the substitution reactions of  $(\text{DTN})\text{W}(\text{CO})_4$  with different phosphorus ligands at various temperatures are summarized in Table V.

Kinetic studies of the reaction of  $(\text{DTN})\text{W}(\text{CO})_4$  with trimethyl, triethyl, triisopropyl, and the constrained phosphite and triphenylphosphine at 66.5 degrees C in xylene are summarized graphically in Figures 24 and 25 in the form of plots of  $k_{\text{obs}}$  vs.  $[\text{L}^*]$  and  $1/k_{\text{obs}}$  vs.  $1/[\text{L}^*]$  respectively. Each of these reactions exhibited the curving

TABLE V  
 RATES OF REACTION OF  $(DTN)W(CO)_4$  WITH  
 PHOSPHORUS LIGANDS IN XYLENE

Ligand	Ligand Conc. moles/liter	Temperature degrees C	$k_{obs}$ $\times 10^4 \text{ sec.}^{-1}$
$P(OCH_3)_3$	0.134	66.5	6.12 (7)
	0.169		6.62 (5)
	0.248		7.52 (1)
	0.322		7.93 (0)
	0.502		8.35 (6)
	1.348		8.97 (7)
	1.643		9.5 (1)
$P(OC_2H_5)_3$	0.114	66.5	6.9 (1)
	0.129		7.17 (8)
	0.173		8.62 (7)
	0.185		9.1 (1)
	0.277		10.8 (2)
	0.459		13.8 (2)
	0.682		14.8 (3)
	0.959		15.5 (1)
	1.098		16.15 (8)
	1.592		16.89 (6)
$P(OCH(CH_3)_2)_3$	0.140	56.5	1.94 (2)
	0.183		2.42 (3)

V Continued

	0.211		2.72 (2)
	0.255		3.11 (4)
	0.341		3.70 (3)
	0.425		4.26 (6)
	0.663		5.73 (5)
	1.017		6.81 (9)
	1.196		7.96 (3)
	0.101	66.5	4.68 (1)
	0.153		6.75 (4)
	0.207		8.25 (4)
	0.228		9.24 (9)
	0.302		11.4 (3)
	0.343		12.59 (7)
	0.493		15.8 (2)
	0.559		17.0 (3)
	0.098	76.5	13.6 (1)
	0.126		16.4 (1)
	0.150		19.44 (7)
	0.206		25.4 (2)
	0.276		31.2 (3)
	0.338		36.5 (3)
	0.435		43.5 (2)
$P(C_6H_5)_3$	0.122	66.5	7.79 (9)
	0.156		8.9 (3)
	0.208		10.8 (2)



V Continued

	0.245		12.9 (7)
	0.317		14.9 (1)
	0.470		17.3 (1)
P(OCH <sub>2</sub> ) <sub>3</sub> CCH <sub>3</sub>	0.100	66.5	10.62 (9)
-fast reaction	0.127		11.9 (1)
	0.153		13.5 (1)
	0.241		17.2 (4)
	0.456		20.8 (4)
-slow reaction	0.101	66.5	2.14 (1)
	0.107		1.99 (5)
	0.123		1.90 (5)
	0.160		1.96 (2)
	0.202		2.05 (1)
	0.227		2.06 (1)
	0.279		2.11 (2)
	0.466		2.20 (3)
P((CH <sub>2</sub> ) <sub>3</sub> CH <sub>3</sub> ) <sub>3</sub>	0.107	56.5	2.39 (1)
	0.136		2.80 (2)
	0.207		3.60 (2)
	0.430		6.10 (9)
	0.598		8.43 (7)
	0.826		10.1 (1)
	1.188		14.18 (8)
	0.082	66.5	6.93 (3)
	0.119		8.45 (6)

V Continued

0.175		9.6 (1)
0.256		12.3 (2)
0.384		16.2 (2)
0.477		19.9 (4)
0.569		22.3 (2)
0.702		28.9 (4)
0.811		32.4 (6)
1.035		36.5 (4)
1.110		41. (1)
1.294		45.3 (6)
0.059	76.5	18.4 (3)
0.098		24.2 (4)
0.155		30.8 (4)
0.197		33.6 (8)
0.244		42.1 (6)
0.324		54.6 (7)

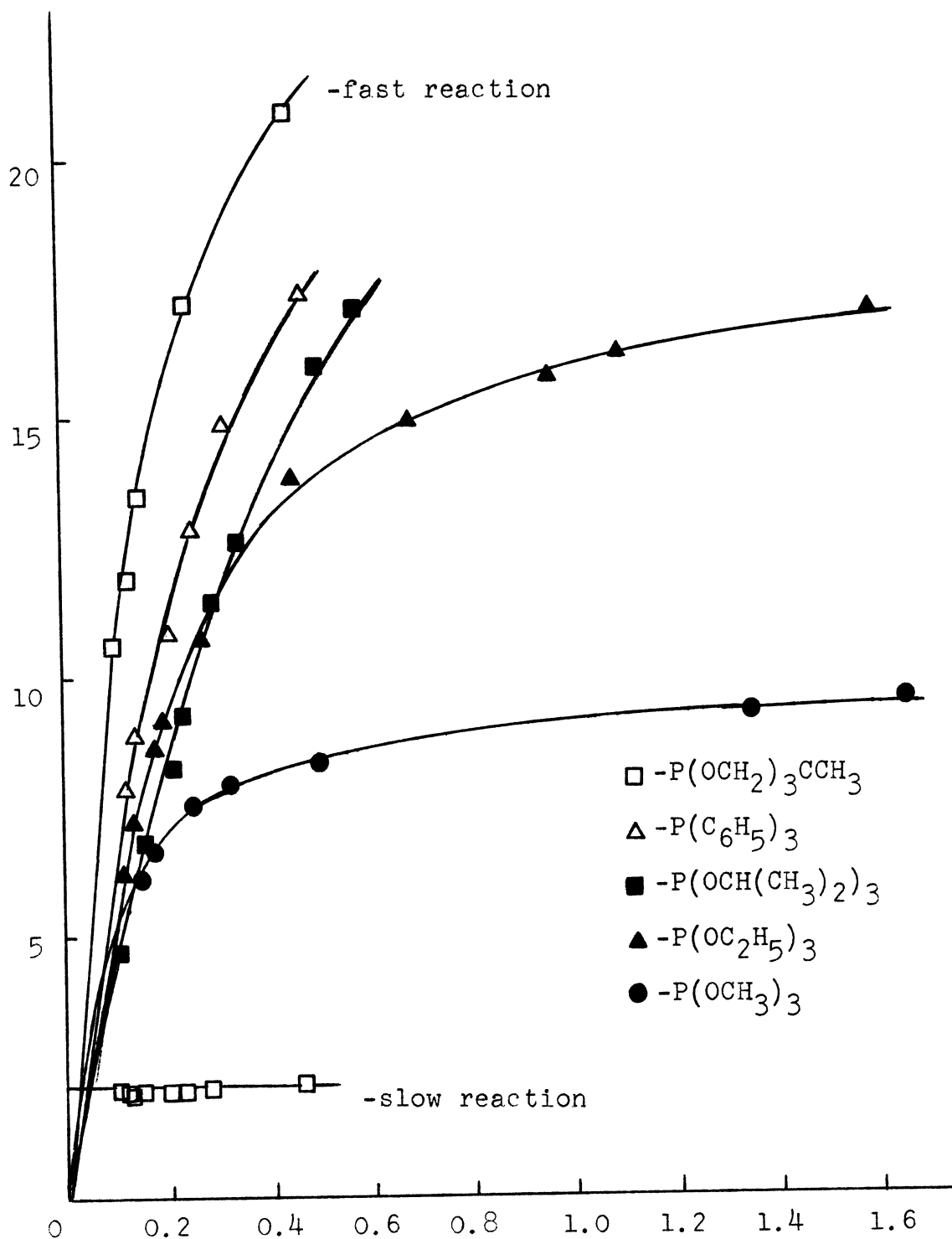


Fig. 24--Plot of  $k_{\text{obs}}$  vs.  $[\text{L}']$  for reactions of various phosphorus ligands with  $(\text{DTN})\text{W}(\text{CO})_4$  in xylene at  $66.5^\circ$ . (Ordinate =  $k \times 10^4 \text{ sec}^{-1}$ , Abscissa =  $[\text{L}']$  in moles/l).

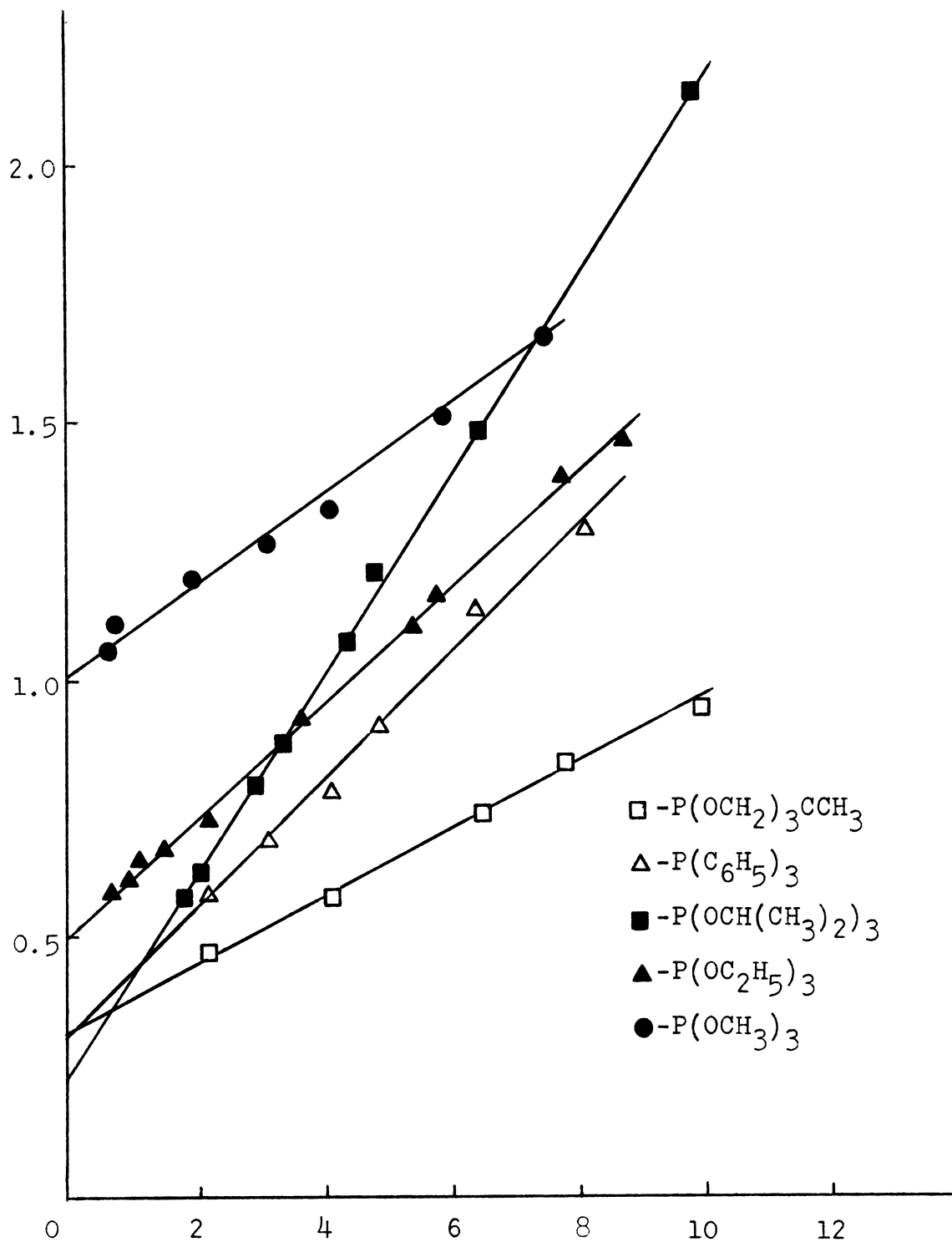


Fig. 25--Plot of  $1/k_{\text{obs}}$  vs.  $1/[L']$  for reaction of  $(\text{DTN})\text{W}(\text{CO})_4$  with various phosphorus ligands in xylene at  $66.5^\circ$ . (Ordinate =  $1/k \times 10^{-3}$  sec, Abscissa =  $1/[L']$  1/mole).

plot of  $k_{\text{obs}}$  vs. ligand concentration and linear reciprocal plot characteristic of mechanism II. (The reaction of  $(\text{DTN})\text{W}(\text{CO})_4$  with the constrained phosphite consisted of two consecutive reactions. The initial rapid reaction was comparable to the reaction of the substrate with other "typical" ligands and will be considered here. The secondary slow reaction will be discussed in a later section.) Values of  $k_1$  and  $k_2/k_{-1}$  were calculated from the intercept and slope of the reciprocal plots as previously discussed. These values are summarized in Table VI.

TABLE VI  
RATE CONSTANTS FOR REACTION OF  $(\text{DTN})\text{W}(\text{CO})_4$   
WITH PHOSPHORUS LIGANDS IN XYLENE

Ligand	Temperature degrees C	$k_1$ $\times 10^4 \text{ sec}^{-1}$	$k_2/k_{-1}$ liter/mole
$\text{P}(\text{OCH}_3)_3$	66.5	9.8 (1)	12.7 (5)
$\text{P}(\text{OC}_2\text{H}_5)_3$	66.5	19.3 (4)	4.71 (9)
$\text{P}(\text{OCH}(\text{CH}_3)_2)_3$	56.5	11.8 (5)	1.40 (2)
	66.5	40.9 (4)	1.284 (3)
	76.5	125. (8)	1.23 (2)
$\text{P}(\text{OCH}_2)_3\text{CCH}_3$	66.5	29. (1)	5.6 (2)
$\text{P}(\text{C}_6\text{H}_5)_3$	66.5	32. (4)	2.5 (1)

The  $k_1$  values of these substitution reactions at 66.5° do

not agree well. However, if the values of  $k_1$  for the trimethyl and triethyl phosphites are not considered, the values of the other  $k_1$ 's at 66.5 C may be averaged to give a value of  $34. (3) \times 10^{-4} \text{ sec}^{-1}$ . The values of  $k_1$  for triisopropyl phosphite, the constrained phosphite, and triphenylphosphine, within two standard deviations, agree with this value, while the  $k_1$  values of trimethyl and triethyl phosphite do not. Dobson and Faber<sup>47</sup> reported  $k_1$  values of  $8.84 \times 10^{-4} \text{ sec}^{-1}$  for trimethyl phosphite and  $18.5 \times 10^{-4} \text{ sec}^{-1}$  for triethyl phosphite under identical experimental conditions. These  $k_1$  values vary by 9.8 per cent and 4.2 per cent respectively from those reported in this study. Dobson and Faber<sup>47</sup> also reported  $k_1$  values of  $38.8 \times 10^{-4} \text{ sec}^{-1}$  for triphenyl phosphite and  $36.0 \times 10^{-4} \text{ sec}^{-1}$  for triisopropyl phosphite. These  $k_1$  values differ by 14.1 per cent and 5.9 per cent respectively from the average  $k_1$  value obtained in this investigation. From these results, it may be concluded that  $(\text{DTN})\text{W}(\text{CO})_4$  reacts with phosphorus ligands via mechanism II, but this mechanism is somehow perturbed in the cases of trimethyl and triethyl phosphite.

Plots of  $k_{\text{obs}}$  versus ligand concentration and reciprocal plots for the reaction of  $(\text{DTN})\text{W}(\text{CO})_4$  with triisopropyl phosphite are shown in Figures 26 and 27 respectively for three different temperatures. Behavior of these plots is consistent with mechanism II at all three temperatures.

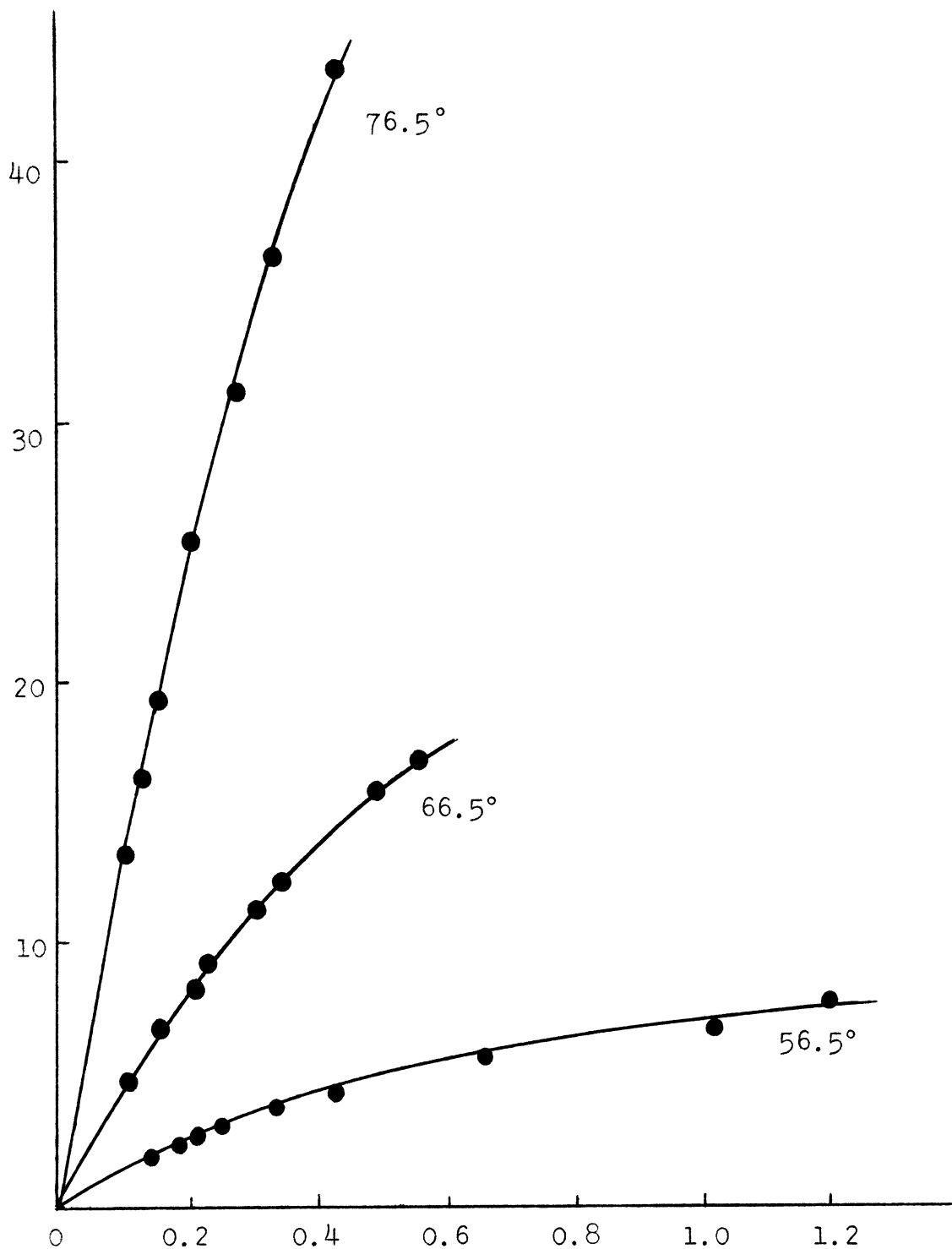


Fig. 26--Plot of  $k_{obs}$  vs.  $[L']$  for reaction of triisopropyl phosphite with  $(DTN)W(CO)_4$  at different temperatures. (Ordinate =  $k \times 10^4 \text{ sec}^{-1}$ , Abscissa =  $[L']$  moles/l).

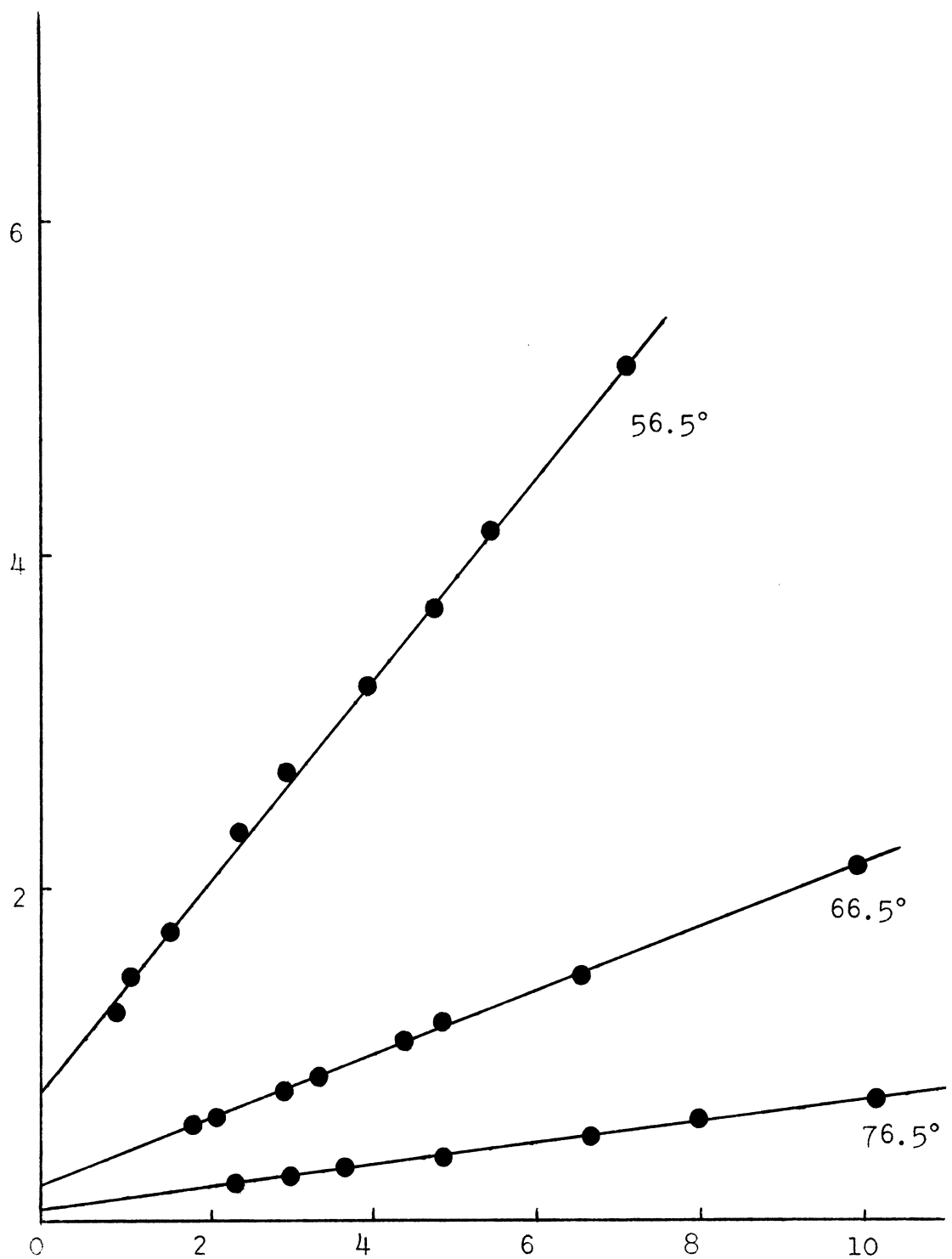


Fig. 27--Plot of  $1/k_{\text{obs}}$  vs.  $1/[L']$  for reaction of triisopropyl phosphite with  $(\text{DTN})\text{W}(\text{CO})_4$  at different temperatures. (Ordinate =  $1/k \times 10^{-3}$  sec, Abscissa =  $1/[L']$  l/mole).



Values of  $k_1$  and  $k_{-1}/k_2$  were calculated from the intercepts and slopes of the reciprocal plots, and these values gave linear Eyring plots, as illustrated in Figure 28. Activation parameters were calculated from these rate constants and are summarized in Table VII.

TABLE VII  
ACTIVATION PARAMETERS FOR REACTION OF  $(DTN)W(CO)_4$   
WITH TRIISOPROPYL PHOSPHITE IN XYLENE

Activation Parameter	Value
$\Delta H_1^*$	26.3 (6) kcal/mole
$\Delta S_1^*$	8. (2) e.u.
$\Delta H_{-1}^* - \Delta H_2^*$	0.8 (4) kcal/mole
$\Delta S_{-1}^* - \Delta S_2^*$	2. (1) e.u.

Plots of  $k_{obs}$  versus ligand concentration and  $1/k_{obs}$  vs.  $1/[L']$  for the reaction of  $(DTN)W(CO)_4$  with tri-n-butylphosphine at three different temperatures are shown in Figures 29 and 30 respectively. As was the case with the  $(DTO)W(CO)_4$  system, the plot of  $k_{obs}$  vs. ligand concentration was linear and the reciprocal plot was non-linear, indicating the presence of a direct attack mechanism at all three temperatures studied. The non-zero intercepts of the plots of  $k_{obs}$  vs.  $[L']$  indicate the coexistence of another

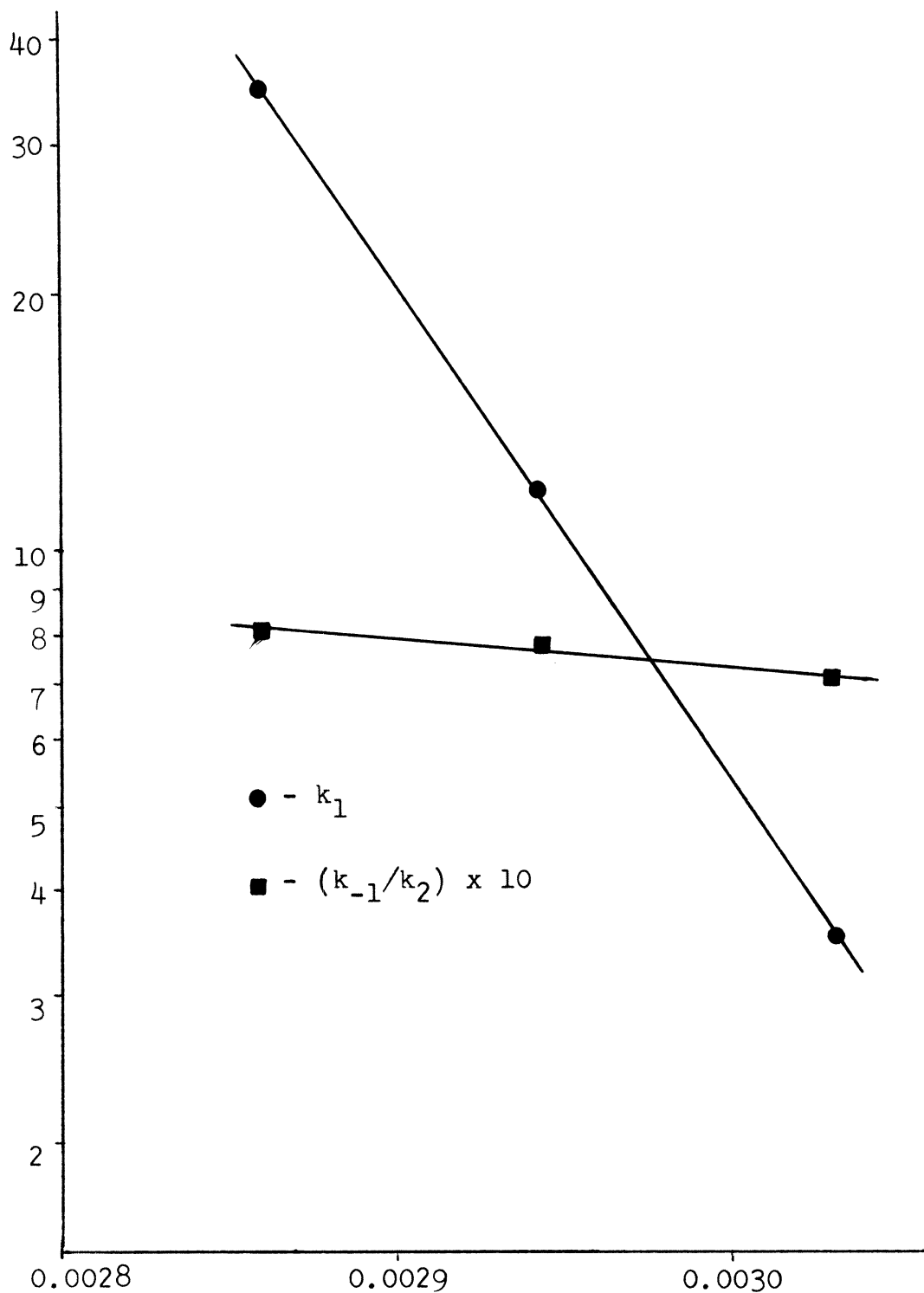


Fig. 28--Eyring plot of rate constants of reaction of  $(\text{DTN})\text{W}(\text{CO})_4$  with triisopropyl phosphite at different temperatures in xylene. (Ordinate =  $k_1/T \times 10^6 \text{ sec}^{-1} \text{ deg}^{-1}$  or  $k_{-1}/k_2$ , Abscissa =  $1/T \text{ degree}^{-1}$ ).

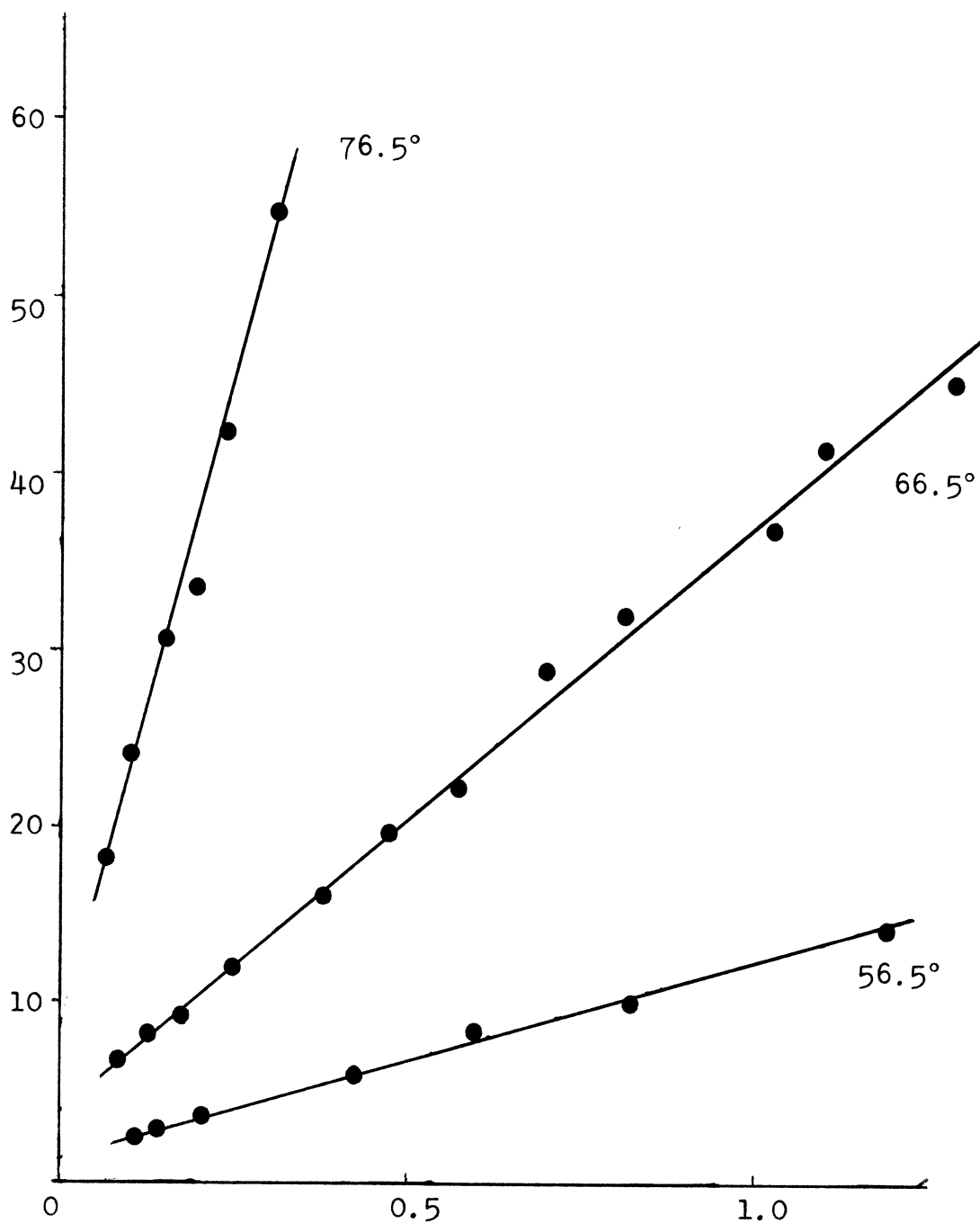


Fig. 29--Plot of  $k_{\text{obs}}$  vs.  $[L']$  for reaction of tri-*n*-butylphosphine with  $(\text{DTN})\text{W}(\text{CO})_4$  in xylene at different temperatures. (Ordinate =  $k \times 10^4 \text{ sec}^{-1}$ , Abscissa =  $[L']$  in moles/liter)

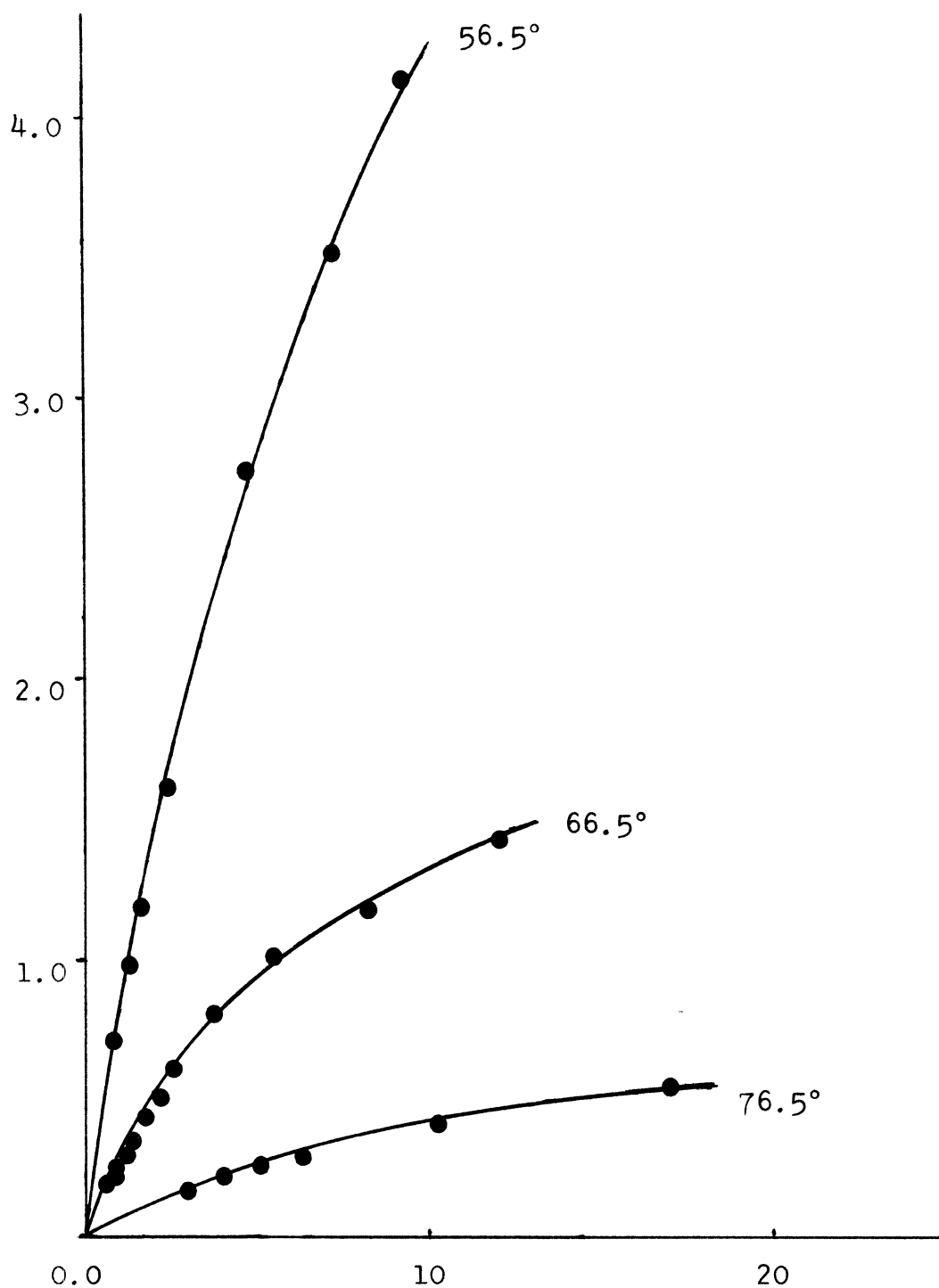


Fig. 30--Plot of  $1/k_{\text{obs}}$  vs.  $1/[L']$  for reaction of tri-*n*-butylphosphine with  $(\text{DTN})\text{W}(\text{CO})_4$  at different temperatures in xylene. (Ordinate =  $1/k \times 10^{-3}$  sec, Abscissa =  $1/[L']$  in liter/mole)

mechanism in this system. Rate constants for these reactions were obtained from the slopes of the plots of  $k_{\text{obs}}$  versus ligand concentration and are given in Table VIII.

TABLE VIII  
SECOND ORDER RATE CONSTANTS FOR REACTION OF  $(\text{DTN})\text{W}(\text{CO})_4$   
WITH TRI-n-BUTYLPHOSPHINE IN XYLENE

Temperature degrees C	Rate Constant $\times 10^4$ liter / mole sec
56.5	10.8 (3)
66.5	32.5 (8)
76.5	133. (8)

From these rate constants, activation parameters for the reaction of  $(\text{DTN})\text{W}(\text{CO})_4$  with tri-n-butylphosphine were calculated. These values were as follows:  $\Delta H^* = 28. (3)$  kcal/mole and  $\Delta S^* = 12. (7)$  e.u.

The plot of  $k_{\text{obs}}$  vs. ligand concentration for the second part of the reaction of  $(\text{DTN})\text{W}(\text{CO})_4$  with the constrained phosphite is included in Figure 24. The linear nature of this plot and the zero slope are indicative of a simple first order reaction, as discussed in Chapter I. This reaction probably corresponds to the loss of DTN by the intermediate  $(\text{DTN})\text{W}(\text{CO})_4\text{P}(\text{OCH}_2)_3\text{CCH}_3$ , followed by rapid steps to yield the final disubstituted product.

## CHAPTER IV

### DISCUSSION

The substitution reaction mechanisms of  $(\text{DTO})\text{W}(\text{CO})_4$  and  $(\text{DTN})\text{W}(\text{CO})_4$  with various phosphorus ligands may be divided into three different categories, dependent upon the identities of both the metal carbonyl complex and  $\text{L}'$ . These may be classified as Path A (mechanism II as shown in Figure 10), Path B (perturbation of mechanism II), and Path C (complex variation of mechanism I as shown in Figure 9).

#### Path A

Mechanism II consists of simple reversible dissociation of one end of the bidentate ligand, followed by attack of  $\text{L}'$  on the resultant five-coordinate intermediate. This path may be identified by the following criteria: curving plots of  $k_{\text{obs}}$  vs. ligand concentration, linear plots of  $1/k_{\text{obs}}$  versus  $1/[\text{L}']$ , and values of  $k_1$  invariant with identity of  $\text{L}'$ . These characteristics are exhibited by the systems  $(\text{DTO})\text{W}(\text{CO})_4$  with trimethyl, triethyl, triisopropyl, triphenyl, and constrained phosphite, and triphenylphosphine and  $(\text{DTN})\text{W}(\text{CO})_4$  with triisopropyl, triphenyl, and constrained phosphite, and triphenylphosphine.

Values of  $k_2/k_{-1}$  for these systems should reflect the discriminatory behavior of the five-coordinate intermediate

in reacting with L' or rechelating to reform starting complex, and may be considered as competition ratios. These competition ratios should be an index of the relative rates of attack of the various L' upon this intermediate, since the value of  $k_{-1}$  must be independent of L', and should vary in the order of nucleophilicity of the different ligands. Calculated values of  $k_2/k_{-1}$  for the reaction of  $(\text{DTO})\text{W}(\text{CO})_4$  with these ligands are given in Table II and vary in the order  $\text{P}(\text{OCH}_2)_3\text{CCH}_3 > \text{P}(\text{OCH}_3)_3 > \text{P}(\text{C}_6\text{H}_5)_3 > \text{P}(\text{OC}_2\text{H}_5)_3 >^{46}$   $\text{P}(\text{OCH}(\text{CH}_3)_2)_3 > \text{P}(\text{OC}_6\text{H}_5)_3$ . Since nucleophilicity is dependent upon both steric and electronic properties, i.e. is greatest for the smallest and most basic L', the observed series is quite reasonable. The above ligands vary in size, as measured by cone angle<sup>55</sup>, in the order  $\text{P}(\text{OCH}_2)_3\text{CCH}_3 <$   $\text{P}(\text{OCH}_3)_3 <$   $\text{P}(\text{OC}_2\text{H}_5)_3 <$   $\text{P}(\text{OCH}(\text{CH}_3)_2)_3 <$   $\text{P}(\text{OC}_6\text{H}_5)_3 <$   $\text{P}(\text{C}_6\text{H}_5)_3$ . Tolman<sup>56</sup> has derived a method of measuring electron donor-acceptor properties of phosphorus ligands based upon carbonyl stretching frequency variation. These parameters have shown an excellent correlation with  $\text{pK}_a$  values<sup>56</sup> and indicate that electron donating abilities of these ligands decrease in the order  $\text{P}(\text{C}_6\text{H}_5)_3 > \text{P}(\text{OCH}(\text{CH}_3)_2)_3 > \text{P}(\text{OC}_2\text{H}_5)_3 > \text{P}(\text{OCH}_3)_3 > \text{P}(\text{OC}_6\text{H}_5)_3 > \text{P}(\text{OCH}_2)_3\text{CCH}_3$ . From the observed variation of competition ratios with  $(\text{DTO})\text{W}(\text{CO})_4$ , it may be concluded that the predominant effect in these systems is exerted by steric considerations, except in the case of triphenylphosphine, in which a strong electron donor effect

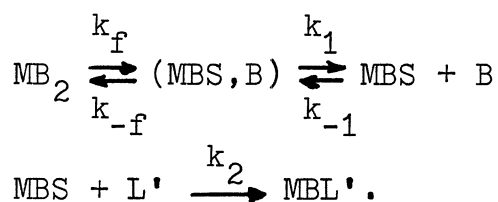
overcomes a large steric factor.

Values of  $k_2/k_{-1}$  for systems in which  $(DTN)W(CO)_4$  follows this path (see Table VI) vary in the order  $P(OCH_2)_3CCH_3 > P(C_6H_5)_3 > P(OC_6H_5)_3^{47} > P(OCH(CH_3)_2)_3$ . This sequence follows the trend established by the reactions of the DTO complex, with the exception of triphenyl phosphite, which has a slightly higher value of  $k_2/k_{-1}$  than predicted.

Although the values of  $k_2/k_{-1}$  observed in these systems do follow definite trends in reactivity, as discussed above, the actual values of these competition ratios exhibit a relatively small variation, e.g., less than ten-fold. This indicates that the five-coordinate intermediate combines with all of the ligands in this series at approximately the same rate. From this observation, it may be concluded that the reaction of the intermediate with  $L'$  is an associative process involving a small activation energy<sup>32</sup>. This conclusion is reached by the following process: if the transition state possessed many properties of the product molecule, i.e. involved a large amount of bond formation, the values of the competition ratios would reflect a marked dependence upon the nature of  $L'$ . However, this dependence is negligible. Therefore, very little bond formation is present in the transition state of the reaction of the five-coordinate intermediate with  $L'$ . The minimal variations of the competition ratios also indicate that  $k_1$  involves essentially complete rupture of the metal-bidentate ligand bond.



Activation parameters were measured for this path for both  $(\text{DTO})\text{W}(\text{CO})_4$  and  $(\text{DTN})\text{W}(\text{CO})_4$ , using triisopropyl phosphite as a typical ligand, and these values were listed in Tables III and VII respectively. Since  $k_1$  is a dissociative process involving little change in the order of the system,  $\Delta S_1^*$  would be predicted to be a low positive value. Therefore, the  $\Delta S_1^*$  value of -12.1 e.u. reported for  $(\text{DTO})\text{W}(\text{CO})_4$  is initially quite surprising. However, Angelici<sup>57</sup> has reported that aromatic solvents, such as xylene, interact quite strongly in the transition state to markedly reduce the entropy of activation. This solvent effect is indicative of an interchange (I) process, such as that discussed by Langford and Gray<sup>58</sup>, although the relatively nonpolar solvent used in these studies should minimize such effects. The interchange model for this system ( $\text{MB}_2$  = substrate complex, S = solvent molecule) would be



However, an I mechanism is assigned when no evidence can be produced for a reactive intermediate<sup>59</sup>, which is not the case in these systems. A strictly dissociative (D) or  $\text{S}_{\text{N}}1$  limiting process is ruled out by the low values of  $\Delta S_1^*$ . Therefore, the "intimate mechanism" for the initial reaction in these systems must be  $\text{I}_d$ , an interchange process of the

dissociative type, which is characterized by the formation of an intermediate with a very short lifetime<sup>59</sup>.

A comparison of enthalpies of activation for the reactions of  $(\text{DTO})\text{W}(\text{CO})_4$  and  $(\text{DTN})\text{W}(\text{CO})_4$  with triisopropyl phosphite reveals that  $\Delta H_1^*$  for the DTN complex is higher than for the DTO complex, contrary to the observed order of reactivity. Therefore, it appears that the larger entropy of activation in the initial dissociative step for  $(\text{DTN})\text{W}(\text{CO})_4$  is responsible for these reaction rates. This entropy effect may arise from the greater steric requirements of the six-membered chelate ring.

It may be assumed that the five-coordinate intermediates formed by the dissociation of one end of the bidentate ligand have approximately the same energies for both the DTO complex and the DTN complex, since  $k_1$  has been shown to involve almost complete rupture of the metal-bidentate ligand bond, as previously discussed. Therefore,  $\Delta H_2^*$  should also be about equal for both complexes, since the intermediates have approximately the same energies and the transition states do not resemble the products, as is indicated by the slight variations in the competition ratios. Since  $\Delta H_2^*$  is approximately equal for both complexes, and  $\Delta H_{-1}^* - \Delta H_2^*$  and  $\Delta H_1^*$  are known for both systems, the potential energy diagrams may be superimposed, as shown in Figure 31. From this diagram, the return of the free end of the bidentate ligand is approximately 9.9 kcal/mole less

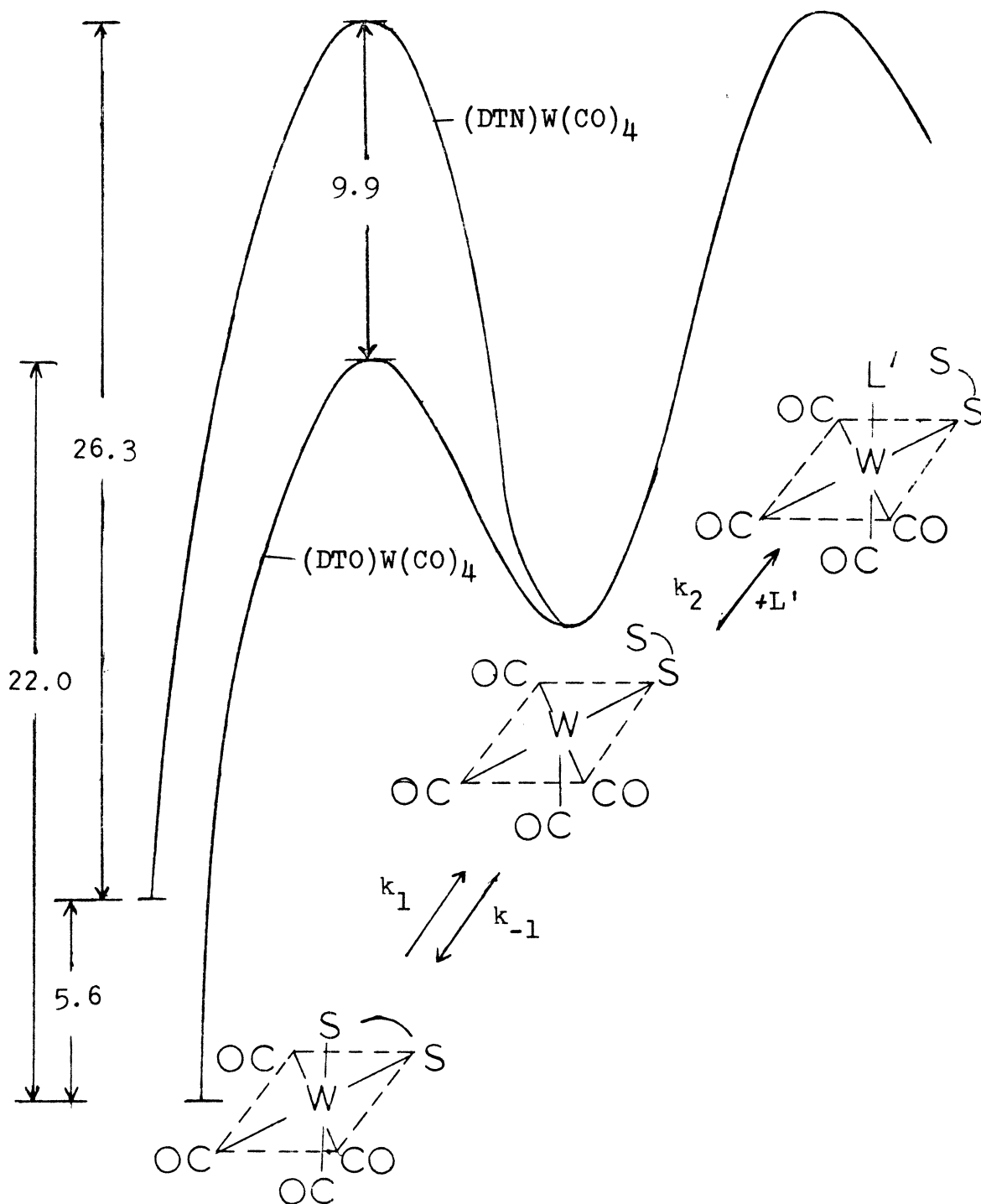


Fig. 31--Potential energy diagram for reaction of (bidentate)W(CO)<sub>4</sub> with triisopropyl phosphite in xylene. (Ordinate = energy in kcal/mole, Abscissa = reaction coordinate)

energetically favorable for  $(DTN)W(CO)_4$ , and therefore the ground state energy for  $(DTN)W(CO)_4$  is approximately 5.6 kcal/mole lower than that of  $(DTN)W(CO)_4$ . This demonstrates the increased stability of the five-membered chelate ring relative to the six-membered ring system, which has been attributed to enthalpy effects rather than entropy factors<sup>30</sup>. Indeed, it has been shown in some systems that the additional ring strain inherent in a six-membered chelate ring is alleviated by lengthening of the metal-bidentate ligand bonds, which may account for the higher ground state energy<sup>60</sup>. However, heats of formation data indicate that five-membered chelate ring systems, relative to six-membered analogs, are stabilized by only 1.3 to 2.2 kcal/mole<sup>30</sup>. The greater difference observed between  $(DTN)W(CO)_4$  and  $(DTN)W(CO)_4$  may be due to structural differences in the molecules caused by steric effects of the larger ring system and its substituents.

The reaction of the constrained phosphite with the DTN complex follows a complex path consisting of initial formation of a stable intermediate via mechanism II followed by unimolecular reaction of this intermediate to form cis and trans  $W(CO)_4(P(OCH_2)_3CCH_3)_2$ , as discussed in Chapter II.

The intermediate formed in the reaction of  $(DTN)W(CO)_4$  with the constrained phosphite has been isolated and identified as the compound  $(DTN)W(CO)_4P(OCH_2)_3CCH_3$ , with the DTN moiety bonded to the metal atom through only one sulfur

donor atom, by examination of the carbonyl stretching spectrum. This spectrum is shown in Figure 32, along with those of the substrate and final product. Similarities among the spectra indicate that the molecule is six-coordinate and of a  $C_{2v}$  local symmetry. A trace amount of the analogous intermediate was detected in the reaction of  $(\text{DTO})\text{W}(\text{CO})_4$  with the constrained phosphite by monitoring this reaction in the infrared, but the decay to products was too rapid at the temperatures required for the initial reaction to permit isolation of the intermediate or to interfere with rate measurements of the initial reaction. Structures of this type, having a bidentate ligand coordinated through only one site, are not unknown. Connor and coworkers<sup>61</sup> prepared and characterized a series of complexes in which only one end of a bidentate phosphorus ligand was bonded to the metal atom, and Knebel and Angelici<sup>62</sup> isolated a number of complexes in which a phosphorus-nitrogen donor bidentate ligand was bonded only through phosphorus by the protonation of the nitrogen. The fact that a stable intermediate is formed only when L' is the constrained phosphite is somewhat unexpected, since  $\text{P}(\text{OCH}_2)_3\text{CCH}_3$  is the weakest electron donor among the ligands used in this study<sup>56,63</sup>. The stability of this complex can be attributed in part to steric effects, since  $\text{P}(\text{OCH}_2)_3\text{CCH}_3$  is the smallest ligand used in this study<sup>55</sup>, but the size differential between it and trimethyl

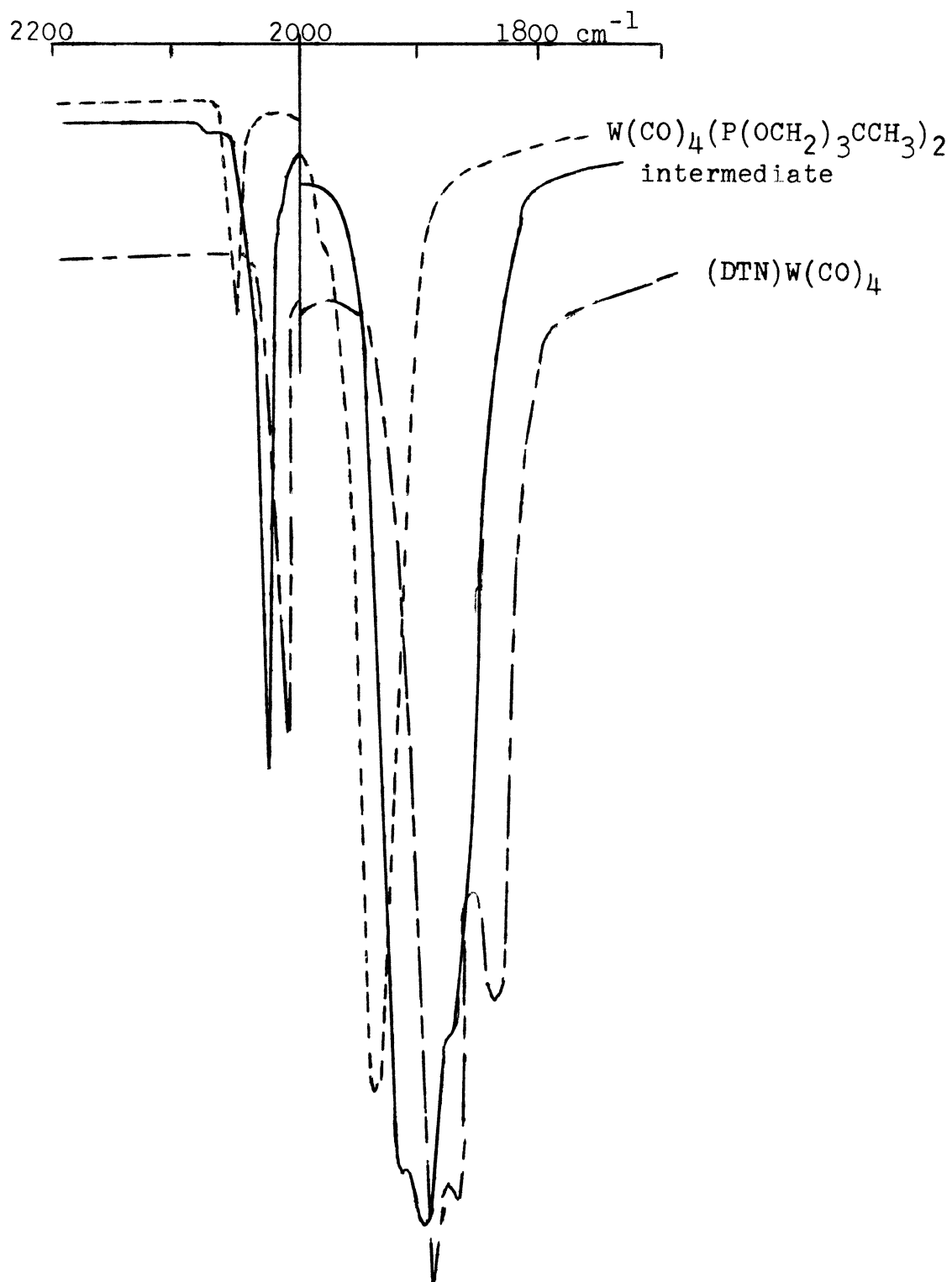


Fig. 32--Carbonyl stretching spectra in chloroform of products and substrate for  $(\text{DTN})\text{W(CO)}_4 + \text{P(OCH}_2)_3\text{CCH}_3$ .

phosphite is not great enough to account for all of the increased stability. Verkade and Piper<sup>63</sup> have noted that the constrained phosphite forms a number of coordination complexes which are not formed by similar, non-constrained phosphites. Chemical shift and coupling constant data indicate that a change in hybridization occurs on constraining the molecule into a bicyclic structure<sup>63</sup>. This change in hybridization should increase the s character of the donor orbital on phosphorus, which would lead to formation of a stronger sigma bond and account for the increased stability of the  $(DTN)W(CO)_4P(OCH_2)_3CCH_3$  complex. The isolation of this species as a reaction intermediate, which is predicted by mechanism II, may be considered strong evidence in support of this mechanism.

#### Path B

Reactions of  $(DTN)W(CO)_4$  with  $P(OCH_3)_3$  and  $P(OC_2H_5)_3$  exhibit the curving plots of  $k_{obs}$  vs. ligand concentration and linear reciprocal plots characteristic of the previously discussed mechanism. However, the reactions of  $(DTN)W(CO)_4$  with these two ligands yield non-common values of  $k_1$ , which is not consistent with this mechanism.

The comparative sizes, as measured by cone angle<sup>55</sup>, of the phosphorus ligands used in this study which exhibited behavior indicative of mechanism II are shown in Table IX.

TABLE IX  
 CONE ANGLES OF PHOSPHORUS LIGANDS

Ligand	Cone Angle deg.
$P(OCH_2)_3CCH_3$	102 (2)
$P(OCH_3)_3$	107 (2)
$P(OC_2H_5)_3$	109 (2)
$P(OCH(CH_3)_2)_3$	114 (2)
$P(OC_6H_5)_3$	121 (10)
$P(C_6H_5)_3$	145 (2)

The two ligands exhibiting perturbed behavior share the common property of small size. The constrained phosphite also shares this property, but it exhibits unique behavior, as previously discussed. This small size may enable the complex to form a seven-coordinate activated complex by reclosure, or partial reclosure, of the chelate ring. If the phosphorus ligand was not strongly bonded to the metal atom, as would be the case with weakly basic trimethyl and triethyl phosphite, although not strongly sigma bonding constrained phosphite, this ring reclosure could result in expulsion of  $L'$  and return to substrate, as illustrated in Figure 33.

This mechanism will yield the steady state rate expression



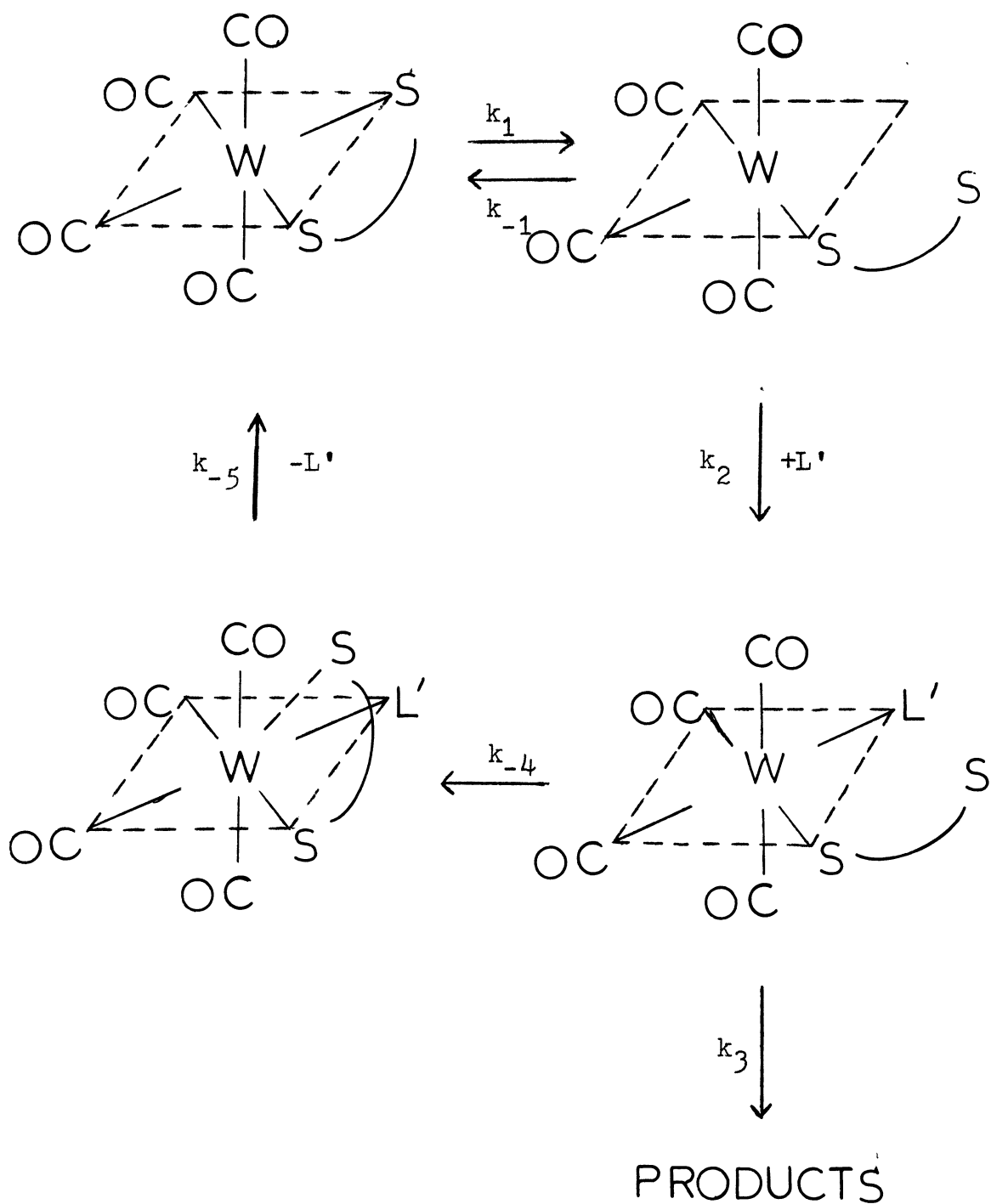


Fig. 33--Substitution reaction mechanism involving chelate ring reclosure with expulsion of  $\text{L}'$ .

$$-\frac{d[\text{Substrate}]}{dt} = \frac{k_1 k_2 k_3 [\text{Bidentate}] [\text{L}']}{k_{-1}(k_3 + k_{-4}) + k_2 [\text{L}'] (k_3 + k_{-4})}$$

Under pseudo first order reaction conditions,  $k_{\text{obs}}$  may be expressed as

$$k_{\text{obs}} = \frac{k_1 k_2 k_3 [\text{L}']}{k_{-1}(k_3 + k_{-4}) + k_2 [\text{L}'] (k_3 + k_{-4})}$$

This expression is of the same general form as that for mechanism II and may be rearranged to yield

$$1/k_{\text{obs}} = k_{-1}(k_3 + k_{-4})/k_1 k_2 k_3 [\text{L}'] + (k_3 + k_{-4})/k_1 k_3$$

A plot of  $1/k_{\text{obs}}$  vs.  $1/[\text{L}']$  for this expression will be linear with a slope of  $k_{-1}(k_3 + k_{-4})/k_1 k_2 k_3$  and an intercept of  $(k_3 + k_{-4})/k_1 k_3$ . This intercept term reduces to  $1/k_1 + k_{-4}/k_1 k_3$ . Therefore, intercepts of reciprocal plots for reactions following this pathway would be greater than for those following the unperturbed path. Since  $k_1$  is independent of  $\text{L}'$ , the true value of  $k_1$  may be obtained from other reactions in which only mechanism II is operative. This enables  $k_{-4}/k_3$  to be calculated by the relationship

$$k_{-4}/k_3 = \text{change in intercept} / \text{true intercept}$$

Using this expression, values of  $k_{-4}/k_3$  were calculated to be 2.51 for trimethyl phosphite and 0.77 for triethyl phosphite. The presence of this term accounts for the non-common values of  $k_1$  calculated for these systems.

The values of  $k_2/k_{-1}$  can be calculated for these

systems as the ratio intercept/slope. These values are included in Table VI, and indicate the competition ratio for trimethyl phosphite to be greater than that of triethyl, as would be predicted on the basis of steric effects.

The presence of a ring closure and return to substrate step in this mechanism accounts for the observed rate law in these  $(DTN)W(CO)_4$  systems. A similar mechanism may account for the rate behavior of the  $(tmpa)W(CO)_4$  systems investigated by Dobson and Faber<sup>47</sup> and Moradi<sup>64</sup>. These systems obey the rate law of mechanism II, but exhibit non-common values of  $k_1$ . The presence of a seven-coordinate transition state formed by ring reclosure has also been invoked to explain the rate behavior of  $(dipy)Cr(CO)_4$  by McKerley, Faber, and Dobson<sup>65</sup>. In the case of this complex, it is postulated that the seven-coordinate activated complex can also react by expulsion of a carbonyl group to form trisubstituted products.

#### Path C

When a very strong nucleophile, such as tri-n-butylphosphine reacts with  $(DTO)W(CO)_4$  or with  $(DTN)W(CO)_4$ , a third reaction path becomes evident. This pathway is characterized by linear plots of  $k_{obs}$  versus ligand concentration and non-linear reciprocal plots. Behavior of this type is indicative of a direct attack mechanism, such as mechanism I in Figure 9. However, the presence of non-zero

intercepts of the  $k_{\text{obs}}$  vs. ligand concentration plots is indicative of a complex mechanism, since a simple direct attack mechanism would exhibit a zero intercept. These criteria are met by the mechanism shown in Figure 34.

The steady state rate law for this mechanism will be

$$-\frac{d[\text{Substrate}]}{dt} = \frac{(k_1k_2 + k_{-1}k_5 + k_2k_5[L'])[L'][\text{Substrate}]}{k_{-1} + k_2[L']}$$

Utilizing pseudo first order reaction conditions,  $k_{\text{obs}}$  will be expressed by

$$k_{\text{obs}} = \frac{(k_1k_2 + k_{-1}k_5)[L'] + k_2k_5[L']^2}{k_{-1} + k_2[L']}$$

Although tri-n-butylphosphine is a very strong nucleophile, the lack of discrimination evidenced by the five-coordinate intermediate with other phosphorus nucleophiles indicates that the value of  $k_2/k_{-1}$  for this system should not be great enough to allow neglect of the  $k_{-1}$  term in the denominator of the complete rate law. If this term could be neglected, the  $k_{\text{obs}}$  expression would reduce to

$$k_{\text{obs}} = \frac{(k_1k_2 + k_{-1}k_5) + k_2k_5[L']}{k_2}$$

which is equal to

$$k_{\text{obs}} = (k_1k_2 + k_{-1}k_5)/k_2 + k_5[L']$$

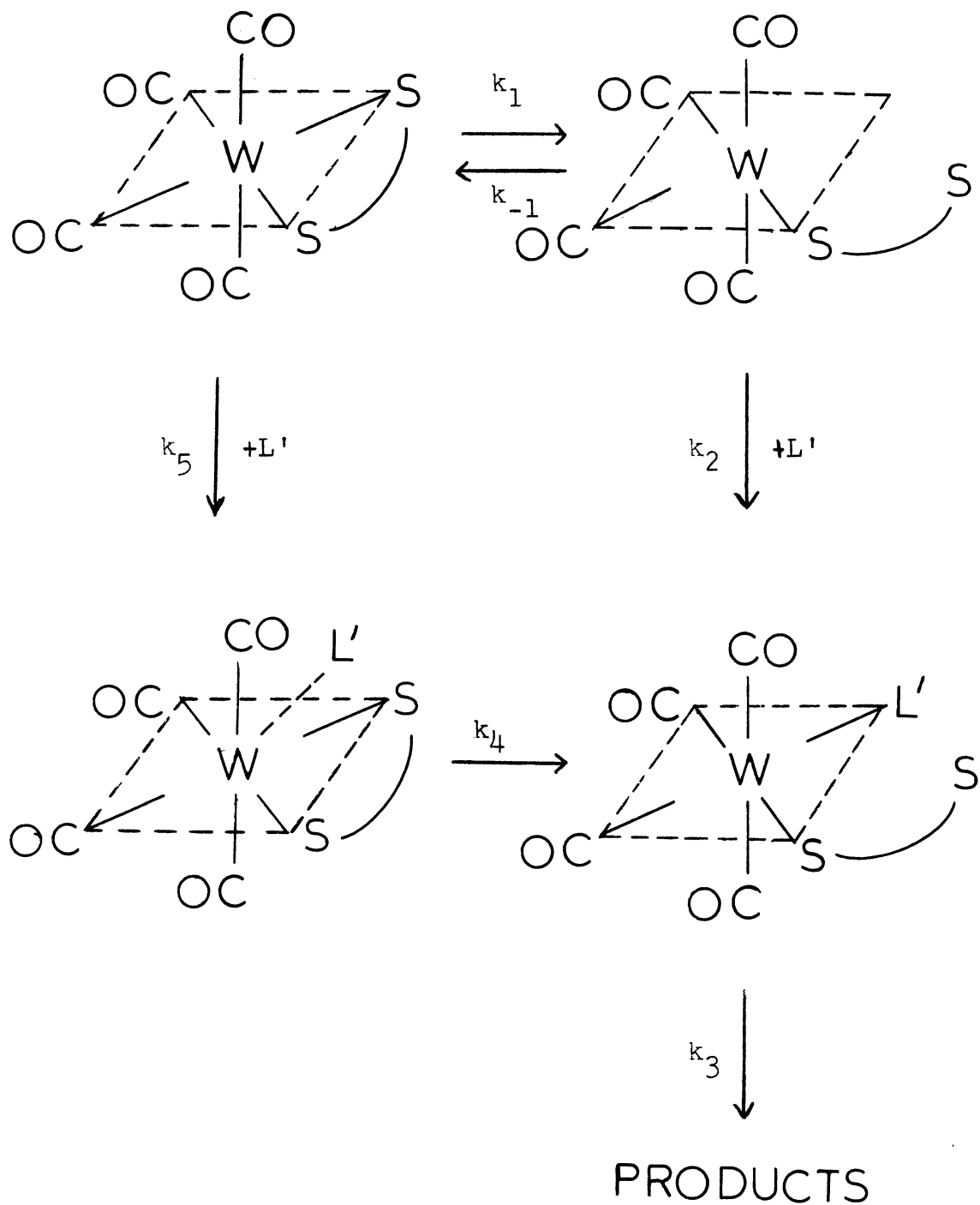


Fig. 34--Substitution reaction mechanism involving reversible dissociation and direct attack of L'.

Although this expression will yield a linear plot of  $k_{\text{obs}}$  vs. ligand concentration with a slope of  $k_5$  and a non-zero intercept, this intercept term will be equal to the value  $(k_1 + k_{-1}k_5/k_2)$ , and the observed intercepts are less than  $k_1$ . Therefore, it is apparent that the  $k_{-1}$  term in the denominator of the rate law may not be neglected.

The rate law may also be rearranged to give the expression

$$k_{\text{obs}} = \frac{k_1 k_2 [\text{L}']}{k_{-1} + k_2 \text{L}'} + k_5 [\text{L}'] .$$

This expression shows the competing mechanisms, and a superimposition of the two rates may give a fairly linear plot over the concentration ranges used in this study, although this plot would deviate from linearity at very low concentrations of  $\text{L}'$ .

The slope of this plot, however, should approximate the value of  $k_5$ . The values of  $k_5$  obtained from these plots are given in Tables IV and VIII. Unfortunately, this mechanism is too complex to allow calculation of any other rate constants. The activation parameters obtained for this system are indicative of an  $I_a$  process, although the similarity of these values to those obtained with triisopropyl phosphite may indicate that the separation of the competing paths is incomplete in this system.

## CHAPTER V

### CONCLUSIONS

The overall mechanism for the reaction of  $(\text{DTO})\text{W}(\text{CO})_4$  and  $(\text{DTN})\text{W}(\text{CO})_4$  with phosphorus ligands in xylene is illustrated in Figure 35. This mechanism may be broken down into three discrete pathways: Path A, governed by  $k_1, k_{-1}, k_2, k_3$ ; Path B, governed by  $k_1, k_{-1}, k_2, k_3, k_{-4}, k_{-5}$ ; and Path C, governed by  $k_1, k_{-1}, k_2, k_3, k_4, k_5$ . The choice of pathway is determined by the identity of the metal carbonyl complex and the steric and electronic nature of  $\text{L}'$ . Path A is followed by "typical" ligands with both  $(\text{DTO})\text{W}(\text{CO})_4$  and  $(\text{DTN})\text{W}(\text{CO})_4$ . Path B is taken by sterically non-demanding ligands, such as trimethyl and triethyl phosphite, with  $(\text{DTN})\text{W}(\text{CO})_4$ , although the constrained phosphite does not react via this mechanism, possibly because of the presence of an exceptionally strong sigma bond between the metal atom and the phosphite, as discussed in Chapter IV. Path C is taken by extremely strong nucleophiles, such as tri-n-butylphosphine, with both  $(\text{DTO})\text{W}(\text{CO})_4$  and  $(\text{DTN})\text{W}(\text{CO})_4$ .

The rate behavior of each system is consistent with this mechanism. Further support of this mechanism is obtained by the isolation of the intermediate species  $(\text{DTN})\text{W}(\text{CO})_4\text{P}(\text{OCH}_2)_3\text{CCH}_3$  formed by attack of  $\text{L}'$  on the five

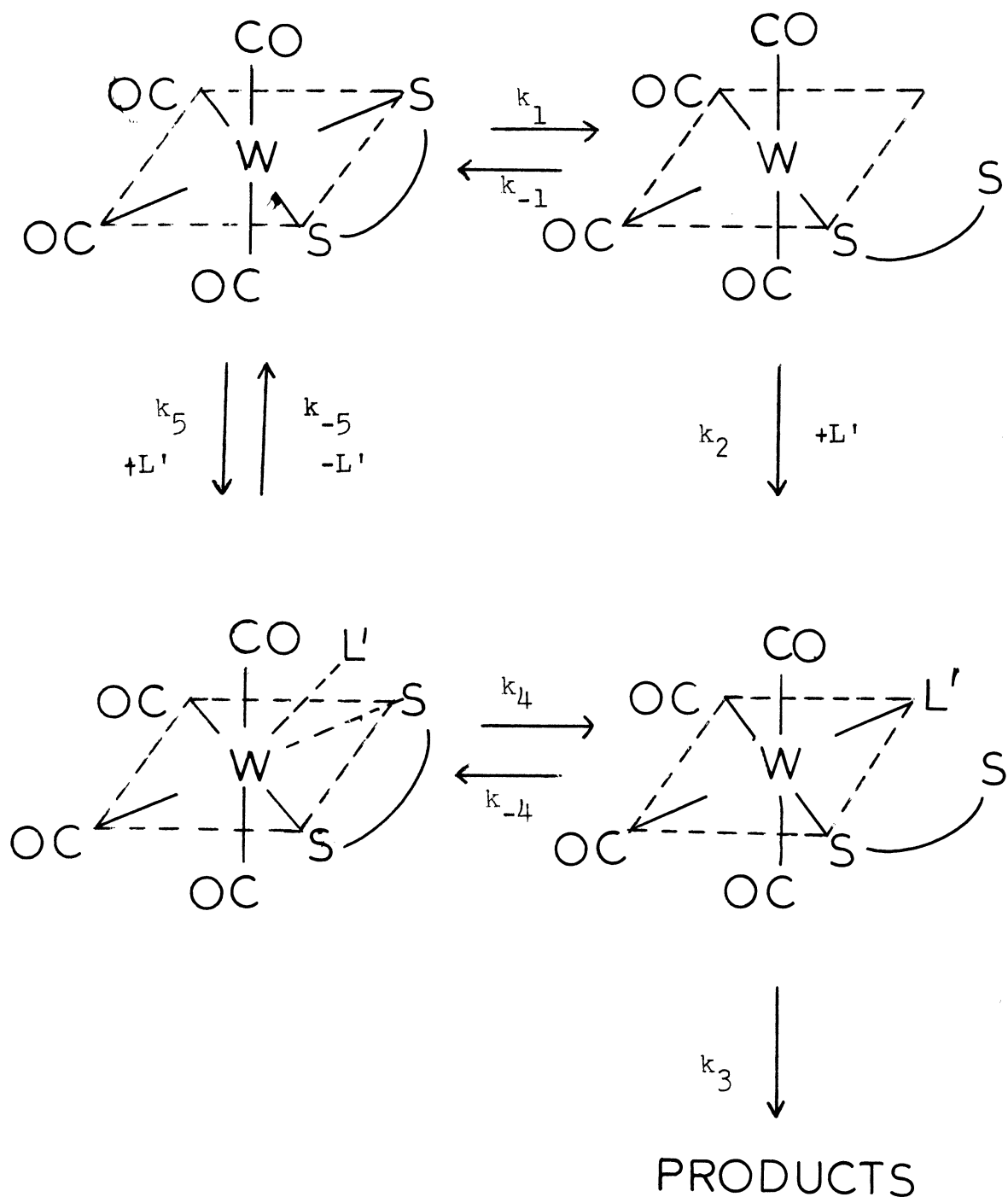


Fig. 35--Substitution reaction mechanism scheme for reaction of tungsten carbonyl complexes containing bidentate sulfur ligands with monodentate phosphorus ligands.



coordinate intermediate formed by dissociation of one end of the bidentate ligand, as predicted by this mechanism. The species  $(\text{DTO})\text{W}(\text{CO})_4\text{P}(\text{OCH}_2)_3\text{CCH}_3$  would be predicted to have approximately the same energy as its DTN analog, but this species could not be isolated because of the lower ground state energy of  $(\text{DTO})\text{W}(\text{CO})_4$  compared to  $(\text{DTN})\text{W}(\text{CO})_4$ . This energy differential causes  $(\text{DTO})\text{W}(\text{CO})_4$  to require much higher temperatures to undergo substitution, and the intermediate is too reactive to be isolated at these temperatures. The presence of a seven-coordinate activated complex is necessitated by the direct attack mechanism evidenced in the reactions of both  $(\text{DTO})\text{W}(\text{CO})_4$  and  $(\text{DTN})\text{W}(\text{CO})_4$  with tri-n-butylphosphine. The principle of microscopic reversibility then dictates the presence of  $k_{-4}$  and  $k_{-5}$ , which are demonstrated in Path B.

Deviation of the activation parameters for  $k_1$  and  $k_5$  from the values predicted for an  $\text{S}_{\text{N}}1$  (limiting) process and an  $\text{S}_{\text{N}}2$  (limiting) process respectively is indicative of an interchange mechanism. Therefore, it is concluded that  $k_1$  represents an  $\text{I}_{\text{d}}$  process and  $k_5$  an  $\text{I}_{\text{a}}$  mechanism.

The presence of Path B in the DTN complex, but not the DTO complex, may be indicative of a difference in structure between the two complexes. It is possible that the ring strain of the six-membered ring system in  $(\text{DTN})\text{W}(\text{CO})_4$  causes a distortion of the octahedral symmetry and makes

possible the reclosure of the chelate ring for this complex, when it is sterically impossible for  $(\text{DTO})\text{W}(\text{CO})_4$ . X-ray crystallographic studies are currently in progress to determine the structure of these compounds.

## BIBLIOGRAPHY

- 1 L. Mond, C. Langer and F. Quincke, J. Chem. Soc., 57, 749 (1890).
- 2 M. Berthelot, Compt. rend., 112, 1343 (1891).
- 3 W. Hieber, Advan. Organometal. Chem., 8, 1 (1970).
- 4 W.E. Trout, J. Chem. Educ., 14, 453 (1937).
- 5 W.E. Trout, ibid., 14, 575 (1937).
- 6 W.E. Trout, ibid., 15, 77 (1938).
- 7 W.E. Trout, ibid., 15, 113 (1938).
- 8 F.A. Cotton and G. Wilkinson, "Advanced Inorganic Chemistry," 3rd ed., Interscience Publishers, New York, N.Y., 1972, pp. 620, 682-708.
- 9 G.R. Dobson, I.W. Stolz and R.K. Sheline, Advan. Inorg. Chem. Radiochem., 8, 1 (1966).
- 10 J.W. Cable and R.K. Sheline, Chem. Rev., 56, 1 (1956).
- 11 P.R. Mitchell and R.V. Parish, J. Chem. Educ., 46, 811 (1969).
- 12 J.E. Huheey, "Inorganic Chemistry," Harper and Row, New York, N.Y., 1972, pp. 280-294.
- 13 R. Poilblanc and N. Bigorgne, Bull. Chem. Soc. France, 1301 (1962).
- 14 L.E. Orgel, Inorg. Chem., 1, 25 (1962).
- 15 F.A. Cotton and C.S. Kraihanzel, J. Am. Chem. Soc., 84, 4432 (1962).
- 16 F.A. Cotton, Inorg. Chem., 3, 702 (1964).
- 17 L.M. Haines and M.H.B. Stiddard, Advan. Inorg. Chem. Radiochem., 12, 53 (1969).
- 18 C.S. Kraihanzel and F.A. Cotton, Inorg. Chem., 2, 533 (1963).

- 19 F.A. Cotton, Inorg. Chem., 3, 702 (1964)
- 20 F.A. Cotton and D.C. Richardson, ibid., 5, 1851 (1966).
- 21 R.J. Angelici, J. Inorg. Nucl. Chem., 28, 2627 (1966).
- 22 R.J. Angelici and M.D. Malone, Inorg. Chem., 6, 1931 (1967).
- 23 R.A. Brown and G.R. Dobson, Inorg. Chim. Acta, 6, 65 (1972).
- 24 R.F. Fenske and R.L. DeKock, Inorg. Chem., 9, 1052 (1970).
- 25 M.E. Hall and R.F. Fenske, ibid., 11, 1619 (1972).
- 26 A.D. Berry, E.R. Corey, A.P. Hagen, A.G. MacDiarmid, F.E. Saalfield and B.H. Wayland, J. Am. Chem. Soc., 92, 1940 (1970).
- 27 G. Keeling, S.F.A. Kettle and I. Paul, J. Chem. Soc., A, 3143 (1971).
- 28 R.T. Jernigan, R.A. Brown and G.R. Dobson, J. Coord. Chem., 2, 47 (1972).
- 29 G.R. Dobson, Annals N.Y. Acad. Sci., 239, 237 (1974).
- 30 F. Basolo and R.G. Pearson, "Mechanisms of Inorganic Reactions," 2nd ed., John Wiley and Sons, New York, N.Y., 1967, pp. 533-540.
- 31 R.J. Angelici, Organometal. Chem. Rev., 3, 173 (1968).
- 32 K.G. Caulton and R.F. Fenske, Inorg. Chem., 7, 1273 (1968).
- 33 J.E. Pardue, M.N. Memering and G.R. Dobson, J. Organometal. Chem., 71, 407 (1974).
- 34 W.D. Covey and T.L. Brown, Inorg. Chem., 12, 2820 (1973).
- 35 L.W. Houk and G.R. Dobson, J. Chem. Soc., A, 317 (1966).
- 36 G.R. Dobson and L.W. Houk, Inorg. Chem. Acta, 1, 287 (1967).
- 37 R.J. Angelici and J.R. Graham, J. Am. Chem. Soc., 87, 5586 (1965).

- 38 J.R. Graham and R.J. Angelici, J. Am. Chem. Soc., 87, 5590 (1965).
- 39 R.J. Angelici and J.R. Graham, Inorg. Chem., 6, 988 (1967).
- 40 J.R. Graham and R.J. Angelici, ibid., 6, 992 (1967).
- 41 G.C. Faber and G.R. Dobson, Inorg. Chim. Acta, 2, 479 (1968).
- 42 D.R. Powers, G.C. Faber and G.R. Dobson, J. Inorg. Nucl. Chem., 31, 2970 (1969).
- 43 G.C. Faber and G.R. Dobson, Inorg. Chem., 7, 584 (1968).
- 44 A. Frost and R.G. Pearson, "Kinetics and Mechanism," 2nd ed., John Wiley and Sons, New York, N.Y., 1961, p. 195.
- 45 G.C. Faber, T.D. Walsh and G.R. Dobson, J. Am. Chem. Soc., 90, 4178 (1968).
- 46 G.R. Dobson, Inorg. Chem., 8, 90 (1969).
- 47 G.R. Dobson and G.C. Faber, Inorg. Chim. Acta, 4, 87 (1970).
- 48 E.K. Plyler, A. Danti, R.L. Blaine and E.D. Tidwell, J. Res. Nat. Bur. Stand., Sect. A, 64, 29 (1960).
- 49 B.P. Federov and I.S. Savel'eva, Izvest. Akad. Nauk SSSR, Otdel Khim Nauk, 223 (1950); Chem. Abstr., 45, 1502a (1951).
- 50 A. Pidcock, J.D. Smith and B.W. Taylor, Inorg. Chem., 9, 638 (1970).
- 51 J.G. Verkade, T.J. Hutteman, M.K. Fung and R.W. King, ibid., 4, 83 (1965).
- 52 A.C. Vanderbroucke, D.G. Hendricker, R.E. McCarley and J.G. Verkade, ibid., 7, 1825 (1968).
- 53 E.P. Ross and G.R. Dobson, J. Inorg. Nucl. Chem., 30, 2363 (1968).
- 54 G.R. Dobson and J.R. Paxson, J. Chem. Educ., 49, 67 (1972).

- 55 C.A. Tolman, J. Am. Chem. Soc., 92, 2956 (1970).
- 56 C.A. Tolman, ibid., 92, 2953 (1970).
- 57 R.J. Angelici and B.E. Leach, Organometal. Chem., 11, 263 (1968).
- 58 C.H. Langford and H.B. Gray, "Ligand Substitution Processes," W.A. Benjamin, New York, N.Y., 1965, ch. 1.
- 59 M.L. Tobe, "Inorganic Reaction Mechanisms," Nelson, London, 1972, pp. 16-23.
- 60 L.J. DeHayes and D.H. Busch, Inorg. Chem., 12, 1505 (1963).
- 61 J.A. Connor, J.P. Day, E.M. Jones and G.K. McEwen, J. Chem. Soc., Dalton, 347 (1972).
- 62 W.J. Knebel and R.J. Angelici, Inorg. Chem., 13, 627 (1964).
- 63 J.G. Verkade and T.S. Piper, "Advances in the Chemistry of the Coordination Compounds," S. Kirshner, Ed., Macmillan Co., New York, N.Y., 1961, pp. 634-639.
- 64 A. Moradi, L.D. Schultz and G.R. Dobson, unpublished results
- 65 B.J. McKerley, G.C. Faber and G.R. Dobson, Inorg. Chem., 14, 2275 (1975).